TURONIAN, CONIACIAN, AND SANTONIAN OSTRACODA FROM SOUTH-EAST AFRICA

By

R. V. Dingle

Marine Geoscience Unit, Department of Geology, University of Cape Town

(With 53 figures and 18 tables)

[*MS accepted 18 January 1985*]

ABSTRACT

Fifty-five species, representing at least twenty genera, are recorded from the Turonian to Santonian strata of Zululand (Mfolozi Valley–False Bay area and Richards Bay borehole), offshore Natal (J(c)–1 borehole), Transkei (Umzamba), and Agulhas Bank. Three species are new: *Cytherelloidea mtubaensis, Cythereis mfoloziensis* and *Unicapella stragulata*. Palaeoecological analyses suggest that depositional environments at the three sites in Zululand all commenced with shallow-water conditions that progressively deepened, but there is evidence of local shallowing in the False Bay area in Upper Santonian times as a result of increased sediment supply. A faunal boundary is recognized between southern outcrops (Umzamba) and Zululand during the Santonian. This is speculated to have been temperature-controlled, and regional considerations of palaeogeography and biogeography suggest that the major ostracod faunal dichotomy across the Turonian–Coniacian boundary in south-east Africa was caused by the influx of warm-water faunas from tropical stocks in the Brazil–Gabon area of the Atlantic. This was initiated by the breakdown of the Walvis–Rio Grande barrier and establishment of a clockwise ocean-current circulation pattern in the southern South Atlantic, which injected warm water into existing north-east flowing currents off the coast of south-east Africa. By comparison with Tanzanian faunas, the timing of this is dated between Lower Cenomanian and Middle Turonian (i.e. between 99 and 89 m.y. ago), and probably coincided with the Lower Turonian transgression recognized in Nigeria (*c.* 91 m.y.).

An ostracod zonation scheme comprising four zones is proposed for the Coniacian–Santonian strata of south-east Africa.

CONTENTS

Ann. S. Afr. Mus. **96** (5), 1985: 123–239, 53 figs, 18 tables.

INTRODUCTION

In south-east Africa there is a widespread hiatus between sediments of mid-Cretaceous age, and overlying strata that were deposited during the Upper Cretaceous transgression (Kennedy & Klinger 1971). Ammonite studies by Kennedy & Klinger (1975) show that at outcrop in the Zululand–Natal region this non-sequence spans uppermost Cenomanian IV to lowermost Coniacian I time, although in north Zululand and offshore Natal, Upper Turonian strata have been proved in oil-exploration boreholes (Du Toit & Leith 1974; McLachlan & McMillan 1979). Preliminary studies showed that this important lithostratigraphic break coincides with a first-order biostratigraphic dichotomy in the ostracod faunas of south-east Africa, and that there is strong evidence for the event having regional significance (Dingle 1982). What makes these phenomena of particular interest is the probability that the faunal change can be related to plate-tectonic events in the South Atlantic, and specifically, the breaching of the Walvis Ridge–Rio Grande Rise archipelago as a faunal barrier between the Equatorial (Brazil–West Africa) and southern Atlantic–south-west Indian ocean provinces. The purpose of this contribution is twofold: to document the Turonian to Santonian

ostracods of south-east Africa; and to make regional faunal comparisons and discuss their palaeogeographical implications.

Known outcrops of Coniacian and Santonian sediments in south-east Africa are limited to the Zululand–Natal coastal plain, northern Transkei (Umzamba), and the western Agulhas Bank (Fig. 1), although borehole and geophysical evidence indicate that they occur extensively beneath younger cover on the continental shelves around southern Africa (Dingle *et al.* 1983). We have examined samples from all three areas, including material from borehole J(c)–1 offshore Natal, but only in Zululand are outcrops extensive and referable to all of the Coniacian and Santonian ammonite stages recognized by Kennedy & Klinger (1975). No Turonian outcrops have been reported from southern Africa, and samples of this age were available only from the J(c)–1 borehole. A summary of the spatial and temporal distribution of the ostracods recovered during this project is shown in Table 1.

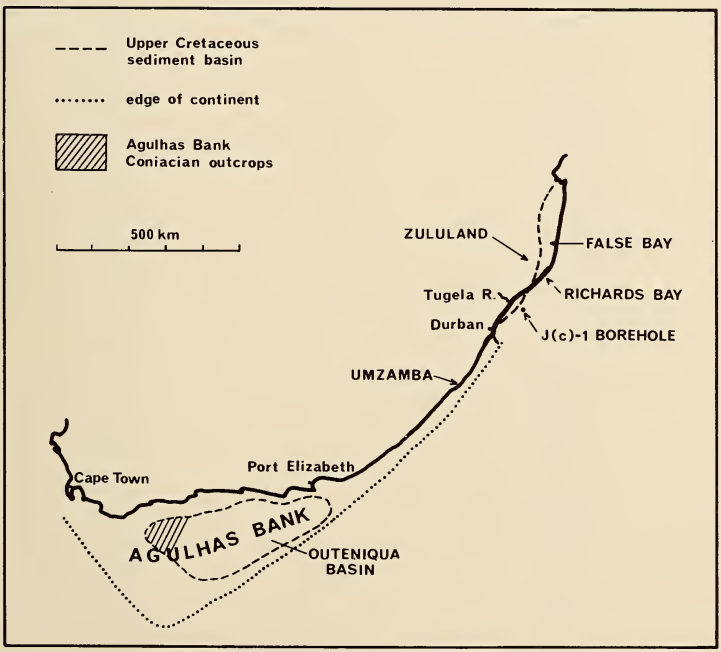

Fig. 1. Turonian to Santonian sample localities in south-east Africa.

TABLE 1

Temporal and spatial distribution of Turonian to Santonian ostracods in south-east Africa.

	Upper Turonian**	Coniacian I	Coniacian II	Coniacian III	Coniacian IV	Coniacian V	Santonian I	Santonian II	Santonian III		Zululand FB	Zululand MV	Zululand BH9	Um.	Ag. Bank
1 *Cytherella* sp. 1929					x							x			
2 *Cytherella* sp. 2351								x—x			x				
3 *Cytherella* sp. 1–4								x—x		*			x		
4 *Cytherelloidea mtubaensis*					x							x			
5 *Cytherelloidea newtoni*					x—	——	——	x—x			x	x	x		
6 *Cytherelloidea umzambaensis*					x—	——	——	x—x		*	x	x	x	x	
7 *Cytherelloidea gardeni*								x—x					x	x	
8 *Cytherelloidea griesbachi*									x—	*			x	x	
9 *Apateloschizocythere?* cf. *mclachlani*			x												x
10 *Amphicytherura tumida*								x—x		*			x	x	
11 *Brachycythere agulhasensis*			x												x
12 *Brachycythere longicaudata*	x—	——	——	x—	x	——	——	x—x		*	x	x	x	x	
13 *Brachycythere rotunda*								x						x	
14 *Brachycythere pondolandensis*								x—x					x	x	
15 *Brachycythere sicarius*								x—x		*	x	x	x	x	
16 *Cythereis klingeri*					x—	——	——	x—x		*	x	x	x		
17 *Cythereis luzangaziensis*	x—	——	——	——	cf. x							x			
18 *Cythereis mfoloziensis*				x								x			
19 *Cythereis transkeiensis*								x—x		*		x	x	x	
20 *Gibberleberis africanus*					x—	——	——	x—			x	x	x	x	
21 *Gibberleberis elongata*									x—	*			x		
22 *Rayneria nealei*					x—	——	——	x—	——	*		x	x	x	
23 *Haughtonileberis haughtoni*	x—	——	——	——	x—	——	——	x—	——	*	x	x	x	x	
24 *Haughtonileberis fissilis*								x—	——	*		x	x	x	
25 *Haughtonileberis vanhoepeni*									x—	*			x		

30 *Bythocypris richardsbayensis*			x	x	x	*	x	x	x		
31 *Paraphysocythere thompsoni*				x	x					x	
32 *Veenia obesa*				x	x					x	
33 *Bairdoppilata andersoni*				x	x	*	x	x	x	x	
34 *Cnestocythere?* sp. 2091					x					x	
35 *Pondoina sulcata*				x	x				x	x	
36 *Unicapella stragulata*			x	x	x		x	x			
37 Indet. sp. 1874				x			x				
38 Indet. sp. 1956			x					x			
39 Indet. sp. 2103				x						x	
40 Indet. sp. 2104				x						x	
41 Indet. sp. 2108				x						x	
42 Indet. sp. 2078					x					x	
43 Indet. sp. 2125				x			x				
44 Indet, sp. 1232			x					x			

J(c)–1	Cen.–Tur.	Coniacian	Santonian								
45 *Bairdoppilata* sp. 2327	x										
46 *Bairdoppilata* sp. 2322			x								
47 *Bairdoppilata* sp. 2336	x		x								
48 *Bythocypris richardsbayensis*	x		x								
49 *Cytherella* sp. 2325		x									
50 *Cytherella* sp. 2317			x								
51 *Krithe* sp. 2329	x										
52 *Krithe* sp. 2332	x										
53 *Dutoitella mimica*			x	*							
54 Indet. sp. 2312	x										
55 Indet. sp. 2314	x										

** = Tanzania, * = extension above Santonian III; FB = False Bay, MV = Mfolozi Valley, BH9 = Richards Bay borehole; Um = Umzamba, Ag. Bank = Agulhas Bank.

TABLE 1

Temporal and spatial distribution of Turonian to Santonian ostracods in south-east Africa.

	Upper Turonian**	Coniacian I	Coniacian II	Coniacian III	Coniacian IV	Coniacian V	Santonian I	Santonian II	Santonian III		Zululand FB	Zululand MV	Zululand BH9	Um.	Ag. Bank
1 *Cytherella* sp. 1929					x							x			
2 *Cytherella* sp. 2351								x—x			x				
3 *Cytherella* sp. 1–4								x—x		*			x		
4 *Cytherelloidea mtubaensis*					x							x			
5 *Cytherelloidea newtoni*					x—			x—x			x	x	x		
6 *Cytherelloidea umzambaensis*					x—			x—x		*	x	x	x	x	
7 *Cytherelloidea gardeni*								x—x					x	x	
8 *Cytherelloidea griesbachi*									x	*			x	x	
9 *Apateloschizocythere?* cf. *mclachlani*			x												x
10 *Amphicytherura tumida*								x—x		*			x	x	
11 *Brachycythere agulhasensis*			x												x
12 *Brachycythere longicaudata*	x—			—x	—x			x—x		*	x	x	x	x	
13 *Brachycythere rotunda*								x						x	
14 *Brachycythere pondolandensis*								x—x					x	x	
15 *Brachycythere sicarius*								x—x		*	x	x	x	x	
16 *Cythereis klingeri*					x—			x—x		*	x	x	x		
17 *Cythereis luzangaziensis*	x—				—cf. x							x			
18 *Cythereis mfoloziensis*				x								x			
19 *Cythereis transkeiensis*								x—x		*		x	x	x	
20 *Gibberleberis africanus*					x—			x—x			x	x	x	x	
21 *Gibberleberis elongata*									x	*			x		
22 *Rayneria nealei*					x—			x—	x	*		x	x	x	
23 *Haughtonileberis haughtoni*	x—				—x			x—x		*	x	x	x	x	
24 *Haughtonileberis fissilis*								x—x		*		x	x	x	
25 *Haughtonileberis vanhoepeni*									x	*			x		
26 *Oertliella pennata*					x—			x—x		*	x	x	x	x	
27 *Oertliella* sp. 476								x—x		*			x		
28 *Paracypris umzambaensis*								x—x		*	x	x	x	x	
29 *Paracypris zululandensis*					x—			x—		*	x	x	x		
30 *Bythocypris richardsbayensis*					x—			x—x		*	x	x	x		
31 *Paraphysocythere thompsoni*								x—x						x	
32 *Veenia obesa*								x—x						x	
33 *Bairdoppilata andersoni*								x—x		*	x	x	x	x	
34 *Cnestocythere?* sp. 2091									x					x	
35 *Pondoina sulcata*								x—x					x	x	
36 *Unicapella stragulata*					x—			x—x			x	x			
37 Indet. sp. 1874								x			x				
38 Indet. sp. 1956					x							x			
39 Indet. sp. 2103								x						x	
40 Indet. sp. 2104								x						x	
41 Indet. sp. 2108								x						x	
42 Indet. sp. 2078									x					x	
43 Indet. sp. 2125								x			x				
44 Indet, sp. 1232					x							x			

	J(c)–1	Cen.–Tur.	Coniacian	Santonian	
45	*Bairdoppilata* sp. 2327	x			
46	*Bairdoppilata* sp. 2322			x	
47	*Bairdoppilata* sp. 2336	x—		—x	
48	*Bythocypris richardsbayensis*	x—		—x	
49	*Cytherella* sp. 2325		x		
50	*Cytherella* sp. 2317			x	
51	*Krithe* sp. 2329	x			
52	*Krithe* sp. 2332	x			
53	*Dutoitella mimica*			x—	*
54	Indet. sp. 2312	x			
55	Indet. sp. 2314	x			

** = Tanzania, * = extension above Santonian III; FB = False Bay, MV = Mfolozi Valley, BH9 = Richards Bay borehole; Um = Umzamba, Ag. Bank = Agulhas Bank.

SAMPLING LOCALITIES

Zululand and Richards Bay

Coniacian and Santonian sediments crop out in river valleys in a north–south swathe along the central part of the Zululand coastal plain between Kwa-Mbonambi in the south (where they are overstepped by Campanian strata), and the Mkuze River in the north. Farther north, along the Pongola River and under the Makatini Flats, no outcrops have been recorded, but they probably underlie Neogene sands. South of Hluhluwe River, Coniacian oversteps the Albian–Cenomanian Mzinene Formation to rest directly on volcanic basement. Kennedy & Klinger (1975) have collected extensively from these exposures, and we have retained their locality and bed-number notation. (Quotation is in the form: locality–bed number/subdivision.) Biostratigraphic subdivision of the two stages follows that of Kennedy & Klinger (1975), and to facilitate international correlation of the ostracod time ranges we quote their ammonite zonation characteristics in Table 2.

South of the Mfolozi valley there are no good natural outcrops, but samples have been obtained from the Richards Bay borehole (BH9), which spans the Santonian–Campanian boundary. At this locality Santonian II rests directly on basement. A similar succession was recorded by Kennedy & Klinger (1975) in an excavation on the Nyokanemi River at Kwa-Mbonambi. These records indicate that Coniacian–Santonian I is missing over a basement feature that Dingle *et al.* (1983) refer to as the Richards Bay Arch. Farther south (Durban), Santonian II is missing, and only Santonian III or Campanian strata are present (Fig. 3).

In Zululand, the Coniacian and Santonian form the lower part of the St. Lucia Formation. It has a basal conglomerate with igneous pebbles, agates, bivalve debris and abundant *Pterotrigonia shepstoni*, but overall consists predominantly of silts with concretionary siltstones and shelly limestones (Kennedy & Klinger 1975; Dingle *et al.* 1983).

Although all the ammonite zones were sampled for ostracods, many of the samples were barren, presumably because of decalcification. The oldest zone that contained ostracods was Coniacian III at locality 16 (28°26,70′S 32°11,42′E), a small quarry on the north side of the Mfolozi River, south of Mtubatuba. Coniacian IV was sampled at locality 15 (28°26,58′S 32°11,40′E) in another small quarry 175 m west of locality 16, and 45 km north-north-east at locality 89 (28°02,27′S 32°21,32′E). The latter consists of hill slopes north of the Hluhluwe River where it debouches into False Bay. No Lower Santonian ostracod-bearing samples were available, but good faunus occurred in samples from outcrops covering the upper part of Santonian II and most of Santonian III. The former are exposed in cliff sections along the western shore of False Bay at locality 74 (27°54,20′S 32°23,78′E). Santonian III faunas were also obtained from locality 74, where the higher beds in the cliff dip to the north-east and crop out along the shore, and at locality 14 (28°28,40′S 32°10,72′E). The latter is near the road

TABLE 2

Kennedy & Klinger's (1975) ammonite zonation of Coniacian to Santonian strata in Zululand.

SANTONIAN

Santonian III

Hauericeras gardeni is abundant. The remainder of the fauna is relatively scarce and is made up of: *Plesiotexanites stangeri* and varieties, *Texanites soutoni, Texanites* spp., *Pseudoschloenbachia, ?Eupachydiscus, Hyphantoceras, Reginaites, Submortoniceras, Bevahites* and diplomoceratids.

Santonian II

Plesiotexanites stangeri and varieties are abundant. The remainder of the fauna consists of: *Texanites soutoni, Texanites* spp., *Hauericeras, Pseudoschloenbachia, ?Eupachydiscus, Hyphantoceras* and diplomoceratids.

Santonian I

Texanites oliveti, Plesiotexanites stangeri, P. densicosta and *P. sparsicosta, Eutexanites, Paratexanites, Hauericeras gardeni, Pseudoschloenbachia, Pseudophyllites indra, ?Karapadites, ?Eupachydiscus, Gaudryceras, Hyphantoceras* and diplomoceratids.

The local base is drawn at the level of the appearance of *Texanites* s.s. in numbers.

CONIACIAN

Coniacian V

Abundant baculitids ornamented only by growth striae. Also forms resembling *Pseudoschloenbachia primitiva* Collignon. *Scaphites, Tetragonites, Protexanites, Texanites* and *Paratexanites* occur.

Coniacian IV

Baculites gr. *capensis* are abundant, and compressed, finely ornamented peroniceratids, *Zuluites* and robustly ornamented *?Gauthiericeras* (e.g. *'Falsebayites', 'Fluminites', 'Hluhluweoceras'* and *'Andersonites'* of Van Hoepen) are locally common. *Tetragonites, Protexanites* and *Paratexanites* also occur.

Coniacian III

Placenticeras, coarsely ornamented peroniceratids *(Zuluiceras), Protexanites, Miotexanites, Paratexanites bailyi, Kossmaticeras* and *?Praemuniericeras* are common.

Coniacian II

Proplacenticeras kaffrarium is abundant. *Peroniceras* gr. *tridorsatum* and *Forresteria* are common. Other types include: *'Eedenoceras' multicostatum, Basseoceras krameri, Kossmaticeras sparsicosta, K. sakondryense, Puzosia* spp., *Pachydesmoceras, Lewesiceras australe, Yabeiceras* spp., *Pseudoxybeloceras matsumotoi, Hyphantoceras reussianum, Allocrioceras* spp., *Baculites bailyi, Scaphites meslei* and *Protexanites.*

Coniacian I

Proplacenticeras kaffrarium is abundant. Other types include *Kossmaticeras theobaldianum, Bostrychoceras indicum, Pachydesmoceras denisonianum* and *Pachydesmoceras* sp.

The local base is drawn at the level of appearance of *Kossmaticeras theobaldianum.*

TURONIAN

No Turonian rocks known from outcrop in Zululand. They occur at depth in boreholes in northern Zululand.

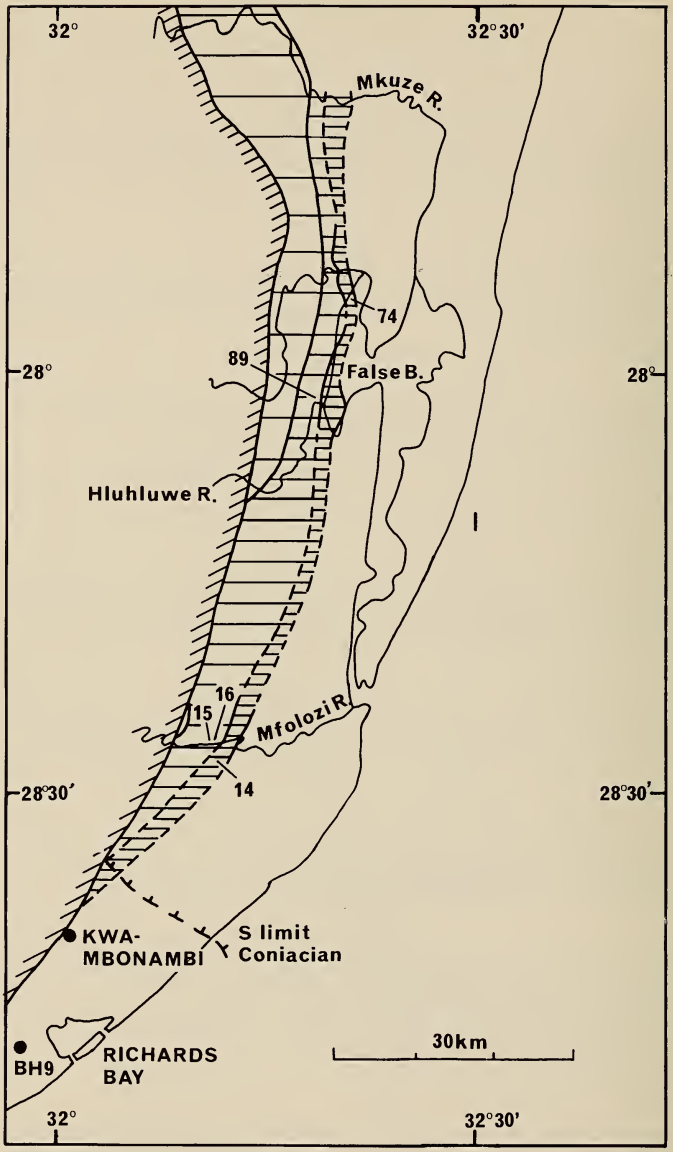

Fig. 2. Sampling localities in Zululand, using the notation of Kennedy & Klinger (1975). See text for co-ordinates and outcrop details. Geology is after Kennedy & Klinger (1975) and Dingle *et al.* (1983) and the key is in Figure 3. BH9 is the Richards Bay borehole.

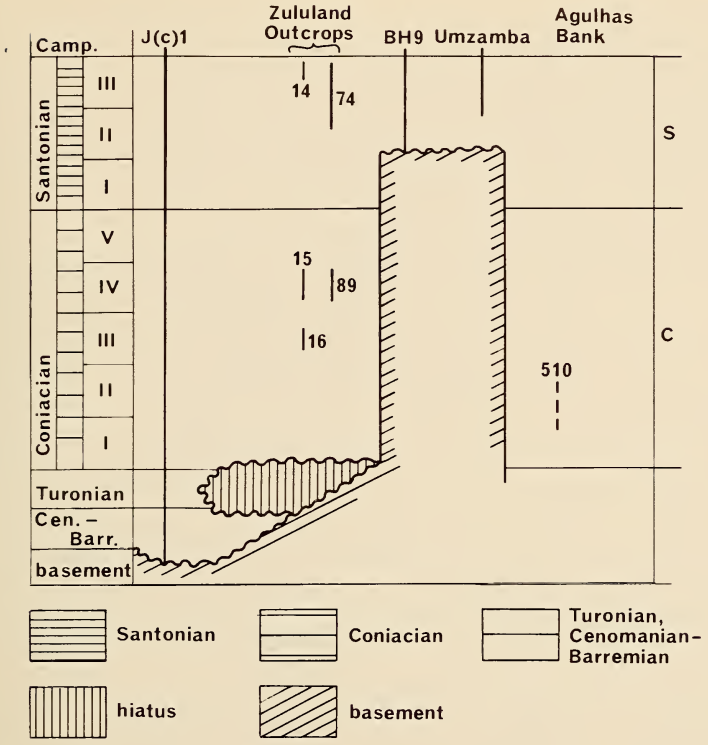

Fig. 3. Correlation chart for sampled sections (see Figs 1 and 2 for locations). Roman numerals indicate ammonite zones after Kennedy & Klinger (1975) (see Table 2 for details). There is some uncertainty as to the ammonite zones represented in the Agulhas Bank outcrops.

bridge over the Msunduzi River due south of River View in the Mfolozi River valley near Mtubatuba.

The Richards Bay borehole BH9 is located at the southern end of the Zululand coastal plain, and 23 cored sections were available for study, covering the whole sequence from immediately above bedrock (Santonian II) to the Santonian–Campanian boundary. The borehole succession and details of sampled horizons are given in Klinger & Kennedy (1977) and Dingle (1980). Ostracods from BH9 have previously been described by Dingle (1980), and serve as an important link between the north Zululand assemblages and the southern assemblages from Umzamba.

Umzamba

The most recent biostratigraphic zonations of this classic locality have been by Klinger & Kennedy (1977, 1980) using ammonites, and Makrides (1979) using foraminifera. Klinger & Kennedy (1980) date the lowermost ammonite-bearing

beds in the Umzamba area (locality C bed 3) as Santonian II (Fig. 4), and place the Santonian II–III boundary within bed 3 at locality A.The latter is the cliff section immediately north of the Umzamba River mouth, from which Dingle (1969) described the ostracods from four horizons, and from which additional material was collected for the present study (31°05,83′S 30°10,50′E). For a comprehensive summary of the stratigraphy and correlation of the Umzamba

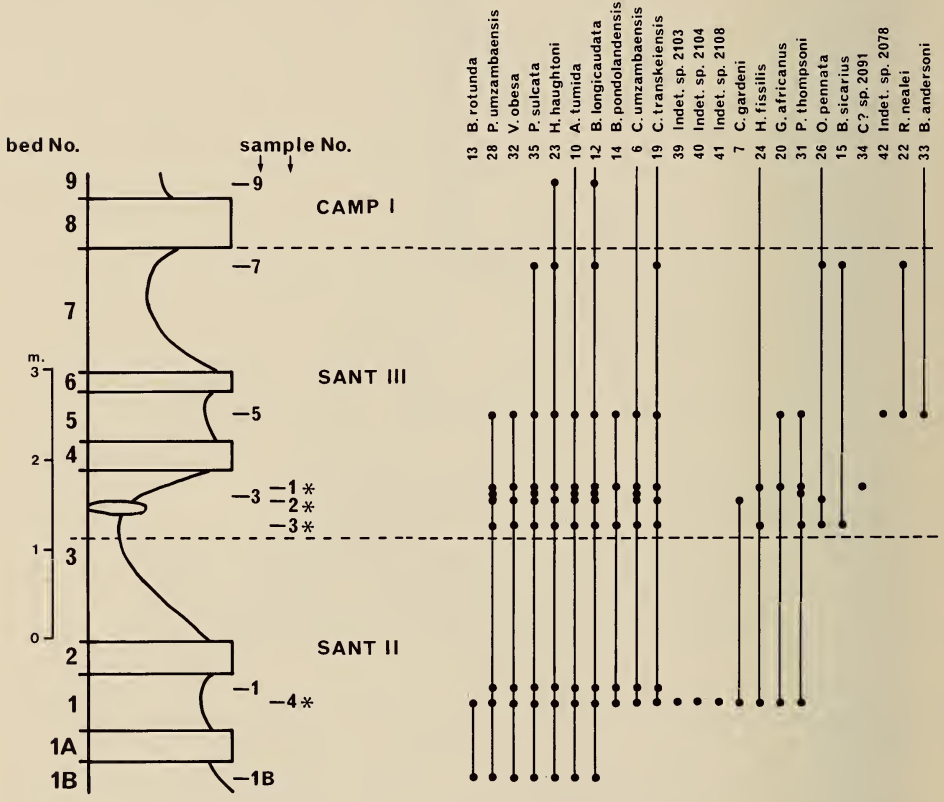

Fig. 4. Measured section at Umzamba Cliff using the bed numbers of Klinger & Kennedy (1980). Ostracod distributions relate to this notation, in addition to that presented by Dingle (1969) (right-hand column, with stars, under 'sample No.'). Ostracod numbers refer to informal taxa numbers on Table 1.

Formation in adjacent outcrops the reader is referred to Dingle *et al.* (1983). It is important to note that at both Umzamba and Richards Bay, Santonian II, which is locally the oldest representative of the Upper Cretaceous transgression, consists of shallow-water sediments deposited in relatively high-energy environments. In contrast, sediments of the same age in north Zululand were probably deposited under relatively deep-water conditions (see Discussion).

Outeniqua Basin (Agulhas Bank)

Three Lower Coniacian samples have been dredged from the western Agulhas Bank during University of Cape Town geological surveys of the sea floor (Fig. 1), and Klinger *et al.* (1976, 1980) have described their ammonite and bivalve faunas (Table 3). One sample (TBD 510) contained ostracods, which were described by Dingle (1971*b*), who quoted a date of Lower–Middle Senonian, based on the presence of the planktonic foraminifera *Globotruncana* sp. ex gr. *G. marginata*, identified by Dr H. P. Luterbacher (University of Tübingen). The ostracods are re-illustrated and their taxonomy is revised.

TABLE 3

Ammonites and bivalves in Lower Coniacian samples from the Agulhas Bank (data from Klinger *et al.* 1976, 1980).

TBD 510: 35°11,70′S 20°30,00′E
Proplacenticeras kaffrarium (Etheridge, 1904)
Scaphites (Otoscaphites?) sp.
TBD 4492: 35°10,00′S 20°53,00′E
Yabeiceras manasoaense Collignon, 1965
TBD 4510: 35°2,50′S 20°39,50′E
Inoceramus (I.) ernsti Heinz, 1928
I. frechi Flegel, 1905

J(c)–1 borehole, offshore Natal

Twenty-five sediment samples (of which 12 contained ostracods) were available from the lower part of the J(c)–1 borehole on the continental shelf off Natal at 29°27,69′S 31°35,66′E in 72 m of water. The borehole penetrated about 2 000 m of Tertiary and Cretaceous strata on the upper part of the Tugela Cone before entering Palaeozoic quartzites, and the section between 2 297 m and 1 927 m (370 m) is considered Upper Cenomanian to Santonian in age (Table 4). The Turonian section (2 197–2 127 m, 70 m) in this borehole is the only one of its age from which material is available in southern Africa. Ostracod faunas from the Campanian to Oligocene sections have previously been described by Dingle (1976, 1981).

PREVIOUS WORK

Chapman's (1904) pioneer work on South African ostracod faunas was undertaken on Santonian material from Umzamba, and was followed by a further publication on a fauna from the same strata in 1923. Unfortunately, all the type material relating to these two studies was destroyed in 1953 (see Dingle 1969 for details). This fact, combined with poor illustrations and ambiguous descriptions in the publications, as well as lack of precise locality details, makes comparative studies with the taxa he identified extremely difficult, and in most cases impossible. Dingle (1969) redescribed the faunas from Santonian II and III strata at the main Umzamba cliff section (Klinger & Kennedy's (1980) locality A), and

TABLE 4

Upper Cenomanian to Santonian ostracods from the J(c)–1 borehole.

Age*	Depth**		Ostracods																		
			Bairdoppilata sp.				*Dutoitella*	*Bythocypris* cf.	*Cytherella* sp.		*Krithe* sp.		Indet.								
	m	ft	2336	2322	2327	Frag.	*mimica*	*richardsbayensis*	2317	2325	2332	2329	sp.	2314	2312	Pyr.	*Ino.*	Charo.			
Sant.	1945	6380															x				
	1981	6500	x	x														x			
	2006	6580															x				
	2018	6620														x	x				
	2030	6660					x	x										x			
	2042	6700							x							x	x				
	2054	6740														x	x				
	2067	6780														x	x				
	2079	6820														x	x				
	2103	6900														x	x				
Con.	2115	6940								x							x				
	2128	6980																			
	2140	7020											x								
	2152	7060			x							x									
Tur.	2176	7140									x		x					x			
	2188	7180																			
	2201	7220										x									
	2213	7260	x					x						x	x						
U. Cen.	2225	7300				x							x								
	2237	7340				x															
	2249	7380																			
	2262	7420																			
	2274	7460																			
	2286	7500											x								
	2297	7540																			
Palaeozoic basement																					

* = stratigraphy after Du Toit & Leith (1974), McLachlan & McMillan (1979), and Dingle *et al.* (1983).
** = original depths in feet shown for correlation with earlier works.
Frag. = fragment, Pyr. = pyrite, *Ino.* = *Inoceramus* prisms, Charo. = charophytes. Indet. sp. refers to various indeterminate fragments

during the course of the present study two additional Santonian II and three Santonian III ostracod-bearing samples were collected. In particular, the upper part of the Santonian III was sampled. The only other descriptions of Santonian ostracods were by Dingle (1980) on the Santonian II and III faunas from the Richards Bay borehole (BH9). There have been no previous published studies on South African Coniacian ostracods, nor on Santonian material from the outcrops in north Zululand.

No Turonian strata are known to crop out in south-east Africa, but details of ostracod populations of this age from Tanzania (Bate & Bayliss 1969) (Table 5), Gabon (Grosdidier 1979), and Brazil and Gabon (Krömmelbein 1964, 1972) form important sources of information for understanding the development of post-mid-Cretaceous ostracod faunas in south-east Africa. Three ostracod-bearing samples of Turonian age were available from the J(c)–1 borehole for the present study.

TABLE 5

Taxa recorded by Bate (*in* Bate & Bayliss 1969) from Tanzania.

A. Sample BM75, Upper Turonian (Luzangazi Stream, north of Wami River).

Ostracoda	Planktonic foraminifera
Cytherura moorei	*Globotruncana helvetica* Bolli
Cytherura luzangaziensis	*Globotruncana linneiana* (d'Orbigny)
Isocythereis sp., Io782	*Globotruncana linneiana coronata* (Bolli)
Curfsina turonica†	*Globotruncana* spp.
Akrogmocythere wamiensis	*Clavihedbergella* sp.
Brachycythere aff. *sapucariensis**†	*Hedbergella delrioensis* (Carsey)
Cythereis luzangaziensis†	*Hedbergella* sp.
Cythereis sp. C, Io793	*Heterohelix* sp.
Paracypris wamiensis	*Praeglobotruncana* sp.
Sphaeroleberis africana	
Cytherella afroturonica	
Cytherelloidea turonica	

* = dominant taxon † = illustrated herein

B. Albian–Cenomanian

Albian	Cenomanian
Ovocytheridea mackinlayi	*Cythereis lindiensis*
Cytherelloidea sp. A	*Cytherella nalukundiensis*
Cythereis sp. A	*Cythereis* sp. B
Cytheropteron africanum	*Cytherelloidea cenomanica*
Cytherella postcontracta	*Majungaella pyriformis*
Majungaella pyriformis	*Cythereis africanus*
Cythereis africanus	
Genus A	
Macrocypris acuticaudata	

A total of 66 fossiliferous samples were available for study (53 from onshore, 12 from the J(c)–1 borehole, and one from the Agulhas Bank), from which 55 species of ostracods have been identified. Microfossils were extracted by washing and sieving, and were photographed with Cambridge S180 and S200 SEMs at the University of Cape Town. Specimens were mounted on double-sided Sellotape or water-soluble glue, and were coated with a gold–palladium mixture. Types and illustrated material are deposited in the South African Museum, Cape Town.

LIST OF GENERA

The genera of Ostracoda discussed in this work are given below:

SYSTEMATIC DESCRIPTIONS

The classification used here is based mostly on the Ostracod *Treatise* (Moore 1961), with various additions necessitated by recent work. Numeric taxonomic categories refer to unique SEM photographic negative numbers in the author's collection.

Abbreviations: ACA = anterior cardinal area; AM = anterior margin; ATE = anterior terminal element; CA = cardinal area; DM = dorsal margin; LV = left valve; MA = marginal area; ME = median element; MPC = marginal pore canal; MS = muscle scars; NPC = normal pore canal; PCA = posterior cardinal area; PM = posterior margin; PTE = posterior terminal element; RV = right valve; SCT = subcentral tubercle; VM = ventral margin.

Subclass OSTRACODA Latreille, 1806
Order PODOCOPIDA Müller, 1894
Suborder PLATYCOPINA Sars, 1866
Family **Cytherellidae** Sars, 1866
Genus *Cytherella* Jones, 1849

Cytherella sp. 1929
Fig. 5A

Remarks

This elongate species with prominent NPC is closest to *Cytherella* morphotype 3 that Dingle (1980) recorded from the Richards Bay borehole. There is a slight difference in their respective AM outlines, but the two may be conspecific.

Age and distribution

Coniacian IV, St. Lucia Formation, locality 15–1 to 15–5, Mtubatuba.

Cytherella sp. 2351
Fig. 5B

Remarks

An inflated species close to *Cytherella* morphotype 4 recorded by Dingle (1980) from the Santonian–Campanian II of the Richards Bay borehole.

Age and distribution

This species occurs consistently, though in small numbers, throughout the Santonian II–III section at locality 74, False Bay.

Cytherella sp. 2325
Fig. 5C

Remarks

A single broken carapace that has a vertically expanded, laterally compressed anterior area, an arched DM, and a convex VM.

Age and distribution

Coniacian, J(c)–1 borehole, 2115 m (6940 ft).

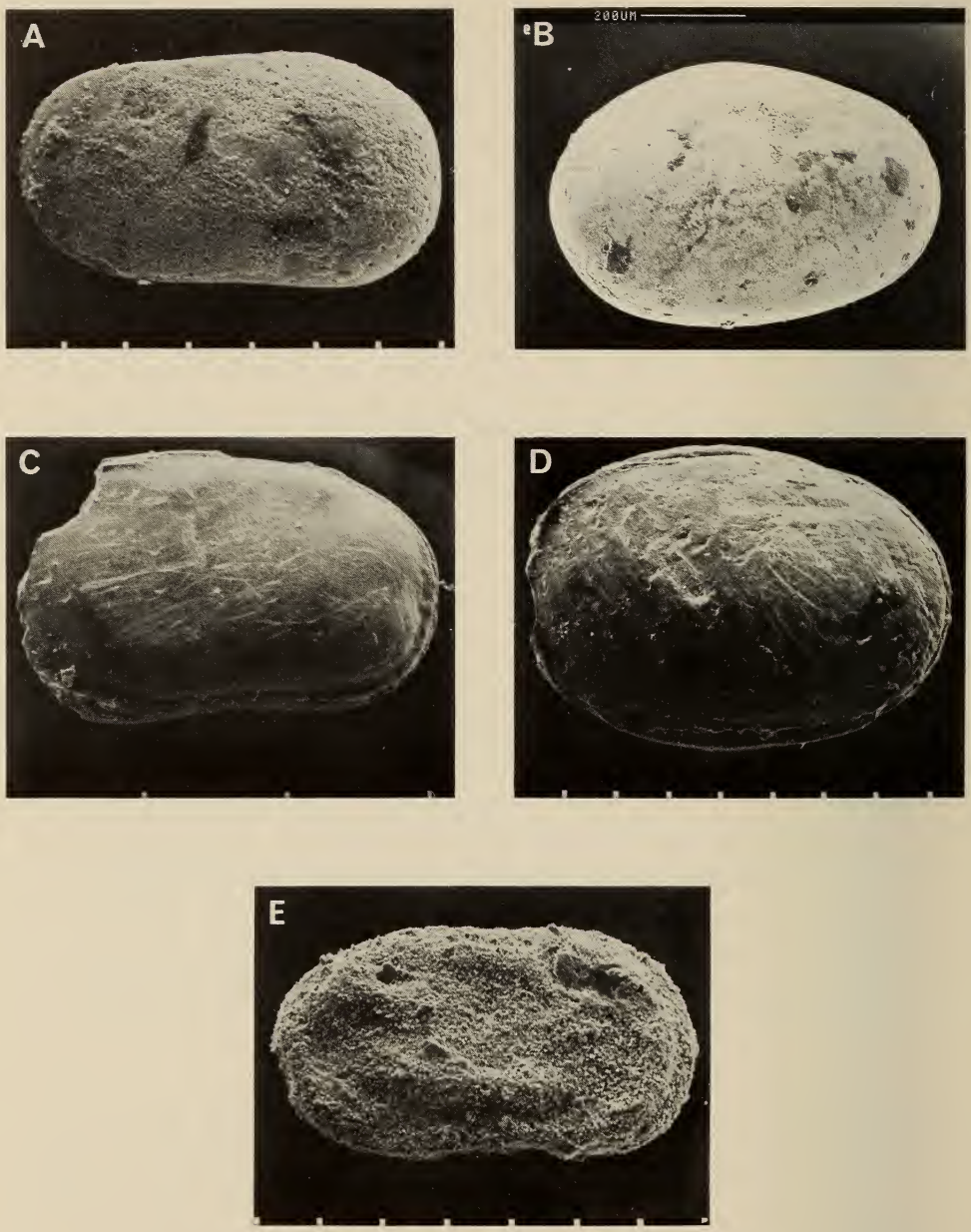

Fig. 5. A. *Cytherella* sp. 1929, SAM–PC6485, LV, locality 15–5, Mtubatuba, Coniacian IV. B. *Cytherella* sp. 2351, SAM–PC6486, RV, locality 74–9, False Bay, Santonian III. C. *Cytherella* sp. 2325, SAM–PC6487, LV, J(c)–1 borehole, 2 115 m, Coniacian. D. *Cytherella* sp. 2317, SAM–PC6488, LV, J(c)–1 borehole, 2 042 m, Santonian. E. *Cytherelloidea mtubaensis* sp. nov., SAM–PC6489, holotype, RV, locality 15–1, Mtubatuba, Coniacian IV, SEM 1954. Scale bars: A, D–E = 100 μ, B = 200 μ, C = 300 μ.

Cytherella sp. 2317

Fig. 5D

Remarks

A single carapace of an ovate species that is similar in outline to *Cytherella* morphotype 2 recorded by Dingle (1980) from the Santonian–Campanian II of the Richards Bay borehole.

Age and distribution

Santonian, J(c)–1 borehole, 2042 m (6700 ft).

Cytherella sp. 1–4 Dingle, 1980

Cytherella spp. 1, 2, 3, & 4. Dingle, 1980: 5–7, fig. 2A–F.
Cytherella sp. Dingle, 1981: 15–17, fig. 5A–F.

Remarks

Dingle (1980) recognized four morphotypes of *Cytherella* that he originally placed in separate categories, but subsequently gathered into one taxonomic unit because it was not possible to consistently discriminate the various valve outlines (Dingle 1981). See Dingle (1980) for representative illustrations.

Age and distribution

Examples of the four morphotypes occur sporadically throughout the Santonian II–III section of the Richards Bay borehole, but only appear in significant numbers in the Campanian. They range upwards into the Maastrichtian III, and two specimens of *Cytherella* (spp. 1929 and 2351) recorded from the Coniacian and Santonian II–III of Zululand outcrops during the present study may be conspecific. Better-quality material and larger populations need to be studied before further progress can be made in resolving the taxonomy of the Upper Cretaceous *Cytherella* species in Zululand.

Genus *Cytherelloidea* Alexander, 1929

This genus is the only one that is well represented above and below the mid-Cretaceous (Turonian–Coniacian) non-sequence in southern Africa, although none of its species range across the hiatus: seven species Berriasian to Cenomanian; seven species Coniacian to Maastrichtian. Of the seven post-Cenomanian species, three appear in the Coniacian (*C. mtubaensis, C. newtoni*, and *C. umzambaensis*); two in the Santonian (*C. gardeni* and *C. griesbachi*); and two in the Campanian (*C. contorta* and *C. mfoloziensis*) (Fig. 6).Three species (*C. mtubaensis, C. newtoni*, and *C. gardeni*) are restricted to Coniacian–Santonian strata, and only one has a relatively long range (*C. umzambaensis*—Coniacian IV to Campanian IV). *Cytherelloidea* is, therefore, a potentially useful genus for biostratigraphic work in the south-east African Coniacian to Maastrichtian sediments.

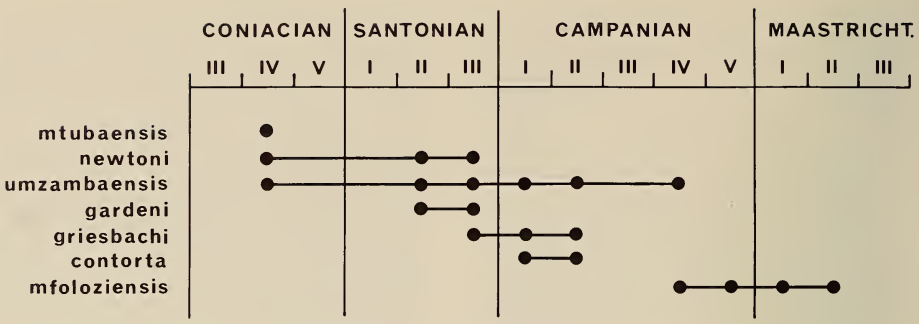

Fig. 6. Ranges of *Cytherelloidea* species in Upper Cretaceous strata of south-east Africa.

Cytherelloidea mtubaensis sp. nov.
Fig. 5E, 7A

Derivation of name

The name *mtubaensis* is derived from the type locality name Mtubatuba, Zululand.

Holotype

SAM–PC6489, RV, locality 15–1, Mtubatuba, Coniacian IV.

Diagnosis

Species with a continuous anterior, ventral, and posteroventral ridge; short elliptical ventromedian and dorsomedian to posterodorsal elevations.

Descriptions

External features. Broadly rounded AM and PM, straight to slightly convex DM, and a weakly concave VM. Surface elevations consist of a continuous, but relatively weak ridge that runs from the anterodorsal area via the VM to about mid-height on the PM. There is a prominent, short pseudo-elliptical ventromedian elevation and an irregular, continuous series of elevations and ridges in the dorsomedian to posterodorsal region. The most prominent part of the latter is at its posterior end. Surface otherwise apparently smooth.

No internal views seen.

Remarks

Only *C. griesbachi* Dingle, 1980 (Santonian III to Campanian III) has a surface rib pattern that is likely to be confused with that of *C. mtubaensis* (Fig. 7), because both have prominent short ventromedian elevations. However, the former has no ribs or elevations that run parallel to the PM, and has a ridge that is continuous around the DM and AM.

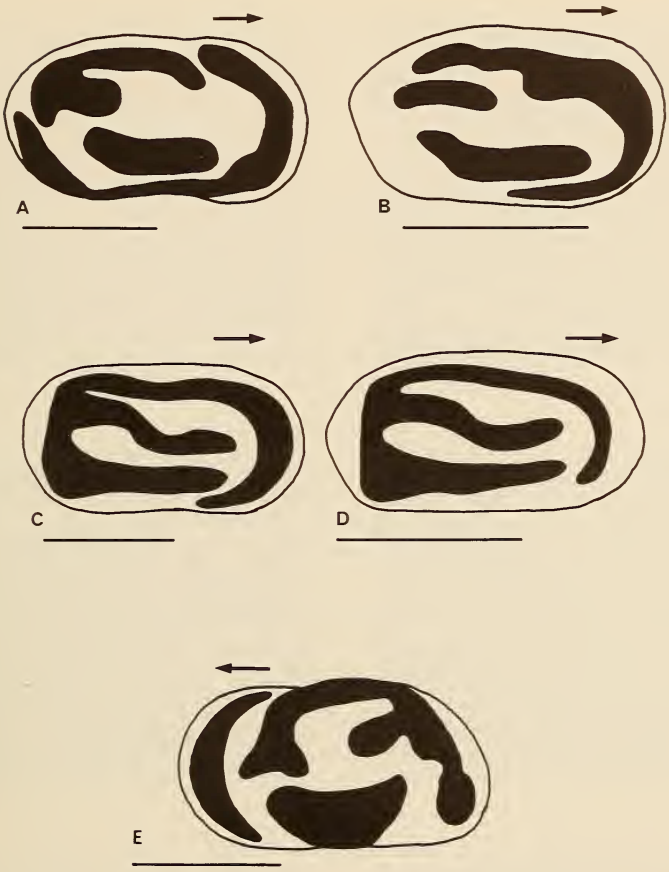

Fig. 7. Sketches of *Cytherelloidea* species, with positive features shaded. A. *C. mtubaensis* sp. nov., SAM–PC6489, holotype, RV, locality 15–1, Mtubatuba, Coniacian IV. B. *C. griesbachi*, holotype, SAM–K5575, RV, BH9 Richards Bay, 88,39 m, Campanian II. C. *C. umzambaensis*, SAM–PC6492, RV, locality 15–7, Mtubatuba, Coniacian IV, SEM 1953. D. *C. umzambaensis*, SAM–PC6491, RV, Umzamba bed 1, Santonian II, SEM 710. E. *C. newtoni*, SAM–PC6490, LV, locality 15–5, Mtubatuba, Coniacian IV, SEM 1919. Scale bars = 300 μ.

Dimensions (mm)

	length	height
PC6489	0,68	0,36

Age and distribution

Cytherelloidea mtubaensis is known only from the Coniacian IV at locality 15–1 at Mtubatuba, Zululand.

Cytherelloidea newtoni Dingle, 1980

Figs 7E, 8A–B

Cytherelloidea newtoni Dingle, 1980: 8–10, figs 3C, 4C.

Remarks

Small numbers of this distinctive species have been recorded from outcrops at Mtubatuba and False Bay, which show no significant morphological differences from the type material of the Richards Bay borehole.

Age and distribution

Cytherelloidea newtoni ranges Coniacian IV (Mtubatuba) to Santonian III (BH9 and False Bay). In the Richards Bay borehole it occurred in sediments deposited in environments that are thought to have ranged from shallow water, high energy, restricted circulation, through shallow water (<100 m), low energy, restricted circulation, to shallow, low-energy, open water (<100 m) (Dingle 1980). *Cytherelloidea newtoni*, although relatively rare, is probably a good stratigraphic indicator for Zululand Coniacian to Santonian strata.

Cytherelloidea umzambaensis Dingle, 1969

Figs 7C–D, 8C–D

Cytherella williamsoniana (*non* Jones, 1849) Chapman, 1904: 236.
Cytherelloidea umzambaensis Dingle, 1969: 351–353, fig. 3; 1980: 7, figs 3A, 4A–B; 1981: 18, figs 7A, 9C.

Remarks

This species is one of the distinctive elements of the Upper Cretaceous ostracod faunas of south-east Africa, and displays a high degree of morphological stability throughout its range. The median longitudinal ridge does show some variability in elevation along the section anterior of the MS depression.

Age and distribution

Cytherelloidea umzambaensis ranges Coniacian IV (Mtubatuba) to Campanian IV (Nibela Peninsula) at outcrop in Zululand, Santonian II to Campanian II in BH9, and Santonian II to Campanian I at Umzamba (type locality). Its distribution in the Richards Bay borehole suggests that it preferred quiet, moderate-depth (100–300 m) environments, but was tolerant of both shallow (<100 m), high-energy and deep (>500 m), low-energy situations.

Cytherelloidea gardeni Dingle, 1971

Fig. 8E–F

non *Cytherelloidea delicata* Dingle, 1969: 353–354, fig. 4.
Cytherelloidea gardeni Dingle, 1971*a*: 353.
Cytherelloidea cf. *C. gardeni* Dingle, 1980: 7.

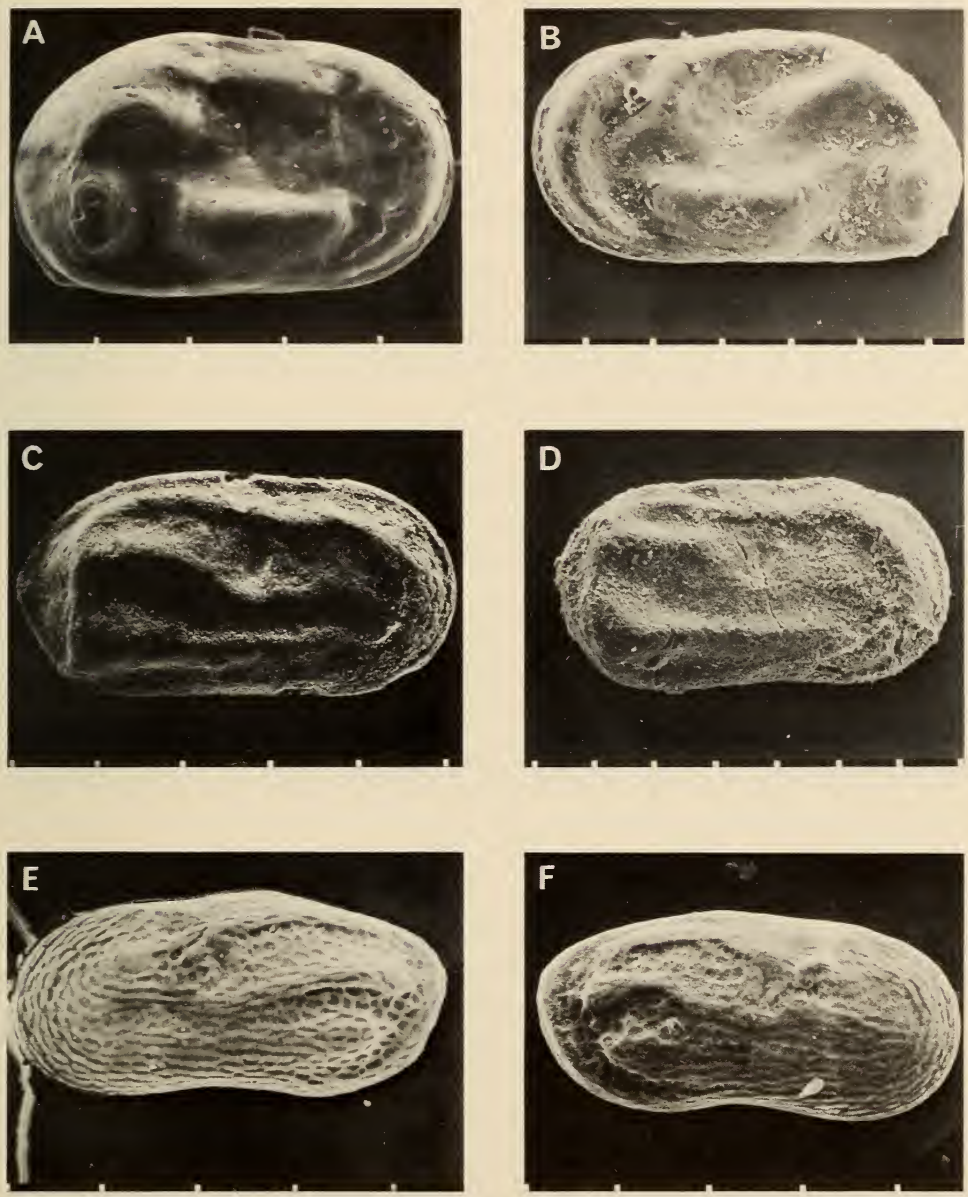

Fig. 8. Genus *Cytherelloidea*. A. *C. newtoni*, SAM–K5574, holotype, RV, BH9 Richards Bay, 120,22 m, Santonian III, SEM 720. B. *C. newtoni*, SAM–PC6490, LV, locality 15–5, Mtubatuba, Coniacian IV, SEM 1919. C. *C. umzambaensis*, SAM–PC6491, RV, Umzamba bed 1, Santonian II, SEM 710. D. *C. umzambaensis*, SAM–PC6492, RV, locality 15–7, Mtubatuba, Coniacian IV, SEM 1953. E. *C. gardeni*, SAM–PC6493, LV, Umzamba bed 3, Santonian III, SEM 714. F. *C. gardeni*, SAM–PC6494, RV, Umzamba bed 3, Santonian III, SEM 717. Scale bars = 100 μ.

Remarks

No additional specimens of this distinctive species have been found in the Zululand outcrops. SEM photographs of Santonian II topotypic material from Umzamba are included here to supplement the inadequate original illustrations by Dingle (1969). The longitudinal rib pattern in the posterior part of the valve is very similar to that of *C. griesbachi*, but the two species have a different valve outline (*C. gardeni* is distinctly elongate), and *C. gardeni* is overall delicately reticulate.

Age and distribution

Cytherelloidea gardeni ranges Santonian II to Santonian III in the Umzamba cliff section, and one specimen was recorded in the lower part of Santonian III in the Richards Bay borehole (BH9).

Cytherelloidea griesbachi Dingle, 1980

Fig. 7B

Cytherelloidea griesbachi Dingle, 1980: 10–11, figs 3B, 4D.

Remarks

A rare species whose rib pattern has similarities with that of *C. mtubaensis*.

Age and distribution

Cytherelloidea griesbachi ranges uppermost Santonian III to Campanian II in the Richards Bay BH9 borehole. One specimen was recorded by Dingle (1980) from Santonian III at Umzamba.

Suborder PODOCOPINA Sars, 1866

Superfamily BAIRDIACEA Sars, 1888

Family **Bairdiidae** Sars, 1888

Genus *Bairdoppilata* Coryell, Sample & Jennings, 1935

Bairdoppilata andersoni Dingle, 1980

Fig. 9A–C

Bairdoppilata andersoni Dingle, 1980: 12–14, fig. 5A–F; 1981: 25–29, figs 11A–D, 13A–B.

Remarks

Specimens from Santonian Zululand outcrops have a prominent posterior beak, but can be accommodated within the intraspecific morphological variations encountered from other areas.

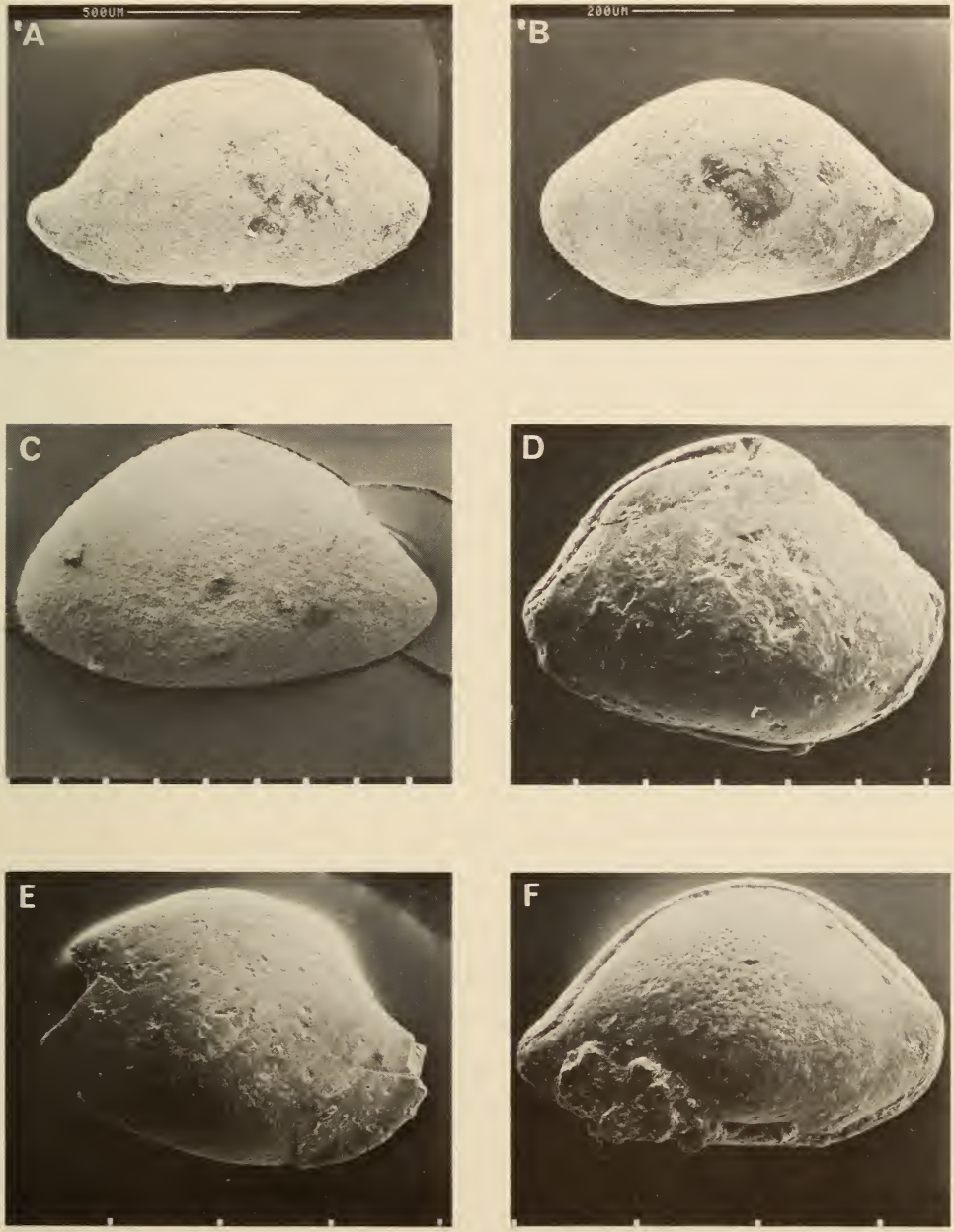

Fig. 9. Genus *Bairdoppilata*. A. *B. andersoni*, SAM–PC6495, LV, locality 74–15, Mtubatuba, Santonian III, SEM 2352. B. *B. andersoni*, SAM–PC6496, RV, BH9 Richards Bay, 139,8 m, Santonian III, SEM 2344. C. *B. andersoni*, SAM–PC6497, RV, Umzamba bed 5, Santonian III, SEM 2076. D. *Bairdoppilata* sp. 2322, SAM–PC6498, LV, J(c)–1 borehole, 1 981 m, Santonian. E. *Bairdoppilata* sp. 2327, SAM–PC6499, LV, J(c)–1 borehole, 2 152 m, Turonian, SEM 2328. F. *Bairdoppilata* sp. 2336, SAM–PC6500, LV, J(c)–1 borehole, 2 213 m, Upper Cenomanian, SEM 2335. Scale bars: A = 500 μ, B = 200 μ, C–D = 100 μ, E–F = 300 μ.

Age and distribution

Bairdoppilata andersoni is one of the temporally and spatially most widespread ostracod taxa in south-east Africa, but is numerically rare in the Santonian strata of Richards Bay, Zululand, and Umzamba. It is known to range Santonian II–Campanian II in BH9, Santonian III–Campanian I at Umzamba, Santonian III–Maastrichtian II (Zululand), and occurs in Maastrichtian III on the Agulhas Bank.

Bairdoppilata sp. 2322

Fig. 9D

Remarks

One badly worn carapace that is probably conspecific with *B.* cf. *africana*, which was illustrated by Dingle (1981, fig. 12F). *Bairdoppilata* cf. *africana* was recorded from Campanian–Maastrichtian sections of the J(c)–1 borehole.

Age and distribution

Santonian, J(c)–1 borehole, 1 981 m (6 500 ft).

Bairdoppilata sp. 2327

Fig. 9E

Remarks

A broken valve whose affinities to other members of the genus in the J(c)–1 borehole are not clear.

Age and distribution

Turonian, J(c)–1 borehole, 2 152 m (7 060 ft).

Bairdoppilata sp. 2336

Fig. 9F

Remarks

Two punctate carapaces of a species that is more elongate than *Bairdoppilata* sp. 2322 and *B.* cf. *africana*.

Age and distribution

Upper Cenomanian–Santonian, J(c)–1 borehole, 2 213 m and 1 981 m (7 260 ft and 6 500 ft).

Genus *Bythocypris* Brady, 1880

Bythocypris richardsbayensis Dingle, 1980

Fig. 10A–B

Bythocypris richardsbayensis Dingle, 1980: 14–16, fig. 6A–E; 1981: 31, fig. 14A–C.

Remarks

This species is sparsely distributed throughout the Coniacian–Santonian strata of south-east Africa, but the oldest recorded specimens show no significant morphological differences from the type specimens (Campanian), or younger material. *Bythocypris richardsbayensis* only becomes abundant in the deeper-water, post-Santonian sediments.

Age and distribution

Coniacian IV–Maastrichtian II (Zululand outcrops), Maastrichtian III (Agulhas Bank), Santonian II–Campanian II (Richards Bay borehole). So far, no specimens have been recorded from Umzamba, presumably because of the shallow-water environments that prevailed there.

Bythocypris cf. *richardsbayensis*

Fig. 10C–D

Remarks

Two carapaces (one crushed) of a species with a similar lateral outline to *B. richardsbayensis*.

Age and distribution

Upper Cenomanian–Santonian, J(c)–1 borehole, 2213 m and 2030 m (7260 ft and 6660 ft).

Superfamily CYPRIDACEA Baird, 1845

Family **Paracyprididae** Sars, 1923

Genus *Paracypris* Sars, 1866

Paracypris zululandensis Dingle, 1980

Fig. 10F

Paracypris zululandensis Dingle, 1980: 17–19, figs 7D–G, 9B; 1981: 35, fig. 16D.

Remarks

Paracypris zululandensis occurs consistently, but in small numbers, in the Coniacian and Lower Santonian strata of the Mfolozi and False Bay areas of Zululand. Dingle (1980) recorded a similar distribution in the Santonian of BH9, but noted that the species becomes relatively more abundant in the deeper-water Campanian section of the borehole.

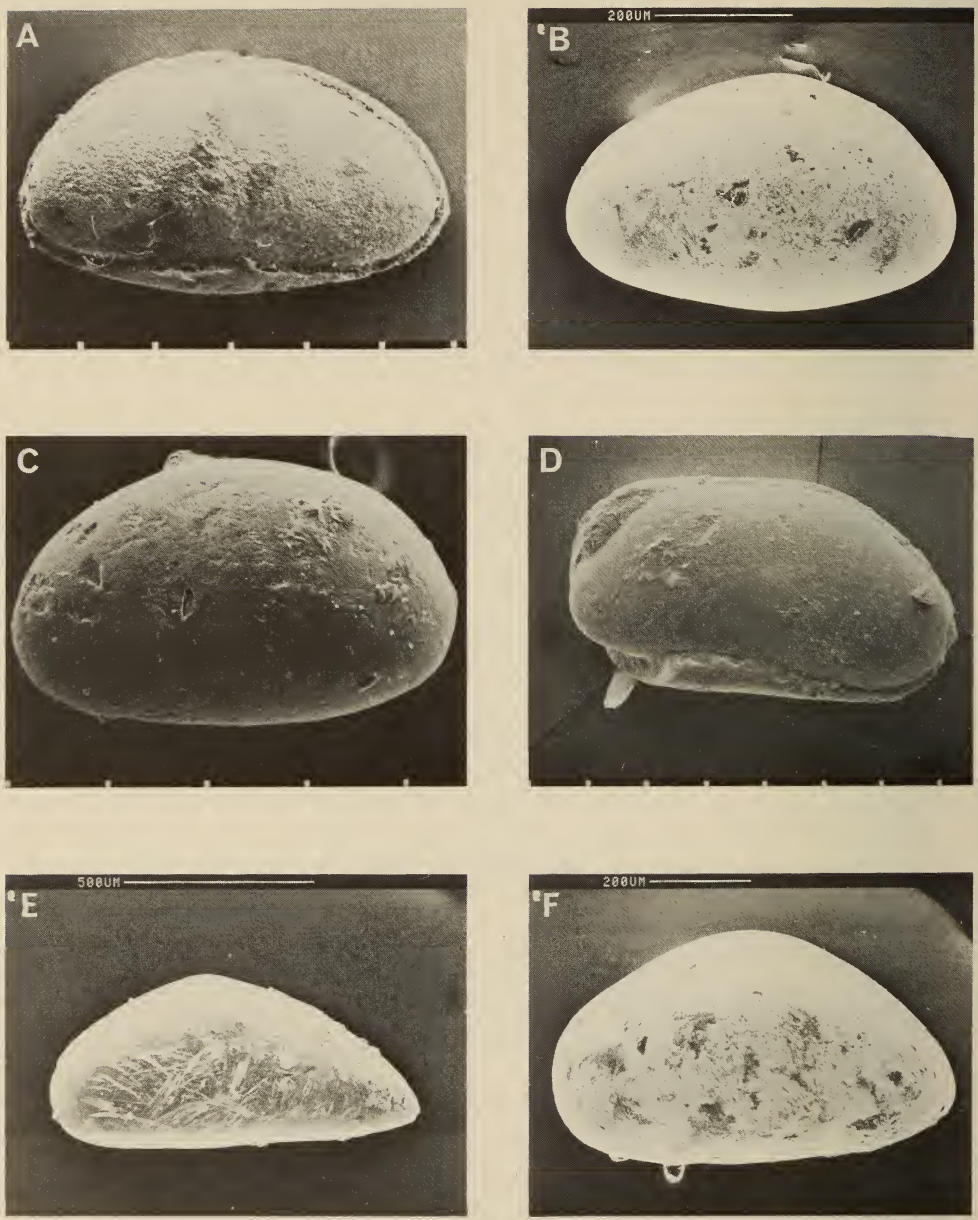

Fig. 10. A. *Bythocypris richardsbayensis*, SAM–PC6501, RV, locality 15–5, Mtubatuba, Coniacian IV, SEM 2133. B. *Bythocypris richardsbayensis*, SAM–PC6502, LV, BH9 Richards Bay, 142,0 m, Santonian III, SEM 2345. C. *Bythocypris* cf. *richardsbayensis*, SAM–PC6503, RV, J(c)–1 borehole, 2 030 m, Santonian–Coniacian, SEM 2324. D. *Bythocypris* cf. *richardsbayensis*, SAM–PC6504, RV, J(c)–1 borehole, 2 213 m, Upper Cenomanian, SEM 2337. E. *Paracypris umzambaensis*, SAM–PC6506, RV, locality 74–11/2, False Bay, Santonian II–III, SEM 2354. F. *Paracypris zululandensis*, SAM–PC6505, RV, locality 74–11/2, False Bay, Santonian II–III, SEM 2348. Scale bars: A, C, D = 100 μ, B, F = 200 μ, E = 500 μ.

Age and distribution

Coniacian IV to ?Maastrichtian I at outcrop in Zululand (Mfolozi and False Bay), Santonian II to Campanian II in the Richards Bay borehole, and Maastrichtian III, Agulhas Bank. Not found at Umzamba.

Paracypris umzambaensis Dingle, 1969

Fig. 10E

Macrocypris simplex (*non* Chapman, 1898) Chapman, 1904: 233, pl. 29 (fig. 22).
Paracypris? umzambaensis Dingle, 1969: 354–356, fig. 5.
Paracypris umzambaensis Dingle, 1980: 17, figs 7A–C, 9A; 1981: 34–35, fig. 16A–C.

Remarks

Paracypris umzambaensis occurs sporadically in the False Bay area, but becomes more abundant farther south, where it is consistently present in small numbers throughout the Richards Bay borehole, and at Umzamba. At the latter locality, it occurs to the exclusion of its close relative *P. zululandensis*. Dingle (1981) suggested that *P. umzambaensis* was more tolerant of deep-water conditions than *P. zululandensis*.

Age and distribution

Santonian III to Maastrichtian II at outcrop in Zululand (False Bay), Santonian II to Campanian II in BH9, Santonian II–III at Umzamba, and late Campanian–early Maastrichtian at Igoda (near East London).

Superfamily CYTHERACEA Baird, 1850

Family **Cytherideidae** Sars, 1925

Genus *Pondoina* Dingle, 1969

Two species of this genus have been recognized in southern Africa: *P. sulcata* (Santonian) and *P. igodaensis* (late Campanian–early Maastrichtian), whilst Krömmelbein (1972) recorded *?Pondoina* sp. from the Turonian Sibang Formation of Gabon, and the ?Coniacian Macau Formation of north-east Brazil. This suggests a Turonian to late Campanian–early Maastrichtian range for the genus. No species referable to the genus was recorded from the Turonian to Maastrichtian of Tanzania by Bate & Bayliss (1969). A link might have been expected in view of the close similarity in some other species between south-east Africa and Tanzania.

Pondoina sulcata Dingle, 1969

Fig. 11A–F

Pondoina sulcata Dingle, 1969: 356–358, fig. 6; 1980: 20, fig. 9C.

Remarks

SEM photographs of topotypic specimens are included here to supplement the original description. In particular, attention is drawn to the strongly

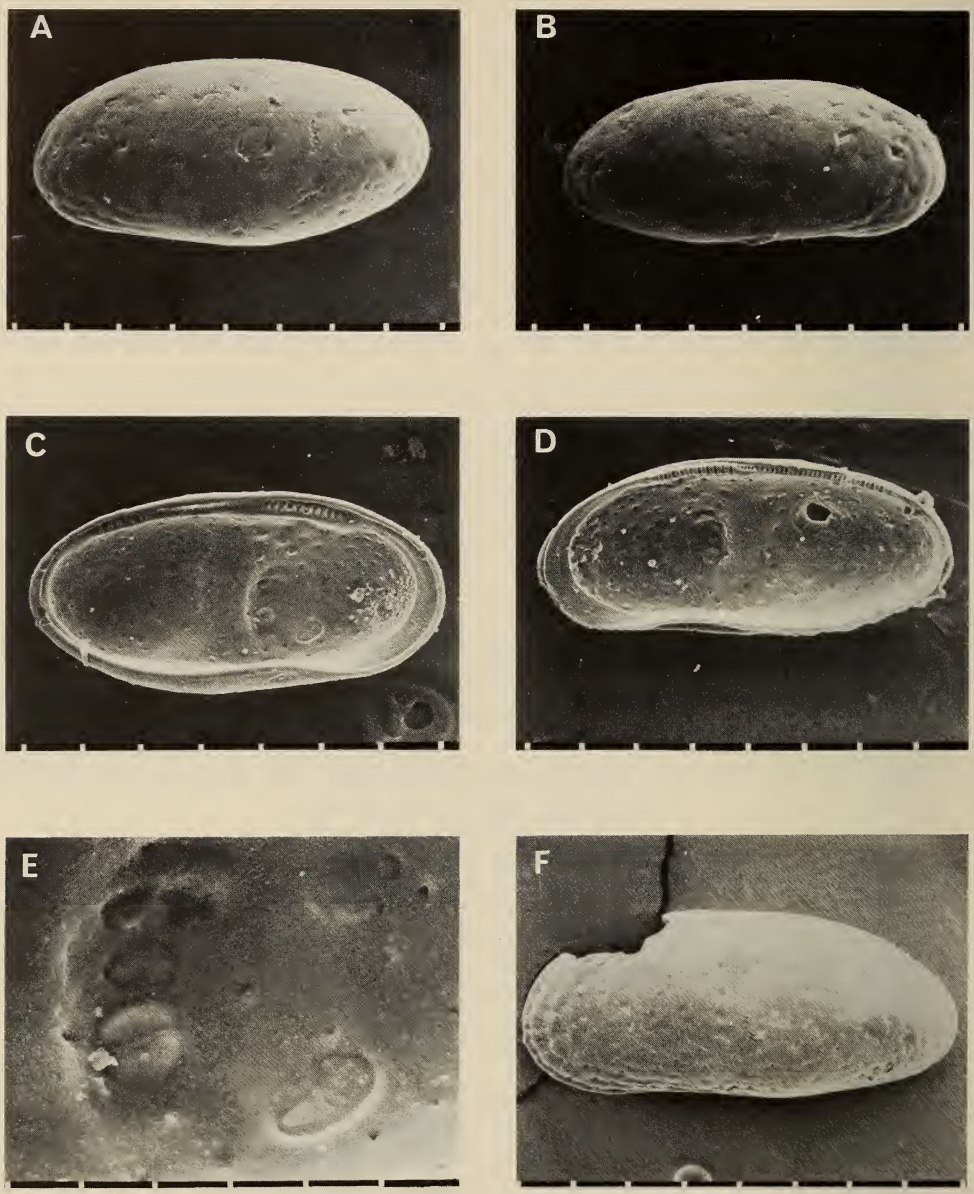

Fig. 11. *Pondoina sulcata*, Umzamba, Santonian III. A. SAM–PC6507, LV, bed 3, SEM 570. B. SAM–PC6508, RV, bed 3, SEM 572. C. SAM–PC6509, internal LV, bed 3, SEM 561. D. SAM–PC6510, internal RV, bed 3, SEM 554. E. SAM–PC6509, muscle scars, LV, bed 3, SEM 569. F. SAM–PC6511, bed 7, SEM 2086.
Scale bars: A–D, F = 100 μ, E = 30 μ.

antimerodont hinge, difference in lateral outline between LV and RV, and the MS (which has a distinctive 'clover-leaf' arrangement of the dorsal two elements of the adductors, and the divided antennal scar).

Age and distribution

Pondoina sulcata ranges Santonian II to Santonian III in its type section at Umzamba, and occurs in small numbers in the lower part of Santonian III in the Richards Bay borehole.

Family **Schizocytheridae** Mandelstam, 1960

Genus *Amphicytherura* Butler & Jones, 1957

Amphicytherura tumida Dingle, 1969

Fig. 12A–E

Amphicytherura (Amphicytherura) tumida Dingle, 1969: 368–370, fig. 13; 1980: 20–21, fig. 10A–F; 1981: 49–50, figs 23C, 25A.

Remarks

This species has not been found at outcrop in Zululand, although it is relatively common in BH9 and at Umzamba, where it can be used as a zone fossil at the top of Santonian III. Some specimens from Santonian III at Umzamba have a slightly extended AM outline compared to the topotypic material in Santonian II.

Age and distribution

Santonian II–Campanian I at Umzamba and Richards Bay borehole.

Genus *Apateloschizocythere* Bate, 1972

Apateloschizocythere? cf. *mclachlani* Dingle, 1981

Fig. 12F

?Amphicytherura sp. Dingle, 1971*b*: 404–405, fig. 7.

Remarks

The five small and poorly preserved specimens recorded by Dingle (1971*b*) have been photographed with SEM. Although generic assignment is still uncertain, they are very similar to a species described by Dingle (1981: 54–57, fig. 26A–B) from the Campanian III of Zululand. The genus has also been recorded from the Maastrichtian III of the Agulhas Bank (*Apateloschizocythere laminata* (Dingle, 1971*b*)).

Age and distribution

Lower Coniacian, sample TBD 510, Alphard Formation, Agulhas Bank.

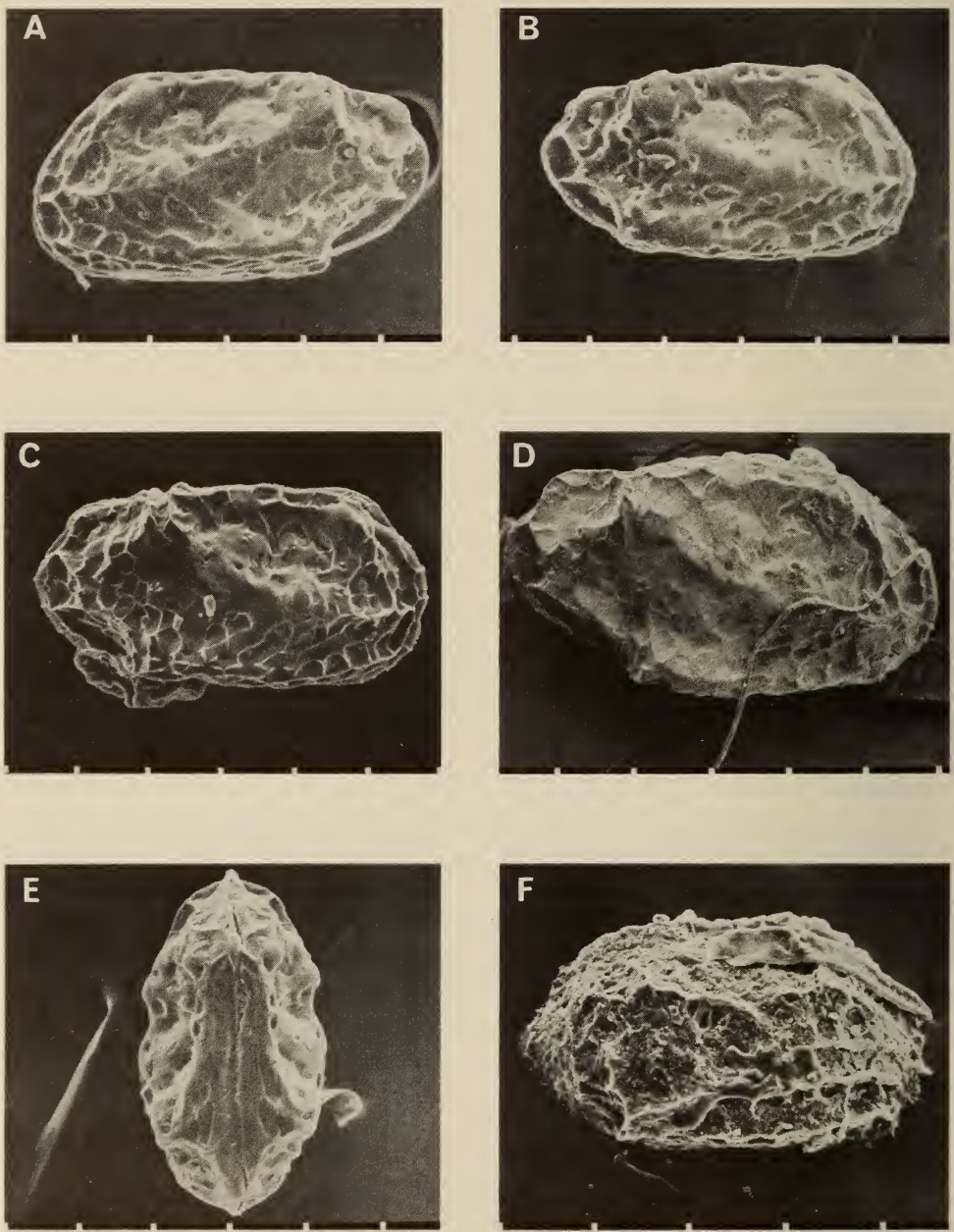

Fig. 12. A–E. *Amphicytherura tumida*. A. SAM–PC6512, LV, Umzamba bed 3, Santonian III, SEM 295. B. SAM–PC6513, RV, Umzamba bed 3, Santonian III, SEM 298. C. SAM–K5594, RV, BH9 Richards Bay, 125,0 m, Santonian III, SEM 317. D. SAM–PC6514, RV, Umzamba bed 3, Santonian III, SEM 2059. E. SAM–PC6515, carapace, dorsal view, Umzamba bed 3, Santonian III, SEM 299.
F. *Apateloschizocythere?* cf. *mclachlani* SAM–PC6516, RV, TBD 510, Agulhas Bank, Alphard Formation, Lower Coniacian, SEM 1882.
Scale bars = 100 μ.

Genus *Cnestocythere* Triebel, 1950

Cnestocythere? sp. 2091

Fig. 13A–B

?Cnestocythere sp. Dingle, 1969: 370–371, fig. 14.

Remarks

This specimen was illustrated by Dingle (1969), but SEM photographs show the hinge to be damaged, so that it may not originally have been merodont. This casts further doubt upon its generic placement. No further specimens of this species have been recovered. An SAM serial number (PC6517) has been allocated to the original specimen, which supersedes UCT number MG–1–2–10.

Age and distribution

Santonian III, Umzamba.

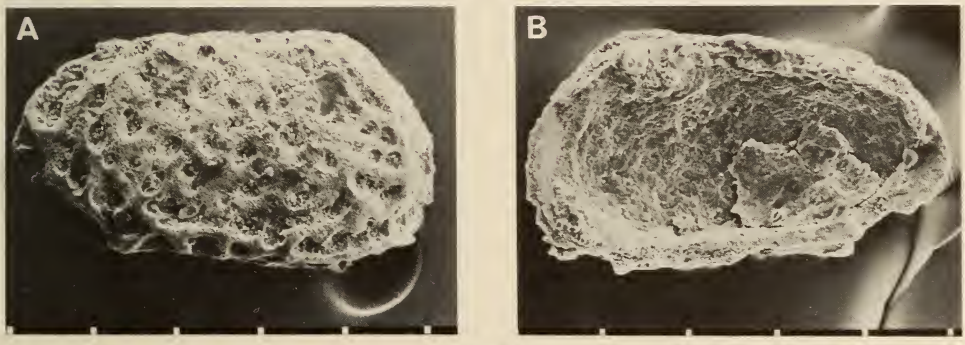

Fig. 13. *Cnestocythere?* sp. 2091, SAM–PC6517, Umzamba bed 3, Santonian III. A. External RV, SEM 2091. B. Internal RV, SEM 2155. Scale bars = 100 μ.

Family **Brachycytheridae** Puri, 1954

Genus *Brachycythere* Alexander, 1933

Brachycythere is one of the key genera for an understanding of the routes and timing of ostracod population movements from the Equatorial Atlantic into the South Gondwana province after the mid-Cretaceous hiatus. In southern Africa, five species have been recognized: two appear in the Coniacian (*B. longicaudata* and *B. agulhasensis*); and three appear in the Santonian (*B. sicarius, B. pondolandensis*, and *B. rotunda*).

Fourteen species of *Brachycythere* have so far been recorded from Africa, and a further seven from nearby areas in the Middle East. Their ranges have been plotted in Table 6, outlines of holotypes and topotypes are illustrated in Figure 14, and their length/height scattergrams are shown in Figure 15. The earliest records are in Cenomanian strata: *B.* cf. *sapucariensis* (Tunisia—Bismuth *et al.* 1981); *B.* gr. *sapucariensis* (Gabon—Grosdidier 1979); *B. sapucariensis* by Schaller (1969, reported in Reyment 1980*a*) from north-east Brazil; and *B.* aff. *ekpo* (Morocco—Oertli 1963). *Brachycythere sapucariensis* and closely related forms have been widely reported from north-east Brazil and various localities in equatorial, west and north Africa, as far east as Tunisia, and range into the Coniacian. As will be discussed below, it is closely related to the main southern African species (*B. longicaudata*). The only other widely reported species is *B. angulata* from Egypt (Turonian), Nigeria (Coniacian), Senegal and Lebanon (Coniacian–Santonian), Cameroon (Santonian), and Israel (Santonian to Maastrichtian).

For the present investigation, it is important to note that the genus *Brachycythere* was well represented in the Equatorial Atlantic and North Africa (probably five species) by Cenomanian–early Turonian times, but that no species of the genus occur in southern Africa or any other South Gondwana locality before the local mid-Cretaceous non-sequence. This hiatus locally ranges in age from late Cenomanian to late Turonian or early Coniacian.

Brachycythere longicaudata (Chapman, 1904)

Figs 16A–D, 17A–D

Cytheridea longicaudata Chapman, 1904: 234–235, pl. 39 (fig. 21). Howe & Laurencich, 1958: 279.

Cythere ?drupracea (*non* Jones, 1884) Chapman, 1904: 234.

Brachycythere longicaudata (Chapman) Dingle, 1969: 358–361, fig. 7; 1980: 25–26, figs 12A–C, 13A–D; 1981: 71–72, fig. 34B–C.

Brachycythere aff. *sapucariensis* Krömmelbein, 1964, Bate, 1969, in Bate & Bayliss: 137–138, 164, pl. 7 (fig. 1) (*partim* (BMNH Io790)).

Remarks

Specimens collected from Coniacian outcrops in Zululand plot within the overall species field on a length/height scattergram, but overlap the subfields of Santonian and Campanian–Maastrichtian material (Fig. 15). This distribution illustrates one aspect of the considerable intraspecific morphological variation that is apparent within the species *B. longicaudata*: generally Santonian specimens are larger and more elongate, whereas the Campanian–Maastrichtian individuals are smaller and somewhat squatter. The new Coniacian samples suggest that the earliest representatives were similar in character to the Campanian varieties and that environmental conditions during Santonian times were favoured by larger and more elongate varieties. Although individuals within the overall Coniacian to Maastrichtian populations could be assigned to separate

TABLE 6

Temporal distribution of the genus *Brachycythere* in Cretaceous strata of Africa and surrounding areas.

Species	Reference	Locality	Cen. L M U	Tur. L U	Coniacian I II III IV V	Santon. I II III	Campanian I II III IV V	Maastr. I II III
gr. *sapucariensis*	Krömmelbein, 1964	G, T, B						
aff. *ekpo*	Oertli (1963)	M						
ledaforma	Masoli (1966)	M						
gr. *angulata*	Grekoff, 1951	A, L, C, S, E, Is						
dumoni	Bismuth & St. Marc, 1981*	T						
longicaudata	This paper	SA, Tz						
agulhasensis	Dingle, 1971*b*	SA						
ekpo	Reyment, 1960	N, E, Is						
IRC 28	Grosdidier, 1973	I						
IRH 34	Grosdidier, 1973	I						
IRE 10	Grosdidier, 1973	I						
IRJ 9	Grosdidier, 1973	I						
IRJ 10	Grosdidier, 1973	I						
sicarius	Dingle, 1980	SA						
pondolandensis	Dingle, 1969	SA						
rotunda	Dingle, 1969	SA						
IRE 5	Grosdidier, 1973	I						
beershevaensis	Honigstein, 1983	Is						
kulatturensis	Guha, 1971	In						
gr. *carinata*	Gowda, 1966	In						
armata	Reyment, 1960	N						
oguni	Reyment, 1960	N						
sp. indet	Reyment, 1960	N						

Notes:

1. *Brachycythere* gr. *sapucariensis* includes cf., aff., as described by: Grosdidier (1979), Bismuth *et al.* (1981), Krömmelbein (1976), Neufville (1973), Reyment (1960).
2. *Brachycythere* gr. *angulata* includes aff.,?, as described by: Grekoff (1951, 1969), Reyment (1960), Apostolescu (1963), Van den Bold (1964), Damotte & St. Marc (1972), Honigstein (1983).
3. *Brachycythere longicaudata* includes Bate (1969).
4. *Brachycythere ekpo* includes cf. Van den Bold (1964), Honigstein (1983).

* = in Bismuth *et al.* 1981.

Abbreviations:
A = Algeria, B = Brazil, C = Cameroon, E = Egypt, G = Gabon, I = Iran, In = India, Is = Israel, L = Lebanon, M = Morocco, N = Nigeria, S = Senegal, SA = South Africa, T = Tunisia, Tz = Tanzania.

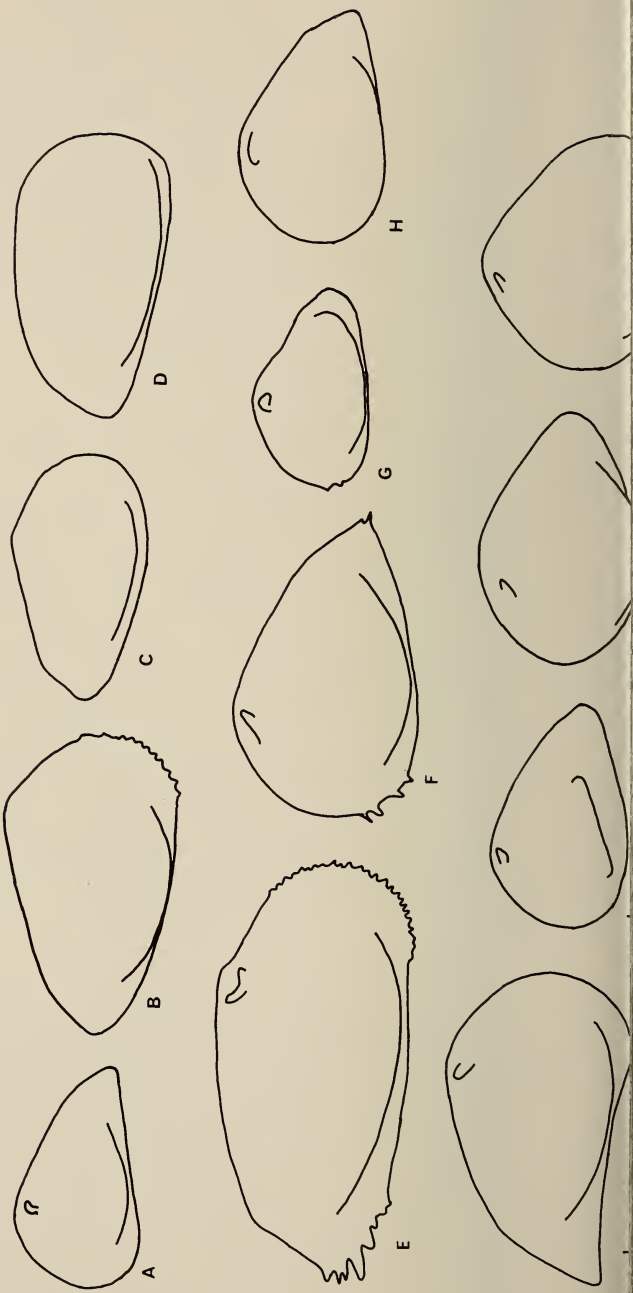
A
B
C
D
E
F
G
H

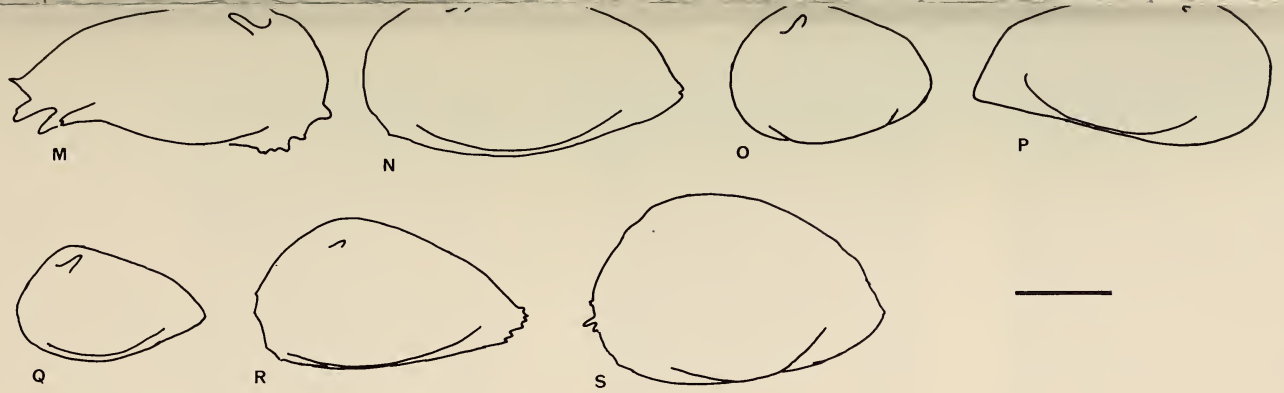

Fig. 14. Comparative outlines of type specimens of *Brachycythere* species from the middle and late Cretaceous of Africa and adjacent areas. See Table 6 for ranges and authorship.
A = *B. sapucariensis*, B = *B. ledaforma*, C = *B. angulata*, D = *B. dumoni*, E = *B. longicaudata*, F = *B. agulhasensis*, G = *B. ekpo*, H = *Brachycythere* IR C28, I = *Brachycythere* IR H34, J = *Brachycythere* IR E10, K = *Brachycythere* IR J9, L = *Brachycythere* IR J10, M = *B. sicarius*, N = *B. pondolandensis*, O = *B. rotunda*, P = *Brachycythere* IR E5, Q = *B. kulatturensis* (not to scale), R = *B. armata*, S = *B. oguni*.
Scale bar = 300 μ.

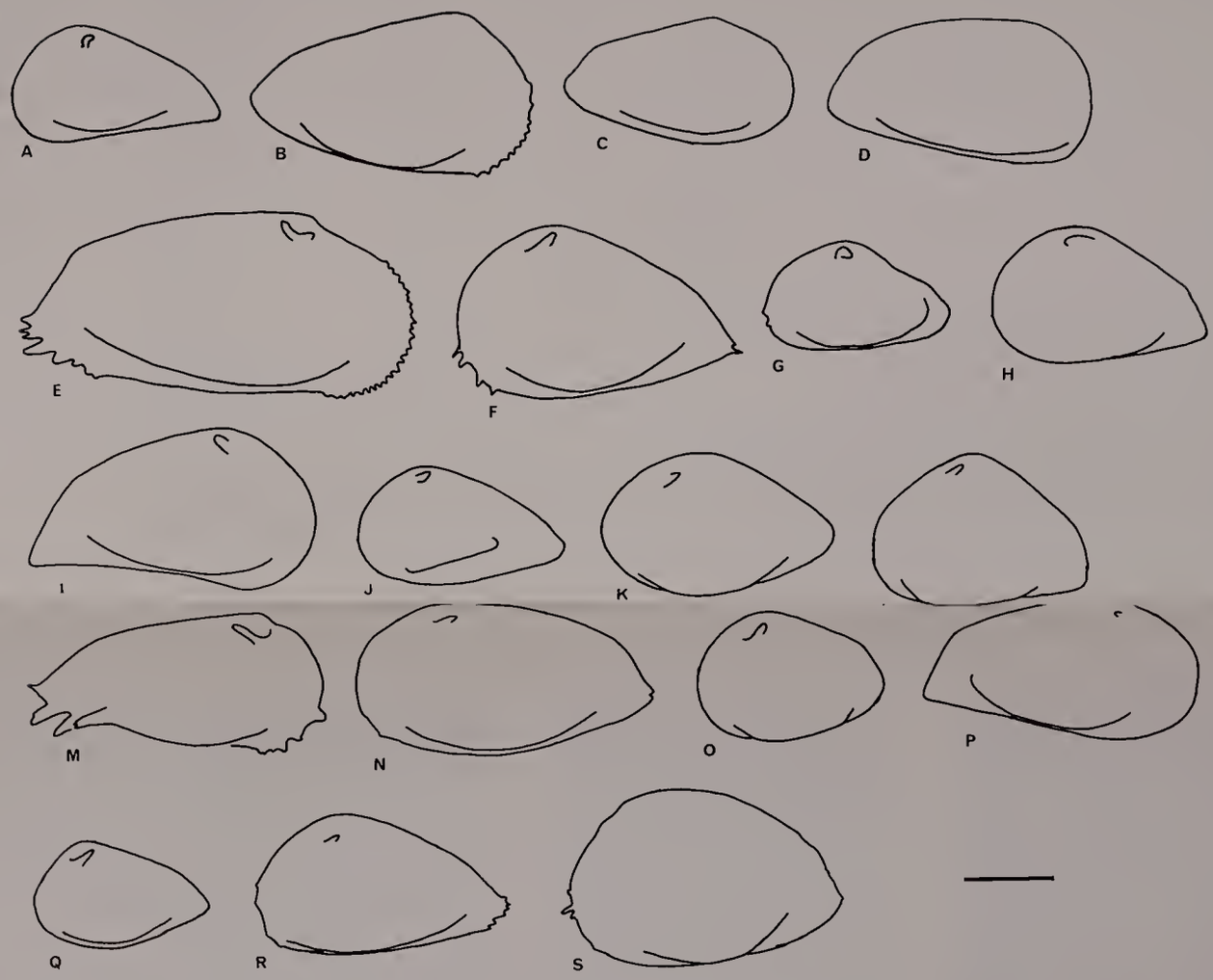

Fig. 14. Comparative outlines of type specimens of *Brachycythere* species from the middle and late Cretaceous of Africa and adjacent areas. See Table 6 for ranges and authorship.
A = *B. sapucariensis*, B = *B. ledaforma*, C = *B. angulata*, D = *B. dumoni*, E = *B. longicaudata*, F = *B. agulhasensis*, G = *B. ekpo*, H = *Brachycythere* IR C28, I = *Brachycythere* IR H34, J = *Brachycythere* IR E10, K = *Brachycythere* IR J9, L = *Brachycythere* IR J10, M = *B. sicarius*, N = *B. pondolandensis*, O = *B. rotunda*, P = *Brachycythere* IR E5, Q = *B. kulatturensis* (not to scale), R = *B. armata*, S = *B. oguni*.
Scale bar = 300 μ.

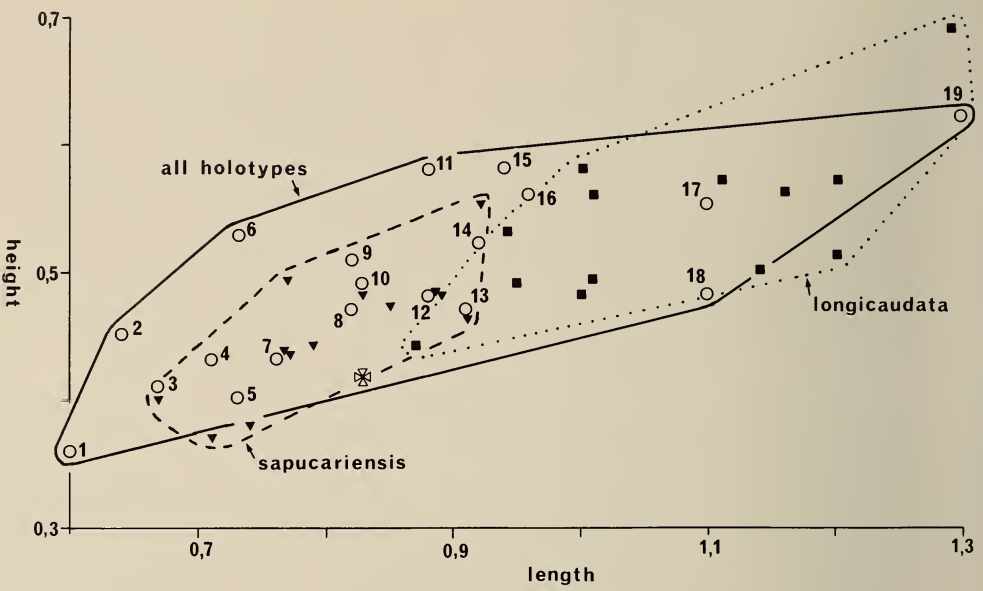

Fig. 15. Length/height scattergram (in mm) of specimens of *Brachycythere*. Solid line and circles = type specimens from the middle and late Cretaceous of Africa and adjacent areas; dashed line and triangles = specimens of *B. sapucariensis* reported in the literature; maltese cross = specimens reported as *B.* aff. *sapucariensis* by Bate & Bayliss (1969).
Key to species: 1 = *B. ekpo*, 2 = *B. rotunda*, 3 = *Brachycythere* IR E10, 4 = *Brachycythere* IR C28, 5 = *B. angulata*, 6 = *Brachycythere* IR J10, 7 = *B. sapucariensis*, 8 = *B. armata*, 9 = *B. kulatturensis*, 10 = *Brachycythere* IR J9, 11 = *B. oguni*, 12 = *B. dumoni*, 13 = *Brachycythere* IR E5, 14 = *B. ledaformis* (as reported by Masoli (1966)), 15 = *B. agulhasensis*, 16 = *Brachycythere* IR H34, 17 = *B. pondolandensis*, 18 = *B. sicarius*, 19 = *B. longicaudata*.

morphotypes on the grounds of lateral outline, such subdividsion has been found impractical because the bulk of the populations would then fall into intermediate categories. In terms of lateral outline (regardless of valve size) this poses problems in discriminating *B. longicaudata* from certain other species, notably *B. sapucariensis*.

On a length/height scattergram of holotypic (and neotypic) specimens of *Brachycythere* from Africa and adjacent areas, the types of *B. longicaudata* and *B. sapucariensis* are widely separated, and in lateral outline are clearly differentiated (Fig. 17). This distinction is also seen in other points of morphological difference: curvature of AM, shape of VM, shape and spinosity of posteroventral area. The two types are Santonian and Coniacian age, respectively. However, several other workers have reported Krömmelbein's Brazilian species from localities in west and north Africa, and if representatives of these materials are compared in shape (but not size) to the general population of *B. longicaudata*, the distinctions become blurred. On a length/height scattergram the *B. sapucariensis*-related specimens plot to the left of the *B. longicaudata* populations and in comparison with other *Brachycythere* type specimens their

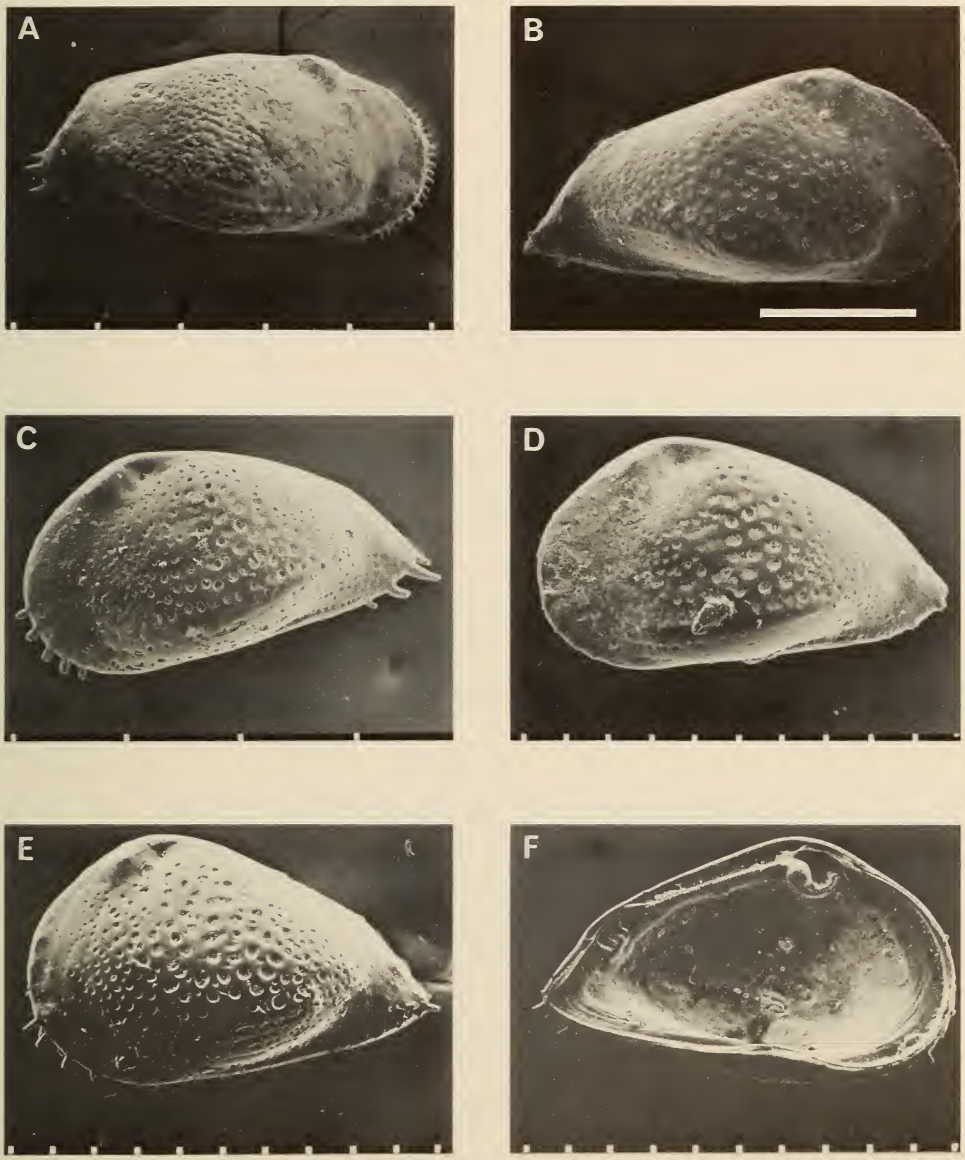

Fig. 16. A–D. *Brachycythere longicaudata*. A. SAM–PC6518, neotype, RV, Umzamba bed 1, Santonian II, SEM 2089. B. BMNH Io790, RV, Wami River area, Luzangazi Stream, Tanzania, Upper Turonian, SP7/848. C. SAM–PC6519, LV, locality 16–1, Mtubatuba, Coniacian III, SEM 1939. D. SAM–PC6520, LV, locality 15–5, Mtubatuba, Coniacian IV, SEM 1922. E–F. *Brachycythere agulhasensis*, TBD 510, Agulhas Bank, Alphard Formation, Lower Coniacian. E. SAM–PC6522, holotype, LV, SEM 1806. F. SAM–PC6542, internal LV, SEM 1807. Scale bars: A–C = 300 μ, D–F = 100 μ.

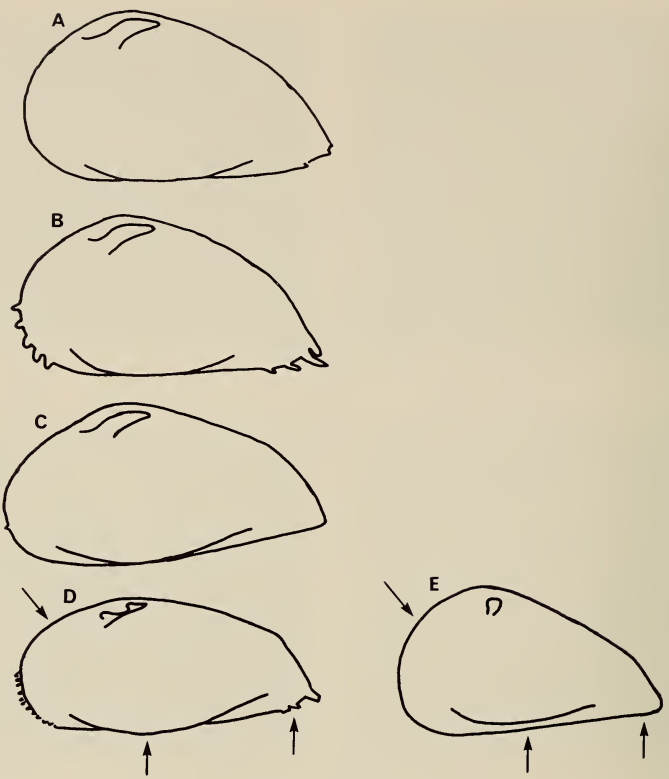

Fig. 17. Outline of *Brachycythere* species, LV. A–D. *B. longicaudata*. A. SAM–PC6520, locality 15–5, Mtubatuba, Coniacian IV, SEM 1922. B. SAM–PC6519, locality 16–1, Mtubatuba, Coniacian III, SEM 1939. C. SAM–K5604, BH9 Richards Bay, 92,27 m, Campanian I, SEM 549. D. SAM–PC6521, Umzamba bed 3, Santonian III, SEM 534. E. *B. sapucariensis*, SMF Xe2990, holotype, Aracaju, Brazil, Coniacian. Arrowed locations show significant differences in lateral outline between *B. longicaudata* and *B. sapucariensis*.

field includes the holotypes of *B. angulata* Grekoff, *B. armata* Reyment, *B. kulatturensis* Guha, and *B. dumoni* Bismuth & St. Marc, as well as several of the morphotypes recorded by Grosdidier (1979) from Iran. At this stage, with the exception of the topotypic material illustrated by Krömmelbein (1964), no consistent subdivision can be made between many members of the two populations other than one based on overall size.

Bate (*in* Bate & Bayliss 1969) recorded *B.* aff. *sapucariensis* from the Upper Turonian of Tanzania. In the subsequent discussion to this paper, Bate (p. 164) compares his specimen more closely with *B. longicaudata*. An SEM photograph of the more elongate specimen recorded by Bate (BMNH Io790) (Fig. 16B) confirms this closeness, and I regard this as the earliest record of Chapman's species.

Age and distribution

The uncertainty engendered by the apparent wide intraspecific morphological variations within *B. sapucariensis* and *B. longicaudata* make temporal and spatial ranges difficult to assign. The type specimens come from the Coniacian Sapucari Formation, eastern Brazil, and Santonian II at Umzamba, respectively. It should be noted that Krömmelbein (1964) originally considered the Brazilian material to be Lower Turonian in age, but has since revised his estimate to Coniacian (?Lower) (Krömmelbein 1976: 543–544).

Taken at face value, the reported distribution of *B. sapucariensis* is Lower Cenomanian to ?Lower Coniacian, with the earliest records from Gabon and Morocco. *Brachycythere longicaudata* has its earliest record in the Upper Turonian of Tanzania, and in southern Africa is known to range Coniacian III (locality 16–1, Mtubatuba) to Maastrichtian II (Nibela) in Zululand, and farther south an incomplete range of Santonian II to Campanian I is recorded at Umzamba. It occurs in the late Campanian–early Maastrichtian at Igoda. The species has not been recorded from the Agulhas Bank (although no Santonian or Campanian faunas have yet been described from this area).

Brachycythere agulhasensis Dingle, 1971

Figs 16E–F, 18A

Brachycythere agulhasensis Dingle, 1971*b*: 399–400, fig. 3.

Remarks

No further specimens of this species have been encountered. SEM photographs of the holotype are included here, and some of the points on which *B. agulhasensis* differs from *B. longicaudata* are emphasized: it has a shorter, but more massive hinge with a particularly deep, rounded ATE, a coarsely crenulate ME, and a relatively short, high PTE; a coarse surface reticulation, and a relatively low length/height ratio (1,61 cf. mean 2,02 for all specimens of *B. longicaudata* plotted on Figure 15). The holotype, originally designated MG–2–1–25, has been transferred to the South African Museum under the number SAM–PC6522.

Age and distribution

Brachycythere agulhasensis is known only from the Lower Coniacian Alphard Formation of the Agulhas Bank (sample TBD 510).

Brachycythere sicarius Dingle, 1980

Fig. 18B

Brachycythere sicarius Dingle, 1980: 27–29, figs 13F, 14A–F; 1981: 72–73, fig. 35A.

Fig. 18. *Brachycythere*. A. *B. agulhasensis*, SAM–PC6522, holotype, MS, LV, TBD 510, Agulhas Bank, Alphard Formation, Lower Coniacian, SEM 1809. B. *B. sicarius*, SAM–PC6523, RV, Umzamba bed 3, Santonian III, SEM 2058. C. *B. pondolandensis*, SAM–PC6524, holotype, LV, Umzamba bed 1, Santonian II, SEM 2112. D. *B. pondolandensis*, SAM–PC6525, RV, Umzamba bed 1, Santonian II, SEM 2115. E. *B. rotunda*, SAM–PC6526, holotype, LV, Umzamba bed 1, Santonian II, SEM 2092. F. *B. rotunda*, SAM–PC6527, RV, Umzamba bed 1B, Santonian II, SEM 2049.
Scale bars: A = 30 μ, B–C = 300 μ, D–F = 100 μ.

Remarks

Morphological similarities suggest that *B. sicarius* evolved from *B. longicaudata* in early Santonian times. It shows a similar range of intraspecific variations to its progenitor, in addition to which the earliest populations suggest that, as in the case of *B. longicaudata*, they lie at the elongate end of the length/height scattergram.

Age and distribution

Santonian II (Richards Bay BH9 borehole) to Maastrichtian I (outcrops) in Zululand, and Santonian III at Umzamba.

Brachycythere pondolandensis Dingle, 1969

Figs 18C–D, 19

Brachycythere pondolandensis Dingle, 1969: 361–362, fig. 8.

Remarks

The holotype and one paratype are re-illustrated here with SEM photographs, which emphasize the fine ribbing and foveolate-like ornamentation of the anterior and posterior regions of this distinctive, but rare, species. The MS pattern is unusual in having a subdivided top scar in the adductor set (Fig. 19). New numbers have been allocated to the re-illustrated specimens following their transfer to the South African Museum: holotype (MG–1–1–6) = SAM–PC6524; paratype (MG–1–1–8) = SAM–PC6525.

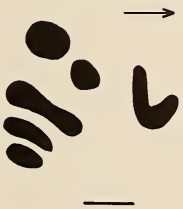

Fig. 19. Muscle scars of *Brachycythere pondolandensis*, SAM–PC6581, LV, Umzamba bed 3, Santonian III, SEM 529. Scale bar = 30 μ.

Age and distribution

Brachycythere pondolandensis has a restricted range in time and space: it occurs in Santonian II and III strata only at Umzamba and Richards Bay BH9 borehole. No specimens were recovered from the Santonian locality 74 (False Bay), but as noted previously (Dingle 1980), the species appears to be particularly susceptible to decalcification and is often poorly preserved in otherwise

well-preserved faunas. Potentially, *B. pondolandensis* is a good Santonian zone fossil for south-east Africa south of 29°S.

Brachycythere rotunda Dingle, 1969

Fig. 18E–F

Brachycythere rotunda Dingle, 1969: 362–363, fig. 9.

Remarks

SEM stereopairs of the holotype show it to have a shallow longitudinal median depression in the vicinity of mid-length, a faint, coarse, widely-spaced reticulate ornamentation in a posteromedian position, a deep circular ocular depression flanked posteriorly by a lateral cheek, and a marked, almost alate upswing of the VM at its posterior extremity. A relatively well-preserved specimen from the lowest Santonian beds at Umzamba is also assigned to the species. It has a coarse reticulate ornament in the posterior area, and a median longitudinal depression. In Figure 15, *B. rotunda* plots to the left-hand side of the length/height scattergram, where it is well displaced from the *B. longicaudata* field, and lies closest to the types of *B. ekpo* and *Brachycythere* sp. IR E10. The holotype, originally designated MG–1–2–2, has been transferred to the South African Museum under the number SAM–PC6526.

Age and distribution

Brachycythere rotunda is rare and is known only from the Santonian II at Umzamba.

Family **Collisarborisidae** Neale, 1975

Genus *Paraphysocythere* Dingle, 1969

Paraphysocythere thompsoni Dingle, 1969

Fig. 20A–C

Paraphysocythere thompsoni Dingle, 1969: 365–366, fig. 11.

Remarks

SEM photographs of topotypic material are included here to supplement the original descriptions. In particular, attention is drawn to the delicate rib pattern in the anterior area and the overall fine intercostal reticulation.

Age and distribution

Although additional material has been collected since Dingle's (1969) original records, neither the spatial nor temporal range of this species has been extended. It is known only from the Santonian II to III of Umzamba. This distribution suggests that it may be a good zone fossil for Santonian strata in south-east Africa south of about 31°S.

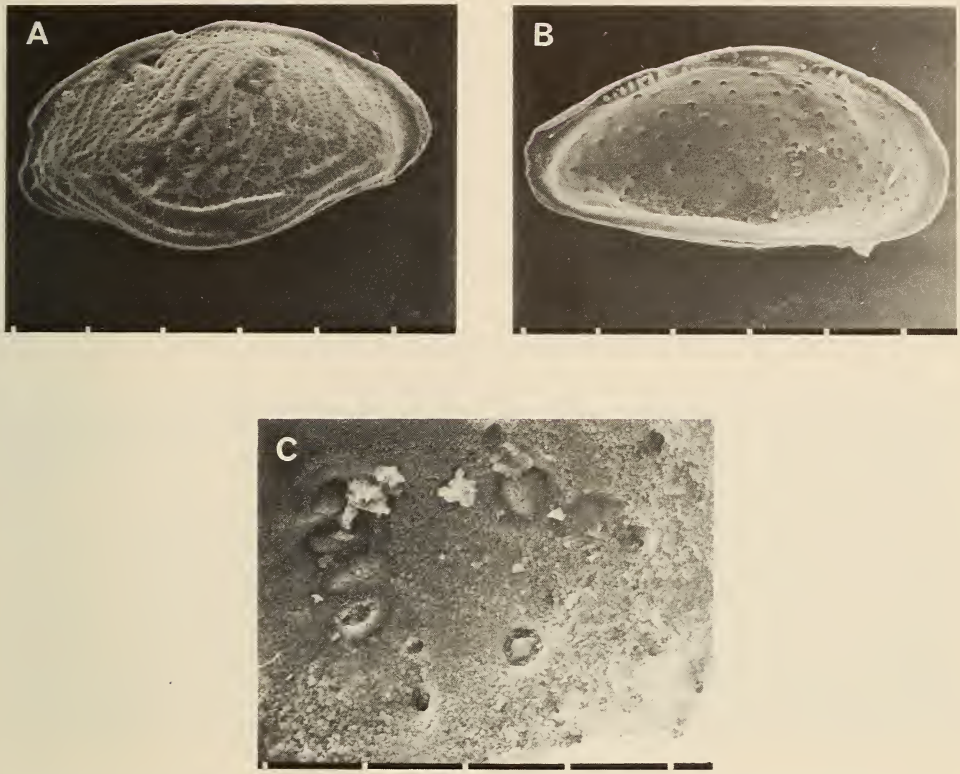

Fig. 20. *Paraphysocythere thompsoni*, Umzamba bed 3, Santonian III. A. SAM–PC6528, LV, SEM 479. B–C. SAM–PC6529, LV. B. Internal view, SEM 480. C. MS, SEM 482. Scale bars: A–B = 100 μ, C = 30 μ.

Family **Progonocytheridae** Sylvester-Bradley, 1948

Subfamily Protocytherinae Lubimova, 1955

Genus *Veenia* Butler & Jones, 1957

Veenia obesa Dingle, 1969

Fig. 21A–F

Veenia obesa Dingle, 1969: 366–368, fig. 12.

Remarks

Despite extensive collecting, no specimens of this distinctive species have been recorded in Zululand at outcrop or in the Richards Bay BH9 borehole. Some of the type material used by Dingle (1969), as well as additional specimens collected from Umzamba during the present study are illustrated here. SEM photographs show that the ATE in RV is somewhat more pointed than originally

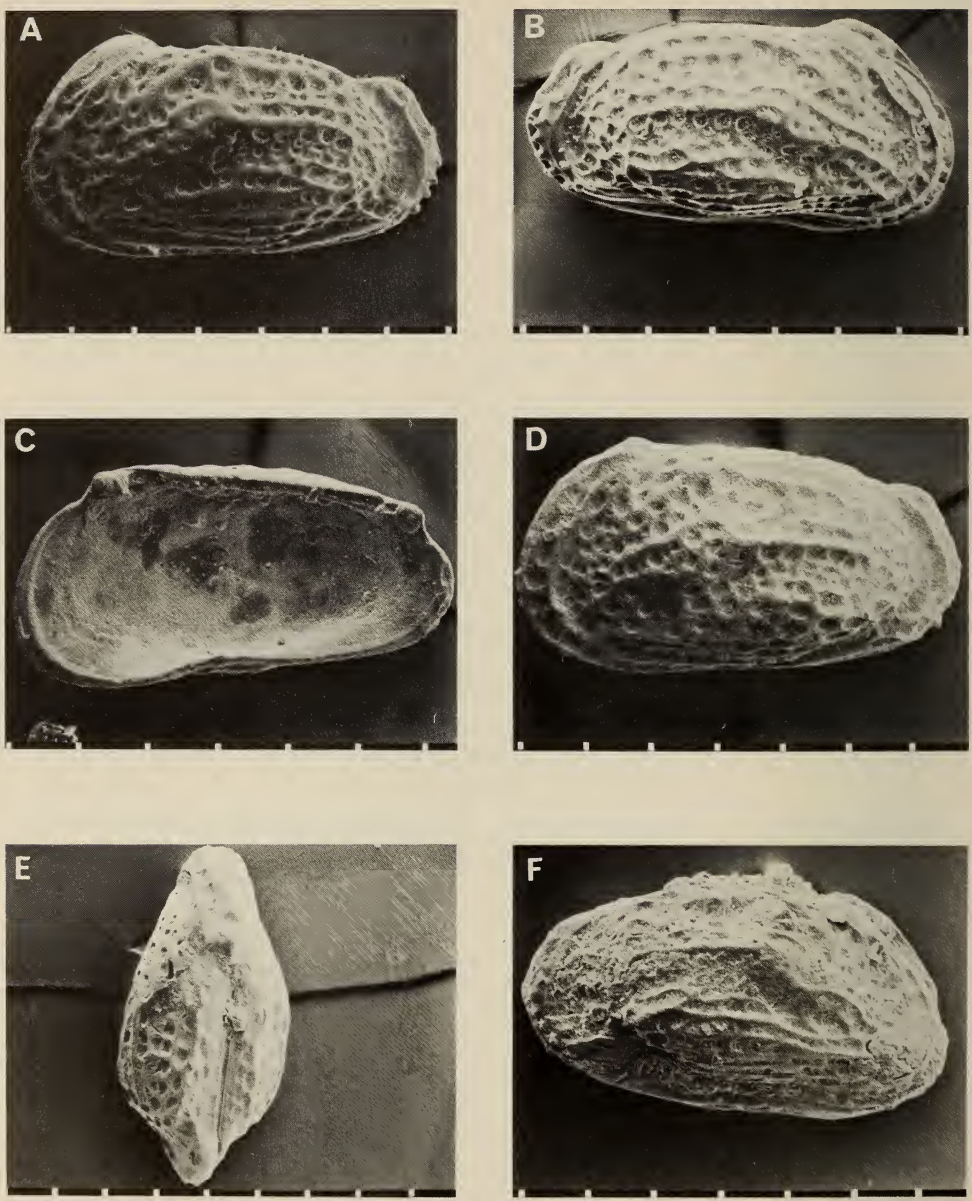

Fig. 21. *Veenia obesa*. A. SAM–PC6530, holotype, LV, Umzamba bed 1, Santonian II, SEM 2095. B. SAM–PC6531, RV, Umzamba bed 1, Santonian II, SEM 2100. C. SAM–PC6532, internal view, RV, Umzamba bed 1, Santonian II, SEM 2097. D. SAM–PC6533, LV, Umzamba bed 5, Santonian III, SEM 2070. E. SAM–PC6534, carapace, dorsal view, Umzamba bed 5, Santonian III, SEM 2071. F. SAM–PC6535, LV, Umzamba bed 1B, Santonian II, SEM 2051. Scale bars = 100 μ.

illustrated, but that the reference to a 'crenulate groove' as the LV ME is unproven and may be the result of poor preservation. Although the MS pattern still cannot be properly observed, the anterior scar is definitely hook-shaped. The oldest specimen recovered, from the lowest beds exposed at the base of the Umzamba cliff section, has a concavity at the posterior end of the VM, but this may be caused by slight crushing of the specimen. New catalogue numbers have been allocated to the type material following transfer to the South African Museum: holotype MG–1–2–6 = SAM–PC6530; paratype MG–1–2–8 = SAM–PC6531; MG–1–2–7 = SAM–PC6532.

Age and distribution

Veenia obesa is confined to Santonian II to III strata at Umzamba, where it reaches 15 per cent of the total ostracod population at the base of the Santonian III zone. It is absent from the highest ostracod-bearing sample collected in Santonian III.

Family **Cytherideidae** Sars, 1925

Genus *Krithe* Brady, Crosskey & Robertson, 1874

This genus, which is indicative of relatively deep-water environments, is relatively abundant in the Campanian IV–Maastrichtian II of Zululand, and has been recorded in the Maastrichtian of the J(c)–1 borehole. The present study records the earliest appearance of the genus in southern Africa (Upper Cenomanian).

Krithe sp. 2329

Fig. 22A–B

Remarks

No internal views were available for this species (2 carapaces), but it differs from *K. nibelaensis*, which is the important Campanian–Maastrichtian Zululand species, by its larger overall size, and lower length/height ratio: *Krithe* sp. 2329 = 1,74; *K. nibelaensis* = 2,07.

Age and distribution

Uppermost Cenomanian (2 201 m, 7 720 ft) to Turonian (2 152 m, 7 076 ft), J(c)–1 borehole.

Krithe sp. 2332

Fig. 22C

Remarks

One crushed carapace of an elongate species. Its valve outline serves to distinguish it from *Krithe* sp. 2329 and *K. nibelaensis*, but its relationship to *Krithe* sp. A from the Maastrichtian of the J(c)–1 borehole (Dingle 1981), which is also relatively elongate, is not known.

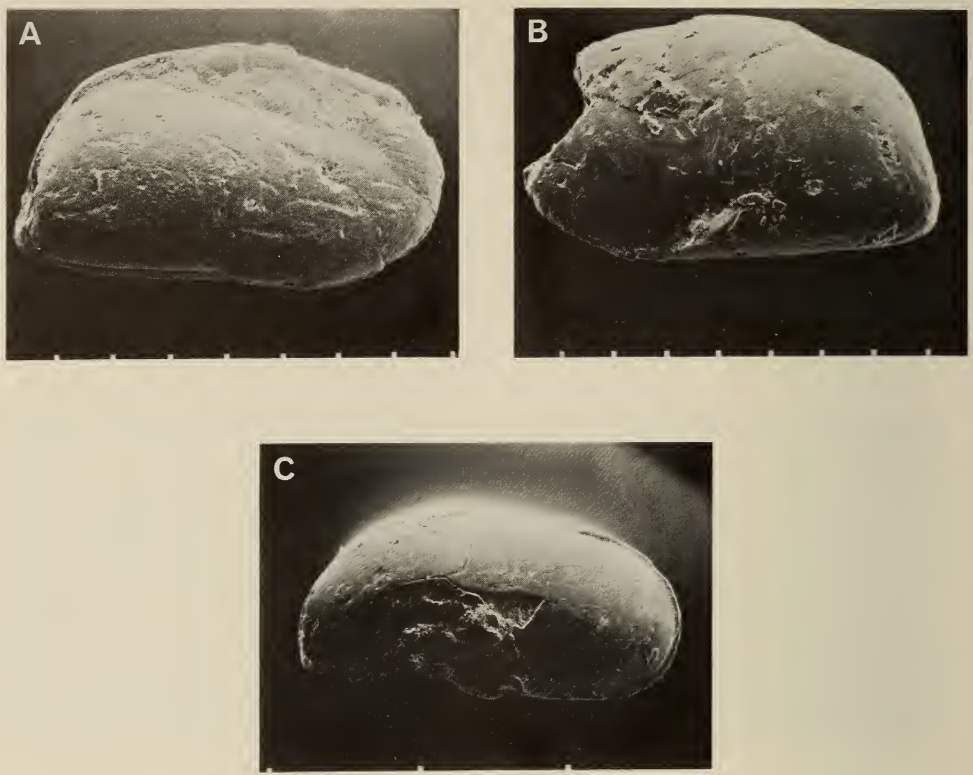

Fig. 22. *Krithe*, J(c)–1 borehole. A. *Krithe* sp. 2329, SAM–PC6536, RV, 2 152 m, Turonian, SEM 2330. B. *Krithe* sp. 2329, SAM–PC6537, LV, 2 201 m, Upper Cenomanian, SEM 2333. C. *Krithe* sp. 2332, SAM–PC6538, RV, 2 176 m, Turonian, SEM 2331. Scale bars: A–B = 100 μ, C = 300 μ.

Age and distribution

Turonian, 2 176 m (7 140 ft), J(c)–1 borehole.

Family **Trachyleberididae** Sylvester-Bradley, 1948

Subfamily Unicapellinae Dingle, 1981

Seven genera have been recognized in this subfamily, which was at its most diverse in the late Cretaceous. All range into the Maastrichtian, and five occur in Campanian strata (Fig. 23). *Unicapella* is the first to appear (Coniacian), but *Herrigocythere, Dutoitella, Paleoabyssocythere*, and *Atlanticythere* all have their first records more or less simultaneously (Campanian) in widely scattered locations (?California, southern Africa, south Atlantic). Benson's (1977) and Dingle's (1981) work suggests that the Southern Hemisphere genera had adapted to relatively deep-water environments during the Cretaceous, and that some persisted into the Tertiary as typical deep-water, cosmopolitan taxa. Similar

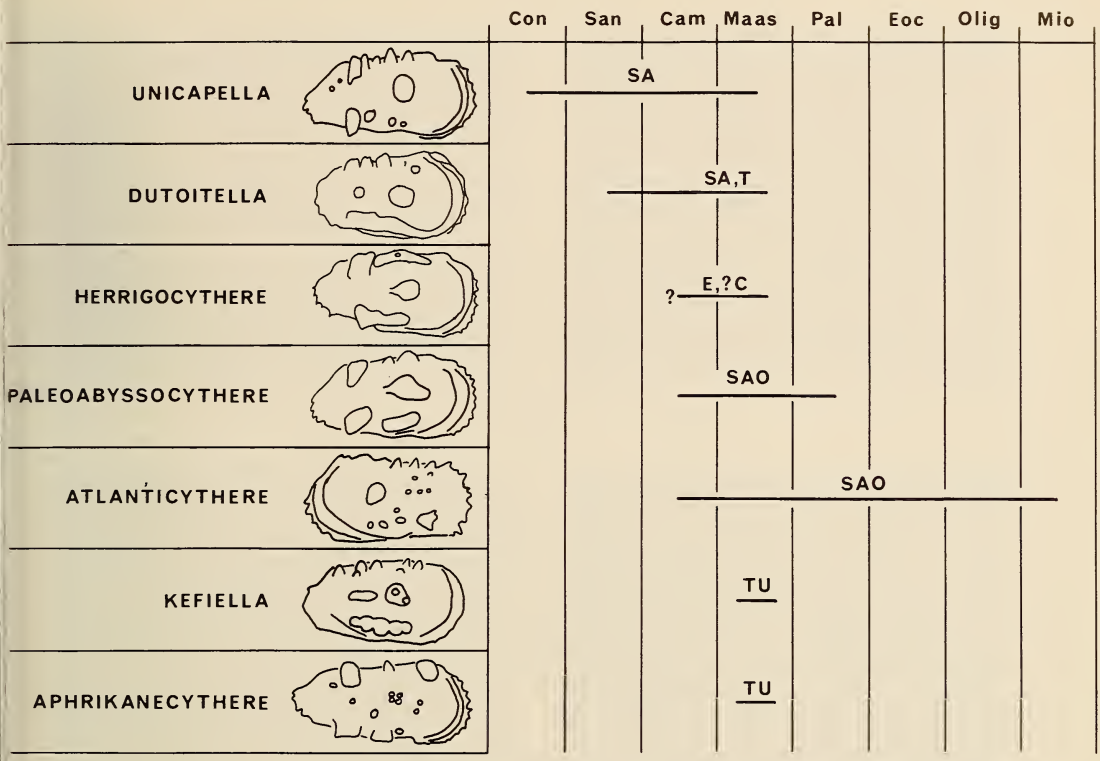

Fig. 23. Ranges of genera of the subfamily Unicapellinae. Key to localities: SA = south-east Africa, T = Tanzania, E = Europe, C = California, SAO = South Atlantic Ocean, TU = Tunisia. References cited in the text.

conclusions were reached by Donze *et al.* (1982) on the Tunisian forms, where *Kefiella* and *Aphrikanecythere* inhabited oxygen-depleted waters (4–5 ml/ℓ) at 400–500 m depths on the upper continental slope.

Genus *Unicapella* Dingle, 1980

Three species of this genus are known from southern Africa, only one of which occurs in Coniacian–Santonian strata (Table 7): *U. stragulata* (Coniacian–Santonian); *U. sacsi* (Campanian–Maastrichtian); and *U. reticulata* (Campanian).

Unicapella stragulata sp. nov.

Fig. 24A–F

Derivation of name

Latin *stragulum* (carpet, rug)—fanciful reference to the carpet-like texture of surface ornamentation.

TABLE 7
Distribution of *Unicapella* and *Dutoitella* in south-east Africa.

	Coniacian	Santonian	Campanian	Maastrichtian	
Unicapella					
stragulata		—			
reticulata			—		
sacsi			—	—	
Dutoitella					
mimica		—	—	—	
dutoiti			—	—	

Holotype

SAM–PC6539, RV, locality 15–7, Mtubatuba, Coniacian IV.

Paratypes

SAM–PC6540, RV, locality 74–13, False Bay, Santonian III.
SAM–PC6541, LV, locality 74–9, False Bay, Santonian ?II.

Diagnosis

Species with short, elliptical ventrolateral ridge, ornamented overall with coarse primary, and fine secondary reticulation.

Description

External features. Elongate nodose appearance. AM broadly rounded with numerous coarse spines, PM bluntly acuminate, asymmetrically so in LV. DM straight, but obscured by lateral surface elevations, VM straight, but obscured about mid-length by slight ventral overhang of lateral surface, and in RV there is a distinct concavity in the anteroventral position. There is a prominent, broad anterior hinge ear in LV. Surface ornamentation dominated by smooth, dome-like SCT. Large complex bullae occur in posteroventral and posterodorsal positions. DM has a line of four high, rounded, perforate tubercles, and VM has a wide, short, rounded and curved ventrolateral ridge that incorporates three indistinct tubercles. Further tubercles occur in posterior and median areas. There is a small indented lip on the anteroventral end of the nodous AM rim. Intercostal and internodose areas ornamented with a coarse but indistinct network of narrow ribs, forming a primary reticulation. There is a secondary fine reticulation that imparts a textured appearance that fancifully resembles a carpet. Large and small punctate nodes act as foci for the primary reticulation.

Internal features. No satisfactory interior views.

Remarks

Unicapella stragulata is very close to *U. sacsi*, and differentiation is based on subtle differences in disposition of surface nodes and primary reticulation patterns in the anterior area. These can be summarized (Fig. 25):

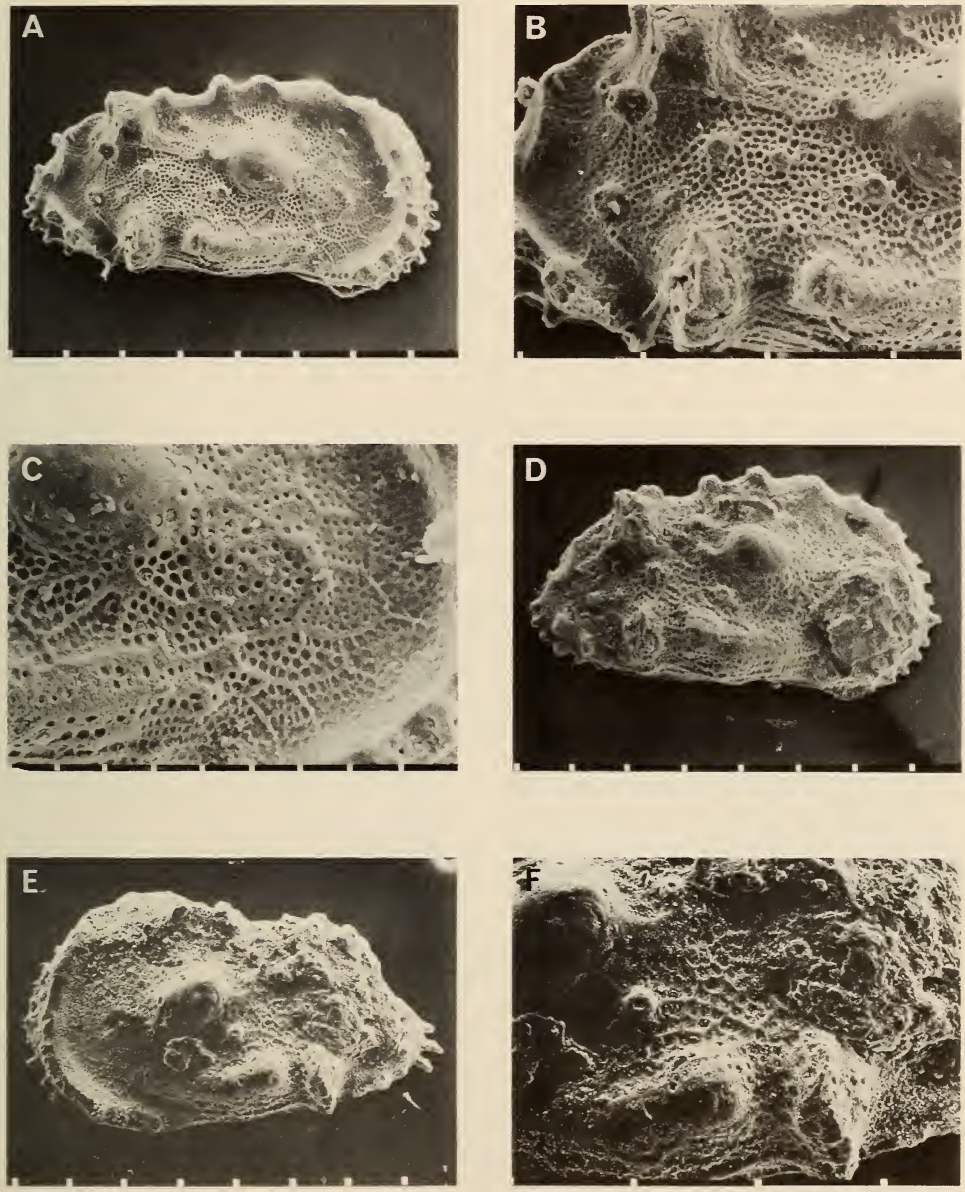

Fig. 24. *Unicapella stragulata* sp. nov. A–C. SAM–PC6539, holotype, RV, locality 15–7, Mtubatuba, Coniacian IV. A. SEM 1948. B. Detail of posterior area, SEM 1951. C. Detail of anterior area, SEM 1950. D. SAM–PC6540, RV, locality 74–13, False Bay, Santonian III, SEM 1868. E–F. SAM–PC6541, LV, locality 74–9, False Bay, Santonian II. E. SEM 1789. F. Detail of area posterior to SCT, SEM 1791. Scale bars: A–B, D–F = 100 μ, C = 30 μ.

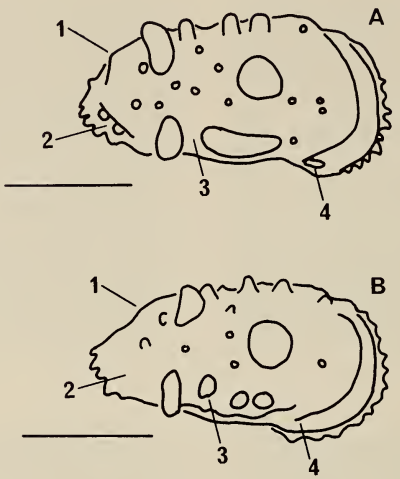

Fig. 25. Comparison of outline of holotypes of *Unicapella*. Significant differences are arrowed. A. *U. stragulata* sp. nov., SAM–PC6539, RV, locality 15–7, Mtubatuba, Coniacian IV, SEM 1948. B. *U. sacsi* SAM–K5610, BH9 Richards Bay, 88,39 m, Campanian II, SEM 343.
Scale bars = 300 μ.

(i) Ventrolateral area: in *U. stragulata* the ornamentation consists of a large bulla and a smooth ridge, whereas in *U. sacsi* there is an additional large node between the bulla and ridge.
(ii) Posterodorsal area: in *U. stragulata* there is a short angled rib in the RV, which is lacking in *U. sacsi*, whereas in *U. sacsi* in both valves there are two small prominent punctate nodes immediately posterior of the posterodorsal bulla.
(iii) Ornamentation of the anterior area: in *U. sacsi* there is a broad band of noticeably fine foveolate ornamentation bounded by the AM rim and a narrow primary rib line. This band is lacking in *U. stragulata*, which has a subtly different primary reticulation pattern, but no noticeable fining in the anteriormost secondary reticulation.

The closeness of the two species strongly suggests that *U. sacsi* developed directly from *U. stragulata* by a slight reorganization of its ornamentation during late Santonian–early Campanian time.

Dimensions (mm)

	length	height
PC6539	0,71	0,36
PC6540	0,70	0,38
PC6541	0,74	0,41

Age and distribution

Unicapella stragulata is known to range Coniacian IV (Mtubatuba) to Santonian III (False Bay) in Zululand.

Genus *Dutoitella* Dingle, 1981

Dutoitella mimica Dingle, 1981

Fig. 26A–B

Genus C sp. Bate, 1969, in Bate & Bayliss: 143, pl. 7 (fig. 15).
Trachyleberis schizospinosa Dingle, 1971*b*: 406–408, fig. 10 (*partim*).
Dutoitella mimica Dingle, 1981: 88–91, figs 37F, 41A–F, 42A–B, 43B, 44B.

Remarks

One worn carapace has been recovered from the J(c)–1 borehole below the levels recorded by Dingle (1981). There is no significant morphological difference between the J(c)–1 specimens and those from the Agulhas Bank. The levels at which this species occur in J(c)–1 are thought to represent intermediate water depths (?100–200 m).

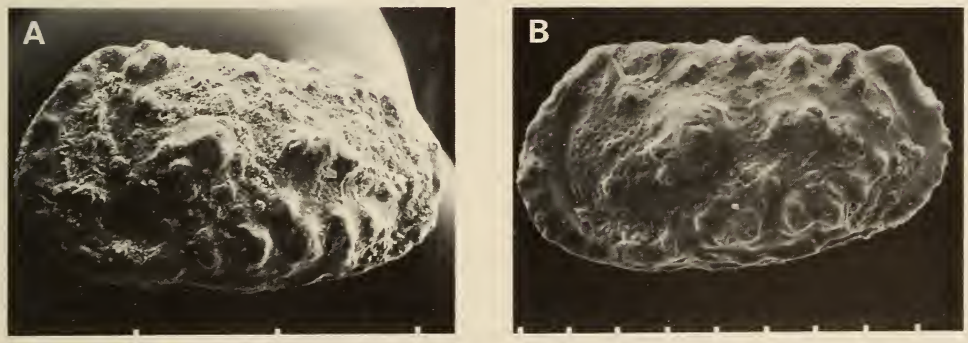

Fig. 26. *Dutoitella mimica*, J(c)–1 borehole. A. SAM–PC6543, LV, 2 030 m, Santonian, SEM 2316. B. SAM–K5752, LV, 1 811 m, Maastrichtian, SEM 1287.
Scale bars: A = 300 μ, B = 100 μ.

Age and distribution

Santonian–Maastrichtian, J(c)–1 borehole: levels 2 030 m (Santonian), 1 871 m (Campanian), 1 811 m (Maastrichtian); Maastrichtian III (sample TBD 818, Agulhas Bank), and Maastrichtian (Tanzania, as Genus C sp. Bate, 1969).

Subfamily Trachyleberidinae Sylvester-Bradley, 1948

Genus *Cythereis* Jones, 1849

Altogether five species of this genus have been recorded from east and south-east Africa in Turonian to Maastrichtian strata (Table 8).

TABLE 8
Distribution of *Cythereis* in south-east Africa.

Locality	Species	Coniacian I II III IV V	Santonian I II III	Campanian I II III
Umzamba	*transkeiensis*		——	——
BH9	*transkeiensis*		—	
	klingeri		——	
Zululand	*transkeiensis*		—	
	klingeri	——		
	mfoloziensis	—		
	cf. *luzangaziensis*	—		

Cythereis klingeri Dingle, 1980
Figs 27A–F, 28A–B, 30C–D, 31A–E

Cythereis klingeri Dingle, 1980: 34–38, figs 18B–F, 19A–F; 1981: 108–109, fig. 52A.

Remarks

Dingle (1980) noted that there is considerable intraspecific morphological variation in this species in samples from the Richards Bay BH9 borehole (Santonian II to Campanian II). In general terms this gives rise to two main morphotypes: FP (with flared dorsal ridges and pointed PM, especially in LV), and SQ (with subdued dorsal ridges and a more quadrate PM in LV). The holotype of the species belongs to the FP morphotype, and although this variety is more abundant in the Campanian and younger sediments, both types do occur in the oldest sediments in the Richards Bay BH9 borehole (Santonian II). The oldest record of *C. klingeri* is in the Coniacian IV, where the species is relatively abundant. Here the specimens are morphologically intermediate between the main FP and SQ morphs, but tend to have more characters typical of the former. This distribution leads to two conclusions: firstly that the two morphs are not sexual dimorphs, and secondly that the FP morph, although more abundant in the younger strata in BH9, was not a later development.

Cythereis klingeri is closely related to *C. luzangaziensis* from the Upper Turonian of Tanzania (Bate & Bayliss 1969) (Figs 28D, 31G–H), but differs principally in the shape of the ventrolateral ridge. In *C. luzangaziensis*, this ridge loops round at its posterior termination to form a narrow but prominent rib on the ventral surface that runs anteriorly, but is not contiguous with the AM rim. This ventral surface rib does not occur in *C. klingeri*. A phylogenetic relationship between the two species seems very probable, with speciation into *C. klingeri* taking place in Coniacian I–III time.

Age and distribution

Cythereis klingeri occurs in Santonian II to Campanian III strata in BH9 borehole, and in Coniacian IV (locality 15–9 to 15–15, Mtubatuba) and

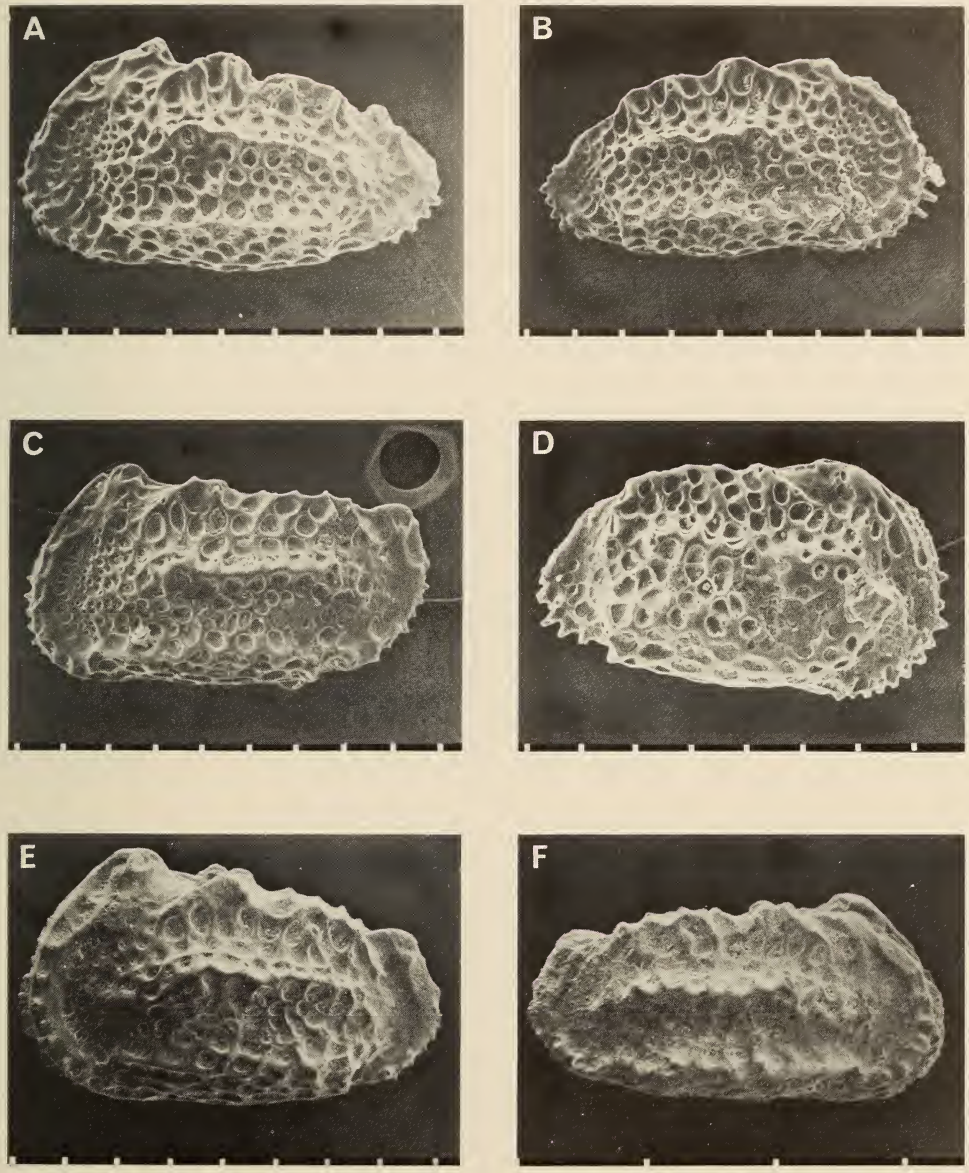

Fig. 27. *Cythereis klingeri*. A. SAM–K5617, LV, BH9 Richards Bay, 82,03 m, Campanian II, FP variety, SEM 158. B. SAM–K5616, holotype, RV, BH9 Richards Bay, 82,03 m, Campanian II, FP variety, SEM 165. C. SAM–K5622, LV, BH9 Richards Bay, 157,0 m, Santonian II, SQ variety, SEM 200. D. SAM–PC6544, RV, BH9 Richards Bay, 151,1 m, Santonian II, SQ variety, SEM 195. E. SAM–PC6545, LV, locality 15–5, Mtubatuba, Coniacian IV, FP variety, SEM 2035. F. SAM–PC6546, RV, locality 15–5, Mtubatuba, Coniacian IV, SQ variety, SEM 2036.
Scale bars: A–E = 100 μ, F = 300 μ.

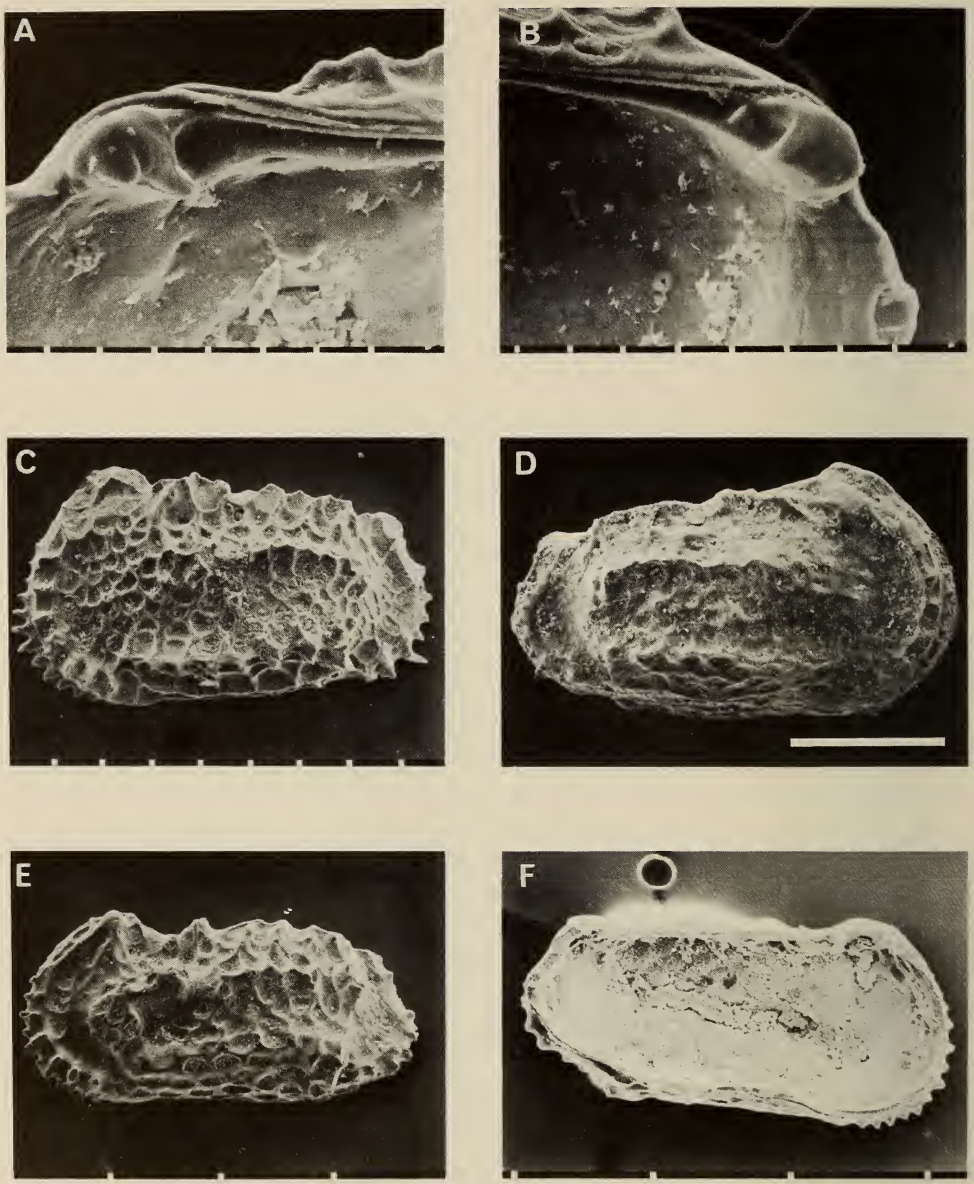

Fig. 28. *Cythereis*. A–B. *C. klingeri*, SAM–K5620, RV, BH9, Richards Bay, 157,0 m, Santonian II. A. ATE, SEM 207. B. PTE, SEM 208. C. *C.* cf. *luzangaziensis*, SAM–PC6547, LV, locality 15–5, Mtubatuba, Coniacian IV, SEM 1936. D. *C. luzangaziensis*, BMNH Io792, holotype, RV, Wami River area, Luzangazi Stream, Tanzania, Turonian, SP7/846. E–F. *C. mfoloziensis* sp. nov., SAM–PC6548, holotype, LV, locality 16–1, Mtubatuba, Coniacian II. E. SEM 1941. F. Internal view, SEM 2159.
Scale bars: A–B = 30 μ, C = 100 μ, D–F = 300 μ.

Campanian II to Maastrichtian II (Mfolozi and Nibela areas) at outcrop in Zululand. It does not occur in Santonian–Campanian strata at Umzamba. Dingle (1981) concluded that it is an environmentally tolerant species, but that it probably preferred relatively shallow (<100 m) water.

Cythereis cf. *luzangaziensis* Bate, 1969

Figs 28C, 31I

Cythereis luzangaziensis Bate, 1969 in Bate & Bayliss: 134, pl. 6 (fig. 10).

Remarks

One specimen showing the characteristic ventrolateral ridge loop has been found in the present study. It differs from the Tanzanian material by having a marked depression (almost a break) between the median longitudinal ridge and the SCT. There is a relatively good population of *C. klingeri* in the sample so I am confident that this specimen is not a morphotype of this species, because there are several distinct differences: shape of anteriormost lobe on the DM ridge, shape of SCT, ventrolateral rib pattern, markedly coarser reticulate ornament and strongly elevated muri and ridges in *C.* cf. *luzangaziensis*. Figures 28D and 31G–H show type specimens of *C. luzangaziensis* for comparison.

Age and distribution

Known only from Coniacian IV (locality 15–13, Mtubatuba) in Zululand.

Cythereis mfoloziensis sp. nov.

Figs 28E–F, 31F

Derivation of name

Locality of type—Mfolozi River valley, Zululand.

Holotype

SAM–PC6548, LV, locality 16–1, Mtubatuba area, Coniacian III.

Diagnosis

Species of *Cythereis* with a complex tubercle lying in an anteroventral position relative to the SCT.

Description

External features. Elongate subquadrate in outline. AM symmetrically rounded, PM triangular with apex just below mid-height. DM and VM straight. Lateral surface carries three prominent longitudinal ridges. Dorsal ridge obscures DM and is flared with a prominent peak at its anterior end. Median ridge is short, descends slightly anteriorly, terminates at about mid-length and is linked to the dorsal ridge by a low saddle. Ventral ridge is straight, terminates posteriorly in a

right-angled bend towards the VM and anteriorly hooks upward to join the complex tubercle. SCT is prominent, rounded and is linked by a short rib to the complex tubercle that lies anteroventrally to it. The latter is formed by a knot of reticulating muri. There is a strong spinose AM rim. Surface overall is coarsely reticulate. The eye tubercle is almost turreted at the prominent ACA.

Internal views. Internal features are poorly preserved. MS not seen, and MA broken. ATE in LV has a prominent process at its anterior end, which indicates a closer relationship to *C. klingeri* than to *C. transkeiensis*, although overall the ATE of *C. mfoloziensis* is less massive than in *C. klingeri*.

Remarks

Cythereis mfoloziensis is closest to *C. klingeri*, from which it differs on the following points: its median ridge does not connect to the SCT, it possesses a tubercle adjacent to the SCT, and has a more prominent posterior termination to the ventrolateral ridge. The distinctive morphology of *C. mfoloziensis* justifies the erection of the species on one specimen only.

Dimensions (mm)

	length	height
PC6548	1,05	0,51

Age and distribution

Known only from the Coniacian III (locality 16, Mtubatuba) of Zululand.

Cythereis transkeiensis Dingle, 1969

Figs 29A–F, 30A–B

?Cythereis ornatissima Reuss, 1846, var. *reticulata* [*non*] Jones & Hinde, 1890, Chapman 1904: 234.

Cythereis transkeiensis Dingle, 1969: 377–378, fig. 18; 1980: 34, fig. 18A; 1981: 109, fig. 52B–C.

Remarks

Closely allied to *C. klingeri, C. transkeiensis* can be distinguished by its massive lateral longitudinal ridges and hinge structure. The holotype is illustrated here (Fig. 30), showing that the hinges of the two species differ as follows: ATE RV in *C. klingeri* resembles a right-hand fist, with external 'thumb', and in *C. transkeiensis* is a left-hand fist; anterior part of ME RV is an enclosed hollow in *C. transkeiensis*, but has no posterior wall in *C. klingeri*; ATE LV in *C. klingeri* has a posterior projection on the anterior wall, while this is lacking in *C. transkeiensis*. Bate's *Cythereis* sp. C (*in* Bate & Bayliss 1969, pl. 7 (fig. 4)) is similar in outline and ornamentation to *C. transkeiensis*.

Age and distribution

Cythereis transkeiensis ranges Santonian II to Campanian I at Umzamba. It is known from Santonian II in Richards Bay BH9 borehole, Santonian III at outcrop in Zululand (locality 14, Msunduzi River), and late Campanian–early

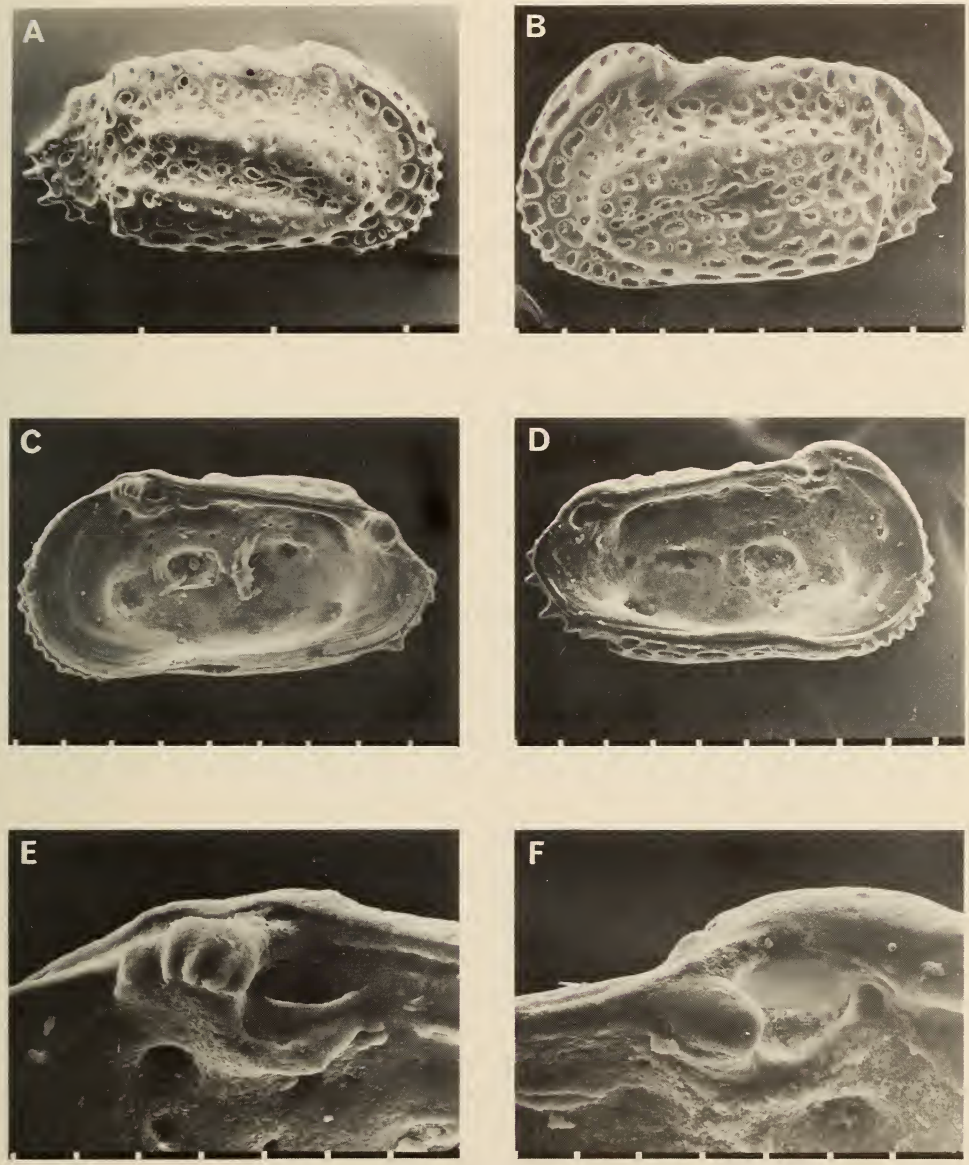

Fig. 29. *Cythereis transkeiensis*, Umzamba. A. SAM–PC6549, holotype, RV, bed 1, Santonian II, SEM 2121. B. SAM–PC6550, LV, bed 3, Santonian III, SEM 145. C. SAM–PC6551, RV, internal view, bed 3, Santonian III, SEM 147. D. SAM–PC6552, LV, internal view, bed 3, Santonian III, SEM 152. E. SAM–PC6551, RV, ATE, bed 3, Santonian III, SEM 149. F. SAM–PC6552, LV, ATE, bed 3, Santonian III, SEM 154.
Scale bars: A = 300 μ, B–D = 100 μ, E–F = 30 μ.

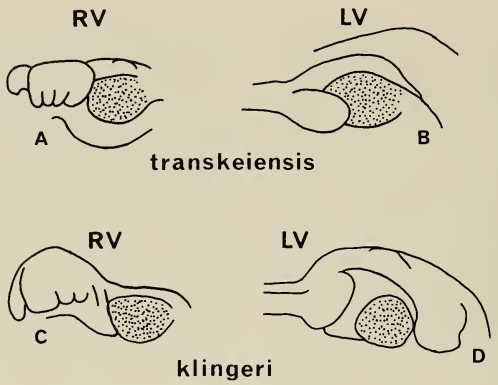

Fig. 30. Comparison of anterior terminal hinge elements of *Cythereis transkeiensis* and *C. klingeri*. A. SAM–PC6551, Umzamba bed 3, Santonian III. B. SAM–PC6552, Umzamba bed 3, Santonian III. C. SAM–K5620, BH9 Richards Bay, 157,0 m, Santonian II. D. SAM–K5619, BH9 Richards Bay, 157,0 m, Santonian II.

Maastrichtian at Igoda. This is a total range of Santonian II to late Campanian–early Maastrichtian. *Cythereis transkeiensis* is rare north of Umzamba, and clearly is a southern analogue of *C. klingeri*, which itself is effectively restricted to Zululand.

Genus *Haughtonileberis* Dingle, 1969

Grosdidier (1979) provisionally assigned five species to *Haughtonileberis* from borehole material in Gabon. These are the earliest records of the genus, with '*Haughtonileberis*' GA C11 (Upper Albian–Upper Cenomanian), followed by three Upper Cenomanian appearances.

The earliest representative in south-east Africa is *H. haughtoni* (Coniacian) (also recorded by Bate & Bayliss (1969) from the Upper Turonian of Tanzania), which ranges into the Lower Campanian. Two other species (*H. fissilis* and *H. vanhoepeni*) are known from the Santonian of south-east Africa.

These records suggest a generic range of Upper Albian to Lower Oligocene (Table 9), with the initial development of the genus in the Equatorial Atlantic (i.e. north of the Walvis Ridge), and rapid migration into the south-west Indian Ocean area by Turonian–Coniacian times.

Haughtonileberis haughtoni Dingle, 1969

Fig. 32A–F

Haughtonileberis haughtoni Dingle, 1969: 372–373, fig. 15; 1980: 39, fig. 21A–E.
Curfsina turonica Bate, 1969, in Bate & Bayliss: 139, pl. 6 (figs 15, 19) (*partim* (BMNH Io783)).

Remarks

Coniacian specimens from south-east Africa are of the squat variety noted by Dingle (1969, 1980) in the topotypic populations, but they possess the sharper,

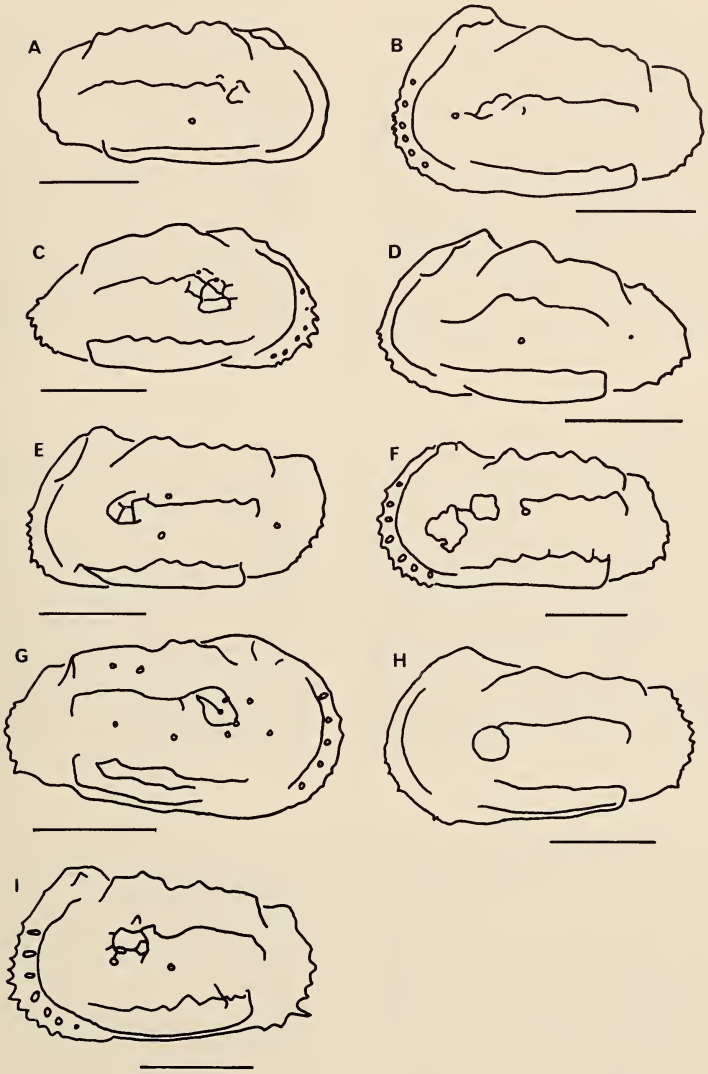

Fig. 31. Comparison of lateral outlines of various species of *Cythereis*. A–E. *C. klingeri*. A. SAM–PC6546, RV, Coniacian IV. B. SAM–PC6545, LV, Coniacian IV. C. SAM–K5616, RV, Campanian II. D. SAM–K5617, LV, Campanian II. E. SAM–K5622, Santonian II. F. *C. mfoloziensis* sp. nov., SAM–PC6548, Coniacian III. G–H. *C. luzangaziensis*, BMNH Io792, holotype, carapace, Turonian. G. RV. H. LV. I. *C.* cf. *luzangaziensis*, SAM–PC6547, LV, Coniacian IV. Scale bars = 300 μ.

TABLE 9
Distribution of *Haughtonileberis* in Africa and adjacent areas.

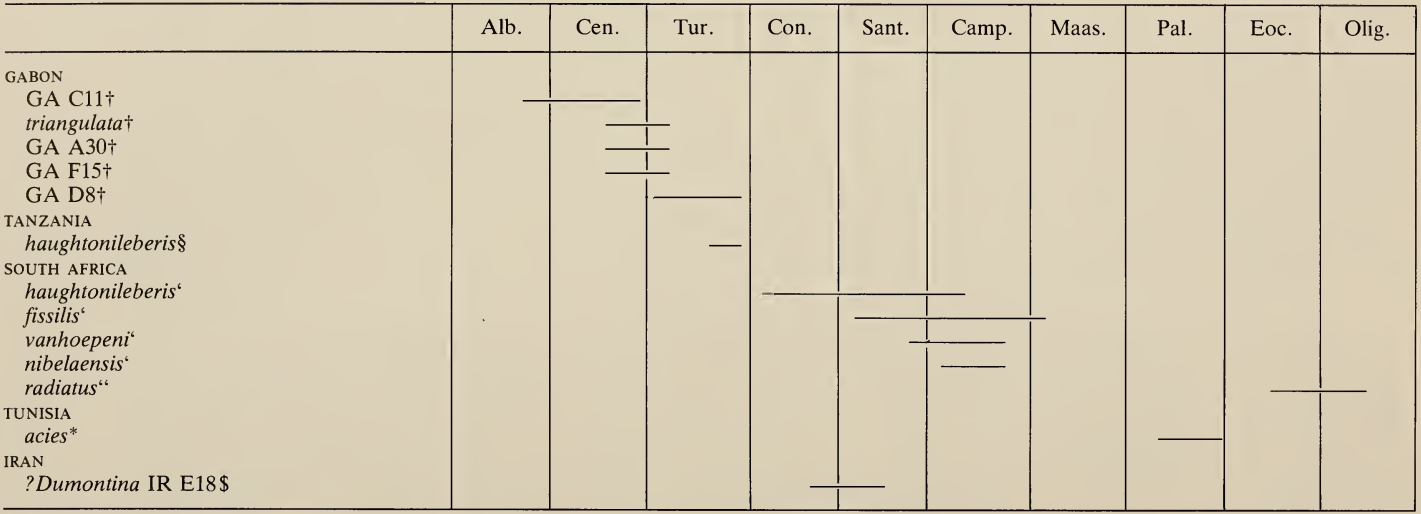

† = Grosdidier (1979)
§ = Bate & Bayliss (1969) one paratype of *Curfsina turonica* (BMNH Io783)
‘ = Dingle (1981)
“ = Dingle (1976)
* = Donze *et al.* (1982)
$ = Grosdidier (1973), similar morphology

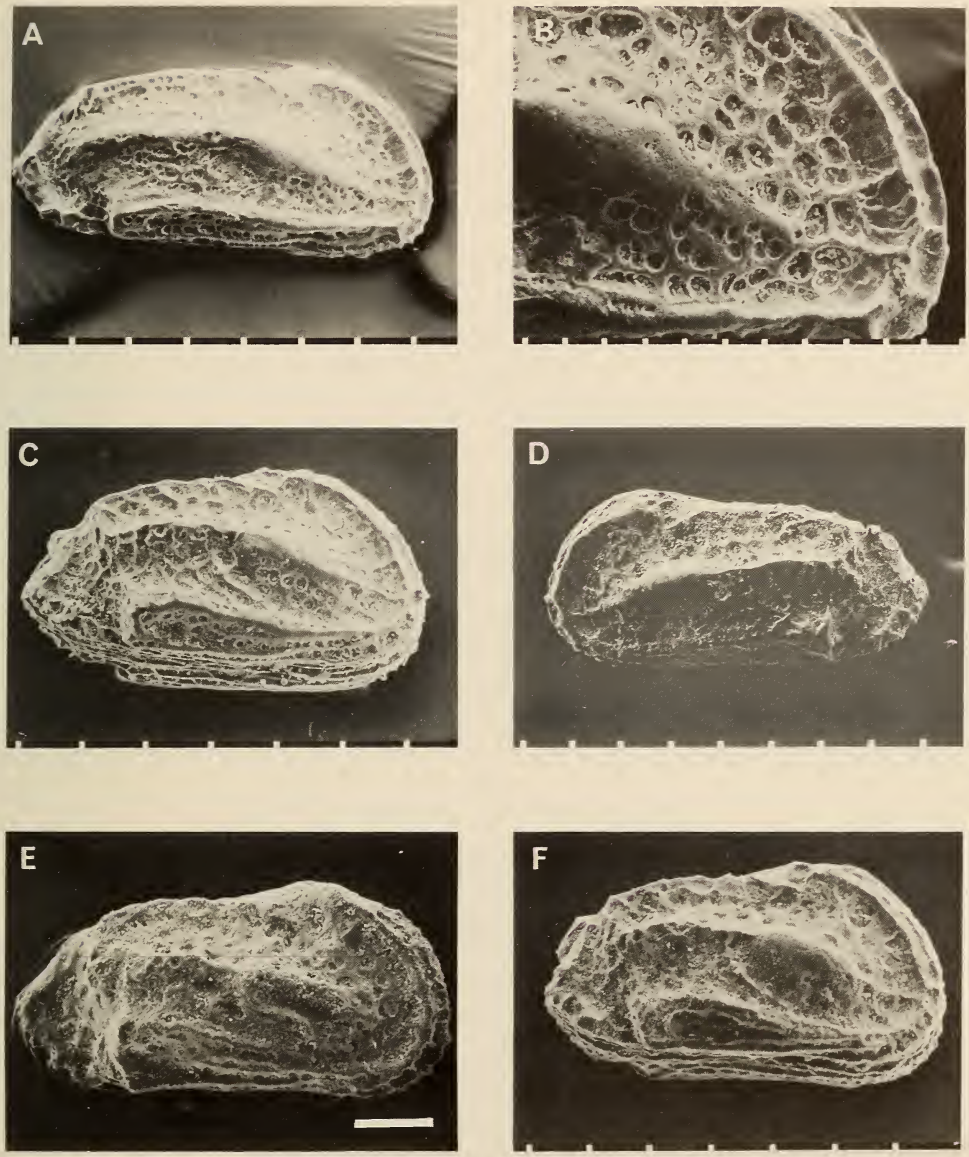

Fig. 32. *Haughtonileberis haughtoni*. A–B. SAM–PC6553, holotype, RV, Umzamba bed 1, Santonian II. A. SEM 2117. B. Detail of anterior area, SEM 2119. C. SAM–PC6554, RV, locality 15–5, Mtubatuba, Coniacian IV, SEM 1945. D. SAM–PC6556, LV, locality 14–3, Mtubatuba, Santonian III, SEM 1780. E. BMNH Io783, RV, described by Bate (*in* Bate & Bayliss 1969) as paratype of *Curfsina turonica*, Wami River area, Luzangazi Stream, Tanzania, Turonian, SP7/854. F. SAM–PC6555, RV, locality 89, Hluhluwe River, Coniacian IV, SEM 1943. Scale bars: A, D–F = 100 μ, B = 30 μ.

narrow posteromedian ridge of the Zululand Campanian faunas. Bate (*in* Bate & Bayliss 1969) illustrated a specimen, which I consider is *H. haughtoni*, as a paratype for his new species *Curfsina turonica* from the Upper Turonian of Tanzania. The holotype (pl. 6 (figs 13, 18, BMNH Io784)) differs significantly from BMNH Io783 in the following points: shape of the ventrolateral ridge, shape of median lateral ridge and SCT, shape of PCA, and shape of PM outline.

Of the five species tentatively assigned to *Haughtonileberis* by Grosdidier (1979) from Gabon, *Haughtonileberis?* GA F15 (Upper Cenomanian–Lower Turonian) is closest to the type species. The main difference is a more prominent upswing in the posterior part of the ventrolateral rib. Otherwise, the general outline, ornamentation, and in particular the shape of the median ridge and adjoined elongate SCT are very similar. The holotype, originally designated MG–1–1–12, has been transferred to the South African Museum under the number SAM–PC6553.

Age and distribution

Upper Turonian of the Luzangazi stream, north of the Wami River, Tanzania; Coniacian IV (locality 15, Mtubatuba) to Campanian I (locality 74, False Bay) at outcrop in Zululand; Santonian II to Campanian I in the Richards Bay BH9 borehole; and Santonian II to Campanian I at Umzamba cliff. This is the longest-ranging species of the genus so far recognized: Upper Turonian to Campanian I. Dingle (1981) concluded that the species was environmentally tolerant (<100 m to 200 m water depths) but that it preferred shallow-water (<100 m), low-energy environments with restricted access to the open ocean.

Haughtonileberis fissilis Dingle, 1969

Fig. 33A–D

Haughtonileberis fissilis Dingle, 1969: 374–375, fig. 16; 1980: 39, fig. 22A–B; 1981: 95, fig. 48F.

Remarks

This species is rare in outcrops in Zululand, where the Santonian specimens belong to the squatter morphotype recognized by Dingle (1980). No significant morphological differences are noted in specimens at the extremes of the species's temporal range. Of the species assigned to *Haughtonileberis* by Grosdidier (1979), '*Haughtonileberis*' GA A30 is closest to *H. fissilis*, having a distinctly split anterior end to the median lateral rib. It differs in having a short oblique dorsal ridge that runs anteriorly from the PCA position. Type material of *H. fissilis* has been transferred to the South African Museum and the new numbers are: MG–1–1–16 = SAM–PC6557, MG–1–1–17 = SAM–PC6559, and MG–1–1–18 = SAM–PC6558.

Age and distribution

Haughtonileberis fissilis ranges Santonian III (Msunduzi River) to Maastrichtian I (Mfolozi River) at outcrops in Zululand, Santonian II to Campanian II in

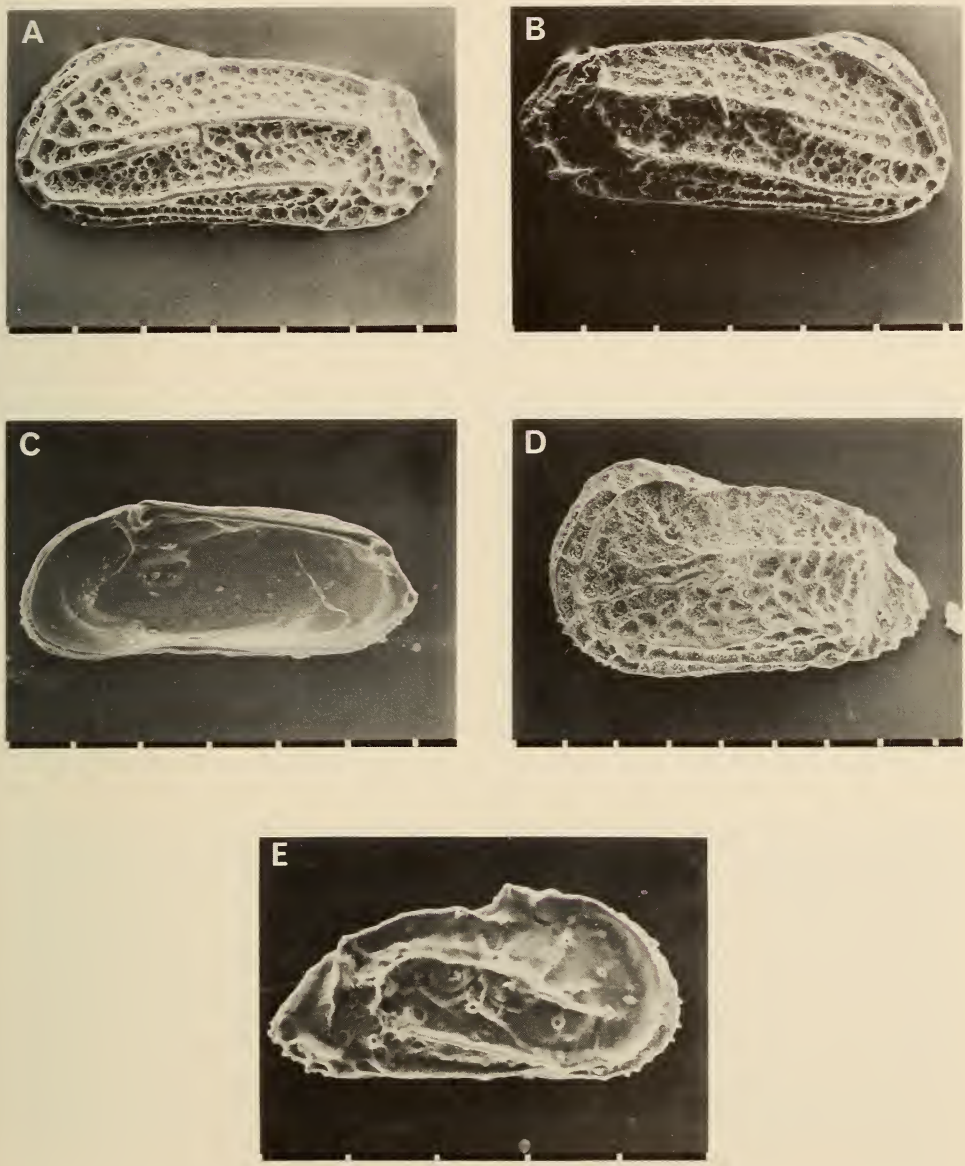

Fig. 33. A–D. *Haughtonileberis fissilis*. A–C. Umzamba bed 1, Santonian II. A. SAM–PC6557, holotype, LV, SEM 2126. B. SAM–PC6558, RV, SEM 2129. C. SAM–PC6559, internal, RV, SEM 254. D. SAM–PC6560, LV, locality 14–1, Mtubatuba, ?Santonian III, SEM 1866. F. *Haughtonileberis vanhoepeni*, SAM–K5632, holotype, RV, BH9, Richards Bay, Campanian I, SEM 32. Scale bars = 100 μ.

the Richards Bay BH9 borehole, and Santonian II to Campanian I at Umzamba. Its total time range in Zululand is Santonian II to Maastrichtian I.

Haughtonileberis vanhoepeni Dingle, 1980

Fig. 33E

Haughtonileberis vanhoepeni Dingle, 1980: 42–44, figs 22H, 23A–F; 1981: 95, fig. 46A.

Remarks

No additional specimens of this species were recovered from Coniacian and Santonian outcrops in Zululand during the present study. None of the species assigned to *Haughtonileberis* by Grosdidier (1979) are close to *H. vanhoepeni*.

Age and distribution

Known only from the Santonian III to Campanian II of the Richards Bay BH9 borehole, and Campanian II to Campanian IV outcrops in Zululand. This gives a total range of Santonian III to Campanian IV, but the Santonian record is restricted to one sample at the very top of Santonian III in BH9. The appearance of *H. vanhoepeni* therefore can be taken as an effective marker for the Santonian–Campanian boundary.

Genus *Oertliella* Pokorny, 1964

This genus first appears in the Coniacian of Zululand, but is relatively rare until the Campanian, where four species are present (Table 10).

Table 10
Distribution of *Oertliella* in south-east Africa.

	Coniacian	Santonian	Campanian	Maastrichtian
pennata				
elongata				
sp. 476				
africana				

Oertliella pennata Dingle, 1980

Fig. 34A–E

Acanthocythereis? aff. *A. horridula* (Bosquet, 1854), Dingle, 1969: 378–380, fig. 19.
Oertliella pennata Dingle, 1980: 46–49, fig. 26A–E; 1981: 98, fig. 48A.

Remarks

With the exception of the Coniacian specimens from locality 15–5, which have more massive spines, those from horizons at outcrop in Zululand are identical to the topotypes from the Richards Bay BH9 borehole.

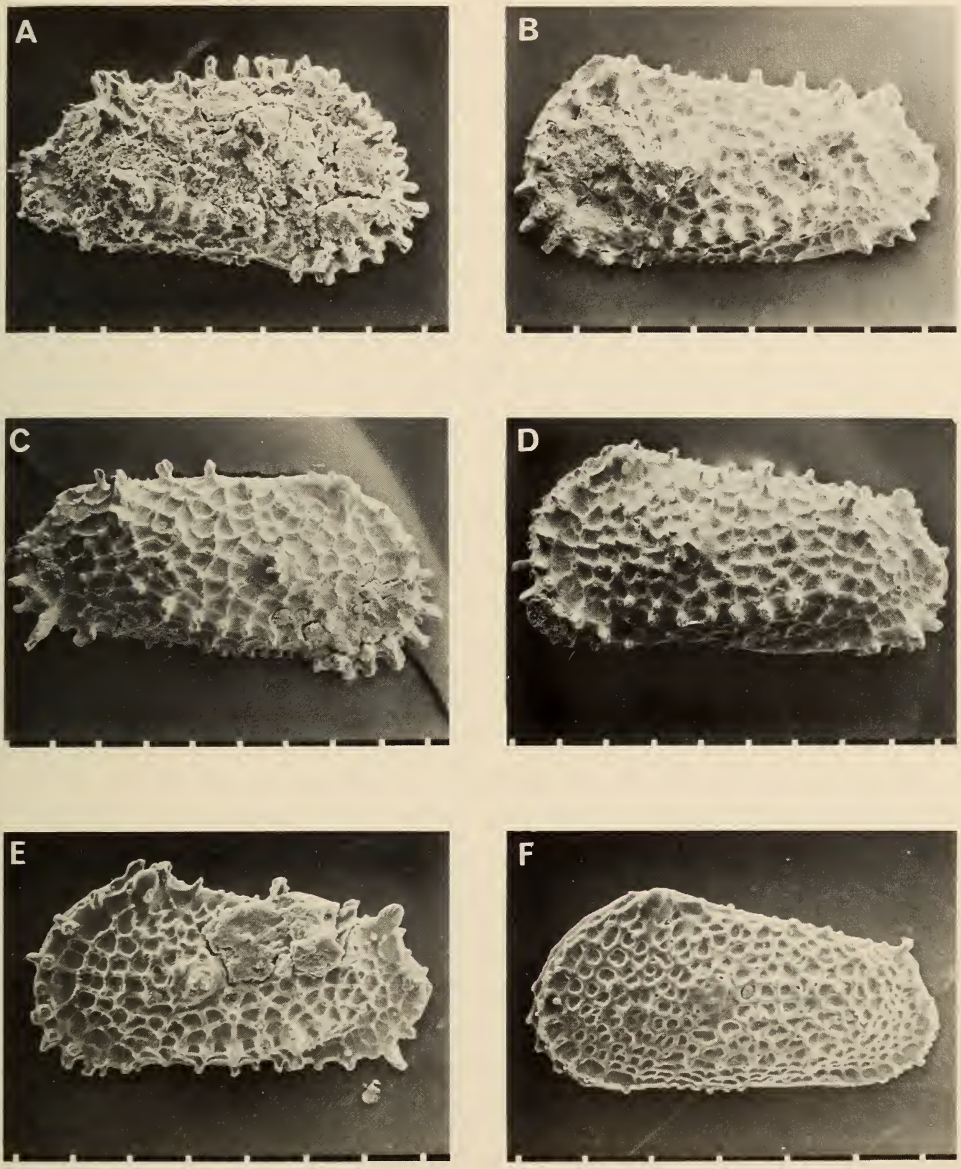

Fig. 34. *Oertliella*. A–E. *O. pennata*. A. SAM–PC6561, RV, locality 15–5, Mtubatuba, Coniacian IV, SEM 1928. B. SAM–PC6562, LV, locality 15–7, Mtubatuba, Coniacian IV, SEM 2135. C. SAM–PC6563, RV, Umzamba bed 7, Santonian III, SEM 2079. D. SAM–PC6564, LV, Umzamba bed 3, Santonian III, SEM 2111. (This is the specimen recorded as *?Acanthocythereis* aff. *A. horridula* by Dingle (1969) (MG–1–2–9)). E. SAM–K5644, holotype, LV, BH9 Richards Bay, 115,9 m, Santonian III, SEM 471. F. *Oertliella* sp. 476, SAM–K5647, LV, BH9 Richards Bay, 115,9 m, Santonian III, SEM 476. Scale bars = 100 μ.

Age and distribution

Coniacian IV to Santonian III (localities 15–5, 15–7, 74–10 and 74–15) at outcrop in Zululand, Santonian III to Campanian II in Richards Bay borehole, and Santonian III to Campanian I at Umzamba.

Oertliella sp. 476

Fig. 34F

Oertliella sp. A Dingle, 1980: 50, fig. 26F.

Remarks

No additional specimens of this species have been recovered during the present study.

Age and distribution

Uppermost Santonian III to Campanian II, Richards Bay BH9 borehole.

Genus *Rayneria* Neale, 1975

Rayneria nealei Dingle, 1980

Fig. 35A–F

Cythereis ?quadrilatera (Roemer) Chapman, 1923: 5, pl. 1 (5).
Rayneria nealei Dingle, 1980: 55–57, figs 28E–F, 29A–F, 30G; 1981: 108, fig. 51F.

Remarks

During the present study several specimens of this species were recorded from Santonian and Coniacian horizons at Umzamba and in Zululand. Compared to type material from the Richards Bay BH9 borehole, which is of Santonian III and Campanian I age, the older populations show several subtle morphological variations. In particular, the valves in lateral outline have a less angular appearance, with the ventromedian ridge being more subdued, while ornamentation in the anterior part of the valve has a distinctly foveolate aspect compared to the more coarsely reticulate ornamentation of the type material. However, one characteristic feature of ornamentation, which both populations display well, is the possession of fine secondary muri within many large individual fossae, which resemble spiders' webs.

Age and distribution

Known from Coniacian IV (Mtubatuba) outcrops in Zululand, Santonian II to lowermost Campanian I in the Richards Bay BH9 borehole, and Santonian III at Umzamba. This gives a total range of Coniacian IV to Campanian I in

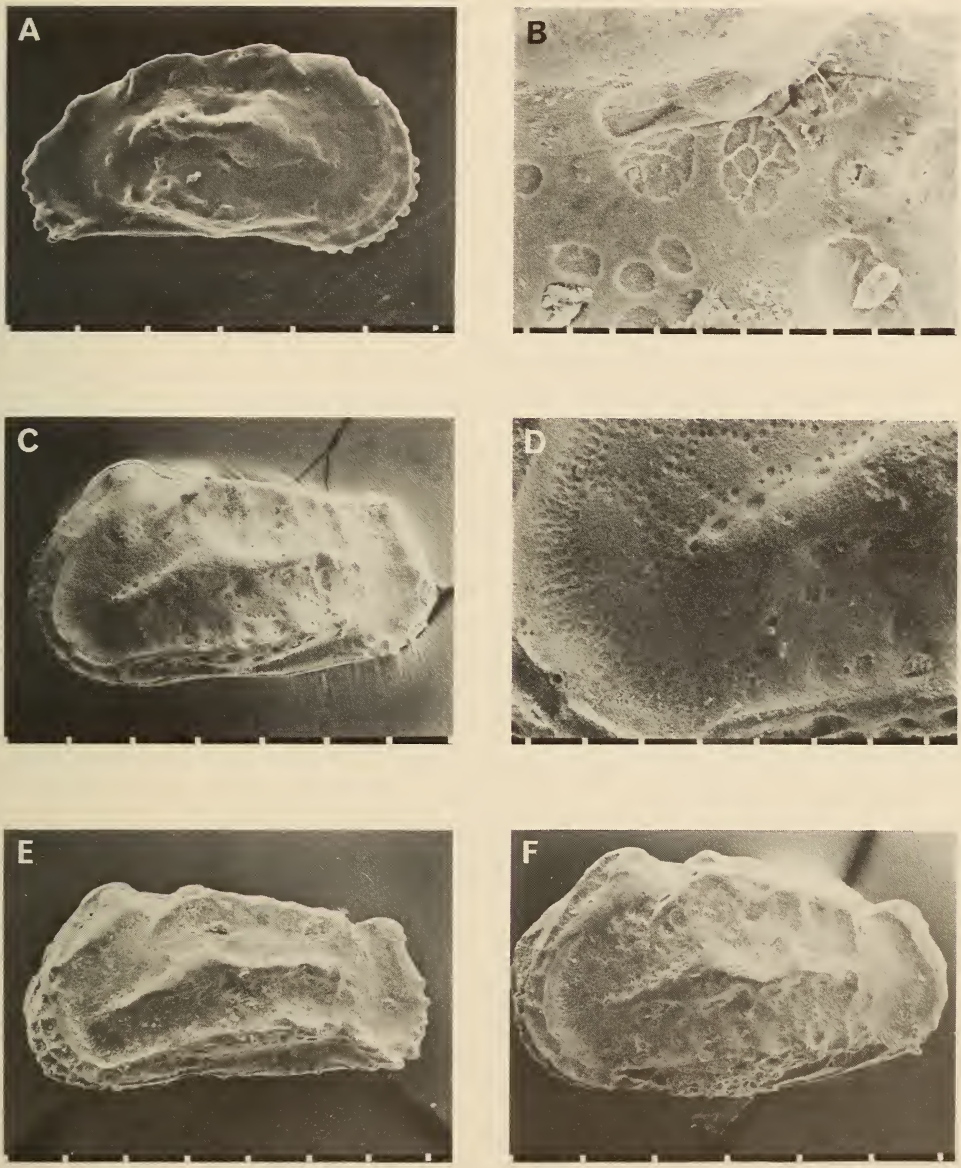

Fig. 35. *Rayneria nealei*. A. SAM–K5652, holotype, RV, BH9, Richards Bay, 139,8 m, Santonian III, SEM 413. B. SAM–PC6567, LV, detail central area, lateral view, Umzamba bed 7, Santonian III, SEM 2083. C–D. SAM–PC6565, LV, Umzamba bed 5, Santonian III. C. SEM 2063. D. Detail anterior area, SEM 2064. E. SAM–PC6566, LV, locality 15–5, Mtubatuba, Coniacian IV, SEM 2042. F. SAM–PC6567, LV, Umzamba bed 7, Santonian III, SEM 2081. Scale bars: A, C, E–F = 100 μ, B = 10 μ, D = 30 μ.

south-east Africa. Dingle (1981) concluded that *R. nealei*'s preferred habitat was water <100 m deep, where environmental conditions ranged from high to low energy.

Genus *Gibberleberis* Dingle, 1969

Three species of this genus have been recorded, all from the Zululand–Umzamba area of south-east Africa. Two of these (*G. africanus* and *G. elongata*) occur in Santonian strata, and the former ranges down into the Coniacian. Although never abundant, the genus is a characteristic element of the Coniacian–Santonian faunas of south-east Africa. Bate (*in* Bate & Bayliss 1969) recorded a closely allied, monospecific genus from the Upper Turonian of Tanzania: *Akrogmocythere wamiensis*. The author has examined the type specimens in the British Museum (Natural History), and noted that the two genera can be distinguished by the lack of a dorsal margin concavity or neck behind the ACA in *Akrogmocythere*, which also has a distinctly down-turned ATE in the LV hinge. In view of the temporal distribution of the two genera, it is possible that *Gibberleberis* evolved from *Akrogmocythere* in the later Turonian or early Coniacian.

Gibberleberis africanus Dingle, 1969

Fig. 36A–C

Gibberleberis africanus Dingle, 1969: 376–377, fig. 17; 1980: 57, figs 30A–D, 31A.

Remarks

Intraspecific morphological variation within *G. africanus* primarily takes the form of differences in the strength and coarseness of the surface rib pattern. The type populations from Umzamba exhibit distinctly coarser reticulation and stronger muri and main rib patterns than those from Zululand, where material from Richards Bay BH9 borehole and outcrops has a more delicate ornamentation. In addition, the Coniacian examples are somewhat plumper and squatter than younger forms, although I have no hesitation in assigning them to the same species.

Age and distribution

Although never abundant, *G. africanus* is ubiquitous in the Coniacian to Santonian strata of the Zululand–Umzamba area. It ranges Santonian II to Santonian III at Umzamba and the Richards Bay BH9 borehole, and Coniacian IV (locality 15, Mtubatuba) to Santonian III (locality 74, False Bay) at outcrop in Zululand. It is a useful marker for Coniacian–Santonian strata in south-east Africa.

Data from the Richards Bay BH9 borehole suggest that *G. africanus* preferred shallow (<100 m), low-energy, open-water conditions (Dingle 1980).

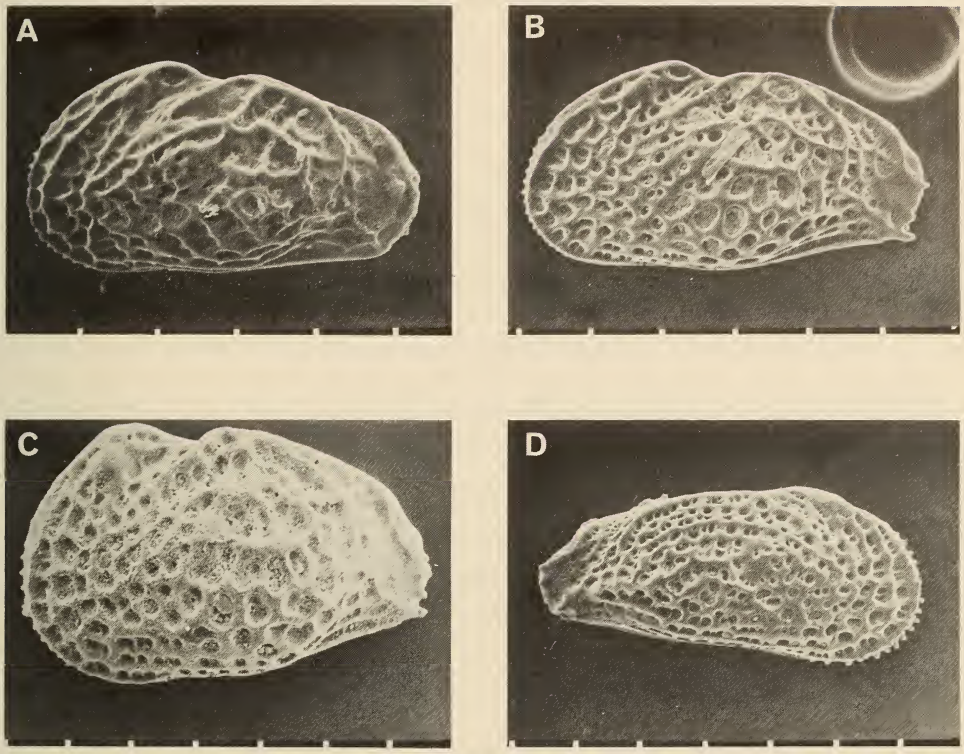

Fig. 36. A–C. *Gibberleberis africanus*. A. SAM–PC6568, LV, Umzamba bed 1, Santonian II, SEM 377. B. SAM–K5658, BH9, Richards Bay, 118,22 m, Santonian III, SEM 395. C. SAM–PC6569, LV, locality 15–7, Coniacian IV, SEM 1947.
D. *Gibberleberis elongata*, SAM–K5660, holotype, BH9 Richards Bay, 124,0 m, Santonian III, SEM 390. Scale bars = 100 μ.

Gibberleberis elongata Dingle, 1980

Fig. 36D

Gibberleberis elongata Dingle, 1980: 57–59, figs 30E–F, 31A; 1981: 111, figs 52D, 53A.

Remarks

This is a relatively rare species, which has not been encountered in Zululand Coniacian–Santonian strata at outcrop.

Age and distribution

Ranges Santonian III to Campanian II in Richards Bay BH9 borehole, and Campanian II at outcrop in Zululand (Nibela Peninsula). It has not been recorded from equivalent strata at Umzamba.

Indeterminate taxa

Indet. sp. 1874

Fig. 37A

Remarks

One poorly preserved carapace of a sub-rectangular, trachyleberid-like species. It has an overall reticulate ornamentation, a nodose dorsal longitudinal ridge, a short ventromedian longitudinal rib, and a large posteroventral spine.

Age and distribution

Santonian III, St. Lucia Formation, locality 74–10, False Bay.

Indet. sp. 1956

Fig. 37B

Remarks

One poorly preserved carapace of a trachyleberid-like species. The carapace narrows posteriorly, and is dominated in the posterior half by three short longitudinal ridges. There is a weak SCT, and an AM ridge. No details of fine surface ornamentation can be seen.

Age and distribution

Coniacian IV, St. Lucia Formation, locality 15–1, Mtubatuba.

Indet. sp. 2078

Fig. 37C

Remarks

One broken valve, probably belonging to *Cytherella*. The outline resembles most closely that of *Cytherella* sp. 2 recorded by Dingle (1980) from the Santonian to Campanian of the Richards Bay borehole.

Age and distribution

Santonian III, bed 5, Umzamba.

Indet. sp. 2103

Fig. 37D

Indeterminate species A Dingle, 1969: 380–381, fig. 20a–c (MG–1–2–1).

Remarks

No additional specimens of this species have been recorded since its original description. SEM photographs emphasize the pseudo-alate ventrolateral ridge.

Fig. 37. Indeterminate taxa. A. Indet. sp. 1874, SAM–PC6570, LV, locality 74–10, False Bay, Santonian III. B. Indet. sp. 1956, SAM–PC6571, locality 15–1, Mtubatuba, Coniacian IV. C. Indet. sp. 2078, SAM–PC6572, RV, Umzamba bed 5, Santonian III. D. Indet. sp. 2103, SAM–PC6573, RV, Umzamba bed 1, Santonian II. E–F. Indet. sp. 2104, Umzamba bed 1, Santonian II. E. SAM–PC6574, LV, SEM 2104. F. SAM–PC6575, RV, SEM 2106. Scale bars = 100 μ.

Age and distribution

Santonian II, bed 1, Umzamba.

Indet. sp. 2104

Fig. 37E–F

Indeterminate species B Dingle, 1969: 381, fig. 20d–g (MG–1–2–3a, b).

Remarks

Two worn valves, which show considerable resemblance to *Veenia obesa*. There are, however, significant points of difference: Indet. sp. 2104 lacks a distinctive SCT, and a median lateral ridge, and the CA in both valves are less prominent than in *V. obesa*. There is a superficial resemblance, mostly in valve outline, to *Akrogmocythere wamiensis* from the Turonian of Tanzania (Bate & Bayliss 1969) but Indet. sp. 2104 lacks the prominent DM ridge.

Age and distribution

Santonian II, bed 1, Umzamba.

Indet. sp. 2108

Fig. 38A

Indeterminate species C Dingle, 1969: 381, fig. 20i–h (MG–1–2–4).

Remarks

A relatively well-preserved carapace of an elongate, delicately reticulate species.

Age and distribution

Santonian II, bed 1, Umzamba.

Indet. sp. 2125

Fig. 38B

Remarks

Poorly preserved carapace and single valve of trachyleberid-like species. Both specimens encrusted with matrix, but prominent features observed are: SCT, posteriorly rising nodose ventrolateral ridge, prominent ACA.

Age and distribution

Santonian III, locality 74–12, False Bay.

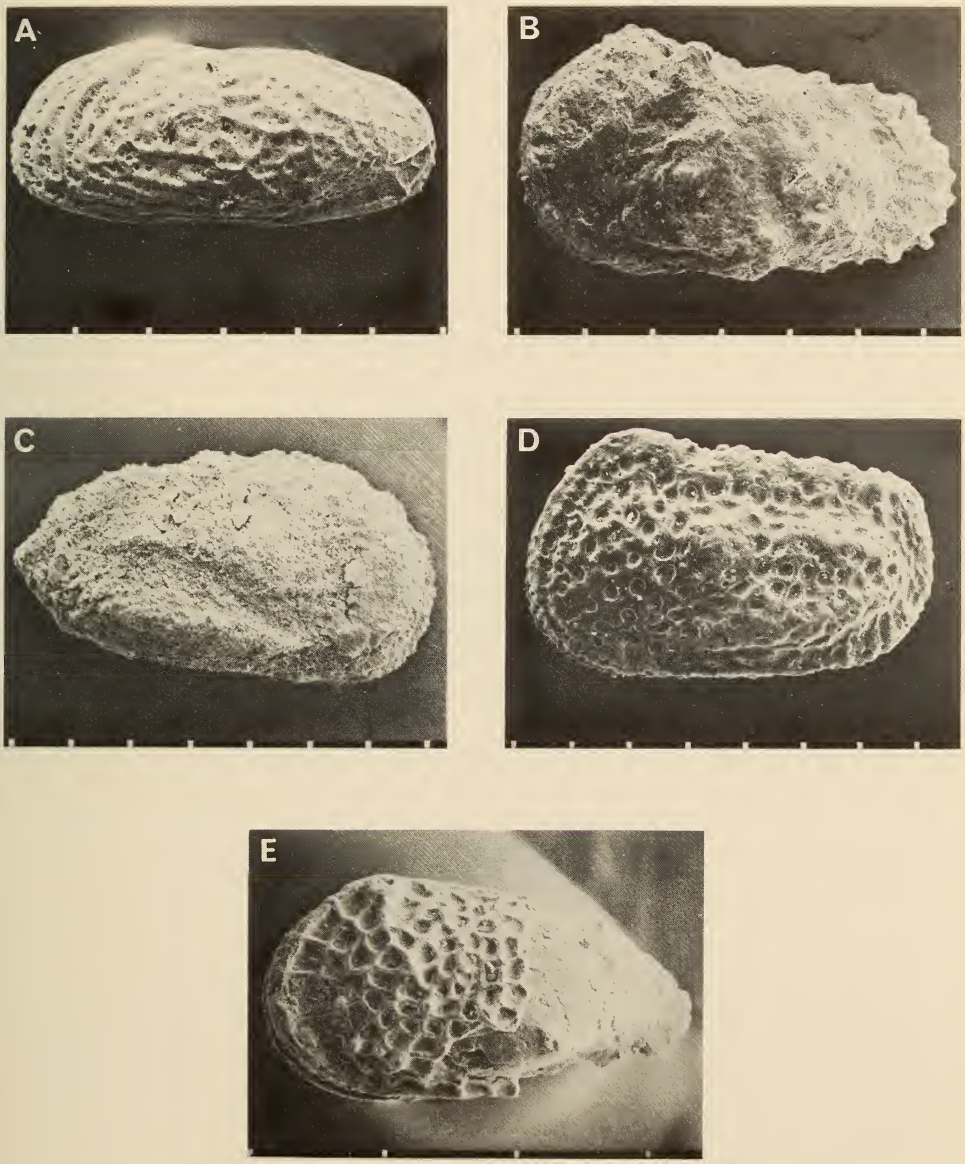

Fig. 38. Indeterminate taxa. A. Indet. sp. 2108, SAM–PC6576, LV, Umzamba bed 1, Santonian II. B. Indet. sp. 2125, SAM–PC6577, LV, locality 74–12, False Bay, Santonian III. C. Indet. sp. 2132, SAM–PC6578, RV, locality 15–1, Mtubatuba, Coniacian IV. D. Indet. sp. 2314, SAM–PC6579, LV, J(c)–1 borehole, 2 213 m, Upper Cenomanian, SEM 2313. E. Indet. sp. 2312, SAM–PC6580, J(c)–1 borehole, 2 213 m, Upper Cenomanian, SEM 2311. Scale bars: A–D = 100 μ, E = 300 μ.

Indet. sp. 2132

Fig. 38C

Remarks

Poorly preserved valve of trachyleberid-like species. Specimen encrusted with matrix, but prominent features observed are: tapering posterior outline, and three short longitudinal ridges in posterior half of valve.

Age and distribution

Coniacian IV, locality 15–1, Mtubatuba.

Indet. sp. 2312

Fig. 38E

Remarks

Fragmented valve of reticulate trachyleberid-like species. Probably possesses a prominent eyespot and conjunctive spines. Superficially similar to some species of *Oertliella*. No closely related species known from Zululand, or J(c)–1 borehole.

Age and distribution

Upper Cenomanian, J(c)–1 borehole, 2 213 m (7 260 ft).

Indet. sp. 2314

Fig. 38D

Remarks

Worn carapace of reticulate cytheracean. In overall shape and ornamentation, this species resembles several members of the genus *Rocaleberis*, which occurs in the Upper Cretaceous (Maastrichtian) of Argentina (e.g. Bertels 1976). Prominent features include: a SCT, three longitudinal ribs, rounded PM and AM, and prominent ACA. No related ostracod species are known from the Cretaceous of southern Africa and the closest correlative may be the record of *Henryhowella* sp. from the Lower Eocene–Upper Oligocene of the J(c)–1 borehole, 1 216–345 m (3 990–1 130 ft) by Dingle (1976). In this regard, the possibility of downhole contamination from younger strata cannot be ruled out.

Age and distribution

Upper Cenomanian, J(c)–1 borehole, 2 213 m (7 260 ft).

DISCUSSION

Fifty-five species of Ostracoda, belonging to at least 20 genera, have been identified from the Turonian, Coniacian, and Santonian strata of south-east Africa, and their temporal and spatial distributions are shown in Tables 1, 11, and 12. In this section, I will first discuss biostratigraphic and palaeoecological aspects of the assemblages from each of the four main areas studied (Zululand, offshore Natal, east coast, and Agulhas Bank), then consider regional correlations, and finally note some implications of ostracod distributions in a Gondwanide setting.

BIOSTRATIGRAPHY AND PALAEOECOLOGY

Zululand

At outcrop in southern Zululand, Kennedy & Klinger (1975) recognized a Coniacian I to Santonian III succession, which is separated from the underlying Cretaceous strata by an uppermost Cenomanian–Turonian non-sequence. The Turonian reported in subcrop by McLachlan & McMillan (1979) occurs farther north. Unfortunately, not all the samples that were collected through the outcrop succession were fossiliferous, but the composite sequence that it has been possible to construct, using material from the Mfolozi Valley, False Bay area, and BH9 at Richards Bay, covers most of Coniacian III to Santonian III time. The main deficiency is lack of data across the Coniacian–Santonian boundary.

Table 11 shows the distribution of ostracods in Zululand, and compares the assemblages from outcrops (Coniacian III to Santonian III) and Richards Bay BH9 (Santonian II to III). Table 12 shows the total time ranges for taxa at both BH9 and outcrop. A total of 34 species in at least 14 genera have been identified from Zululand, with 24 species (12 genera), and 24 species (13 genera) from outcrop and BH9, respectively (Table 11). Fourteen species are common to the two regions (42% similarity, although the latter figure rises to 58% if the Santonian species only are considered).

Palaeoenvironmental analyses have previously been carried out on the Santonian section of the Richards Bay borehole BH9 (Dingle 1980), and the techniques applied in that study have been employed here. In addition, because of the continuous record, and good preservation of the material from this borehole, the results will serve as a standard for comparison. This earlier work need only be summarized here and the results reviewed in the light of new data.

Because of the relatively small numbers of specimens recovered from some of the samples collected at outcrop, and the discontinuous nature of these outcrops, any palaeoenvironmental predictions made from the ostracod populations must be regarded as tentative. The only sections that give a continuous enough record to be of use are those in the Mfolozi Valley (localities 15 and 16), and at False Bay (locality 74), where Coniacian III–IV and Santonian II–III, respectively, are exposed (Figs 2, 3). The ostracod populations of these two areas

TABLE 11
Distribution of Coniacian to Santonian ostracods in Zululand.

Outcrop								BH9		
Coniacian			Santonian			Camp.	Species	Santonian		Camp.
III (16)	IV (89, 15)	V	I	II (74)	III (74, 14)	I		II	III	I
x							*Cythereis mfoloziensis*			
x	x			x	x	x—*	*Brachycythere longicaudata*	x	x	x—*
	x						*Cytherella* sp. 1929			
	x						*Cytherelloidea mtubaensis*			
	x						Indet. sp. 1956			
	x						Indet. sp. 2132			
	x						*Cythereis* cf. *luzangaziensis*			
	x						*Rayneria nealei*	x	x	x
	x			x	x		*Cytherelloidea newtoni*	x	x	
	x				x		*Haughtonileberis haughtoni*	x	x	x
	x			x	x	x—*	*Paracypris zululandensis*	x	x	x—*
	x			x	x		*Gibberleberis africanus*	x	x	
	x			x	x	x—*	*Cythereis klingeri*	x	x	x—*
	x			x	x	x—*	*Bythocypris richardsbayensis*	x	x	x—*
	x			x	x	x—*	*Cytherelloidea umzambaensis*	x	x	x—*
	x				x		*Oertliella pennata*		x	x—*
	x			x	x		*Unicapella stragulata*			
				x			Indet. sp. 2125			
				x	x		*Cytherella* sp. 2351			
				x	x	x	*Paracypris umzambaensis*	x	x	x—*
				x		x—*	*Haughtonileberis fissilis*	x	x	x—*
					x		Indet. sp. 1874			
					x		*Cythereis transkeiensis*	x		
					?x	x—*	*Bairdoppilata andersoni*	x	x	x—*
						x—*	*Brachycythere sicarius*	x	x	x—*
							Cytherella sp. 1–4	x	x	x—*
							Brachycythere pondolandensis	x	x	
							Pondoina sulcata		x	
							Amphicytherura tumida		x	x
							Cytherelloidea gardeni		x	
							Gibberleberis elongata		x	
							Oertliella sp. 476		x	x—*
							Cytherelloidea griesbachi		x	x—*
						x—*	*Haughtonileberis vanhoepeni*		x	x
Species extant:										
2	16			14	16	10	33 Con.–Sant. species 14 genera	16	23	17(+6 Camp. forms)
17			17				42 % similarity 14 spp. common	24		

( ) numbers in parentheses are localities
* = range extends above Campanian I

TABLE 12

Comparison of ranges of ostracods in Zululand (outcrops & BH9) and Umzamba.

Zululand							Species	Umzamba		
Con.			Santonian			Camp.		Sant.		Camp.
III	IV	V	I	II	III			II	III	
x							*Cythereis mfoloziensis**			
x	x			x	x	x	*Brachycythere longicaudata*	x	x	x
	x						*Cytherella* sp. 1929			
	x						*Cytherelloidea mtubaensis**			
	x						Indet. sp. 1956			
	x						Indet. sp. 2132			
	x						*Cythereis* cf. *luzangaziensis**			
	x			x	x		*Cytherelloidea newtoni**			
	x			x	x		*Gibberleberis africanus*	x	x	
	x			x	x	x	*Haughtonileberis haughtoni*	x	x	x
	x			x	x	x	*Rayneria nealei*		x	
	x			x	x	x	*Paracypris zululandensis**			
	x			x	x	x	*Cythereis klingeri**			
	x			x	x	x	*Bythocypris richardsbayensis**			
	x			x	x	x	*Cytherelloidea umzambaensis*	x	x	x
	x			x	x	x	*Oertliella pennata*		x	x
	x			x	x		*Unicapella stragulata**			
				x			Indet. sp. 2125			
				x	x		*Cytherella* sp. 2350			
				x	x		*Brachycythere pondolandensis*	x	x	
				x	x	x	*Cytherella* sp. 1–4*			
				x	x	x	*Paracypris umzambaensis*	x	x	
				x	x	x	*Haughtonileberis fissilis*	x	x	x
				x	x	x	*Bairdoppilata andersoni*		x	x
				x	x	x	*Brachycythere sicarius*		x	
					x		Indet. sp. 1874			
					x		*Cythereis transkeiensis*	x	x	x
					x		*Pondoina sulcata*	x	x	
					x		*Cytherelloidea gardeni*	x	x	
					x		*Gibberleberis elongata**			
					x	x	*Amphicytherura tumida*	x	x	x
					x	x	*Oertliella* sp. 476*			
					x	x	*Cytherelloidea griesbachi**			
					x	x	*Haughtonileberis vanhoepeni**			
							*Brachycythere rotunda***	x		
							Indet. sp. 2103**	x		
							Indet. sp. 2104**	x		
							Indet. sp. 2108**	x		
							*Veenia obesa***	x	x	
							*Paraphysocythere thompsoni***	x	x	
							Cnestocythere? sp. 2091**		x	
							Indet. sp. 2078**		x	
Species extant:										
2	16			19	27	17	42 Con. – Sant. species 36 % similarity	17	19	8
17			28				15 spp. common	23		

* confined to Zululand—13
** confined to Umzamba—8

Richards Bay & Umzamba: 32 spp, 15 common, 47 % similarity

are detailed in Table 13. Plotting these data on a Cytheracea–Cytherellidae–Bairdiacea+Cypridacea triangular diagram (CCBC plot; see Dingle 1980, 1981 for discussion) (Figs 39, 40) reveals several trends that are potentially significant as palaeoecological indicators.

The five Coniacian samples are cytheracean-dominant and cluster towards the top of the diagram close to the fields considered by Dingle (1980) in his study of the Richards Bay borehole BH9 as shallow-water (<100 m), high- and low-energy environments (assemblages 1 and 3) (Fig. 39). The composition of the Coniacian ostracod populations (Table 14) is very similar to that of the Santonian of Richards Bay (Dingle 1980), and similar environments of deposition are inferred. Factors significant in making this comparison are: (i) dominance of *Brachycythere longicaudata, Cythereis klingeri*, and *Haughtonileberis haughtoni*; (ii) dominance of the cytherellid component by species of *Cytherelloidea*; (iii) absence of *Bairdoppilata* in the Bairdiacea+Cypridacea component, which is composed of *Bythocypris* and *Paracypris*. At Richards Bay, the lower-energy environment (assemblage 3) is characterized by the dominance of *Cythereis klingeri*, so it may be possible to differentiate high- and low-energy assemblages within the Coniacian populations on the grounds of variations in the cytheracean element (Fig. 41).

In contrast, the Santonian II and III ostracod populations from the False Bay area plot in areas on the CCBC diagram that are considered predictive of relatively deep water (see Dingle 1981, fig. 75). There appear to be two distinct fields in the assemblages, one of which contains the Santonian II and lower Santonian III populations, and the other with the upper Santonian III populations (Fig. 39). The former lies in a region of the CCBC diagram for which there is no previous documentation, but which borders on field 7 that contained Maastrichtian assemblages that were considered predictive of deep water (>500 m) (Dingle 1981). Spread of the data points within the Santonian II–III field (Fig. 39) may not be significant because some of the samples contain few specimens. Its ostracod population is dominated by bairdiacean/cypridacean forms and, although *Bairdoppilata* is present, it is *Bythocypris richardsbayensis* that is the main element. In this respect, the Santonian II–III assemblages differ significantly from those of the Maastrichtian assemblage that was used to define field 7. Further important differences are the lack of blind cytheraceans, and typical deep-water markers such as *Krithe*. Furthermore, the presence of various cytheracean elements that are dominant in shallow-water assemblages (e.g. *Brachycythere longicaudata, Cythereis klingeri*, and *Haughtonileberis haughtoni*) suggests that the Santonian II–III field represents deposition in water significantly shallower than field 7. However, because of the overall subordination of cytheracean types, it is considered somewhat deeper than fields to the north of the '*Bythocypris*' line. Overall, the characteristics of this field seem closer to those of 4a (which has a predictive water depth of 100–200 m) than 7, and is referred to as 4c; a predictive intermediate water depth of 300 m is tentatively assigned to it.

TABLE 13

Distribution of ostracods from Zululand outcrops, expressed as percentages of total population.

	Coniacian III	Coniacian IV				Santonian II	Santonian III							
Locality no.	16	15				74	74							
Bed no.	1	1	3	5	7	9	10	10	11	11	12	13	14	15
Subdivision							1	2	1	2				
CYTHERACEA	100	65	100	84	91	35	21	—	33	66	46	47	50	42
Cythereis mfoloziensis	33													
Haughtonileberis haughtoni				10	29		7				15	13		4
Brachycythere longicaudata	66			21	26	16			33		31	27	50	13
Cythereis cf. *luzangaziensis*				2										
Gibberleberis africanus					10	6								17
Rayneria nealei				5	10									
Cythereis klingeri		65	100	40	10	10	7			66				
Oertliella pennata				6	3		7							8
Unicapella stragulata					3	3						7		
CYTHERELLIDAE	—	24	—	10	10	32	14	—	—	33	23	20	—	13
Cytherelloidea mtubaensis		18												
Cytherelloidea newtoni				2		6						13		
Cytherella spp.		6		8		23	14			33	15	7		13
Cytherelloidea umzambaensis					10	3					8			
BAIRDIACEA & CYPRIDACEA	—	12	—	8	—	42	71	100	67	—	31	34	50	42
Bythocypris richardsbayensis		12		5		29	57				31	7	50	17
Paracypris umzambaensis						3		100				27		
Bairdoppilata andersoni														25
Paracypris zululandensis				3		10	14		67					
Smoothed data (3 point means)														
Cytheracea	83	88	83	92	98	26	19	18	33	48	53	48	46	46
Cytherellidae	12	8	11	7	10	21	17	5	11	19	25	14	11	7
Bairdiacea & Cypridacea	6	4	7	3	4	53	71	79	56	49	22	38	42	46
No. valves per sample	3	17	2	63	31	31	14	3	6	3	13	15	8	24

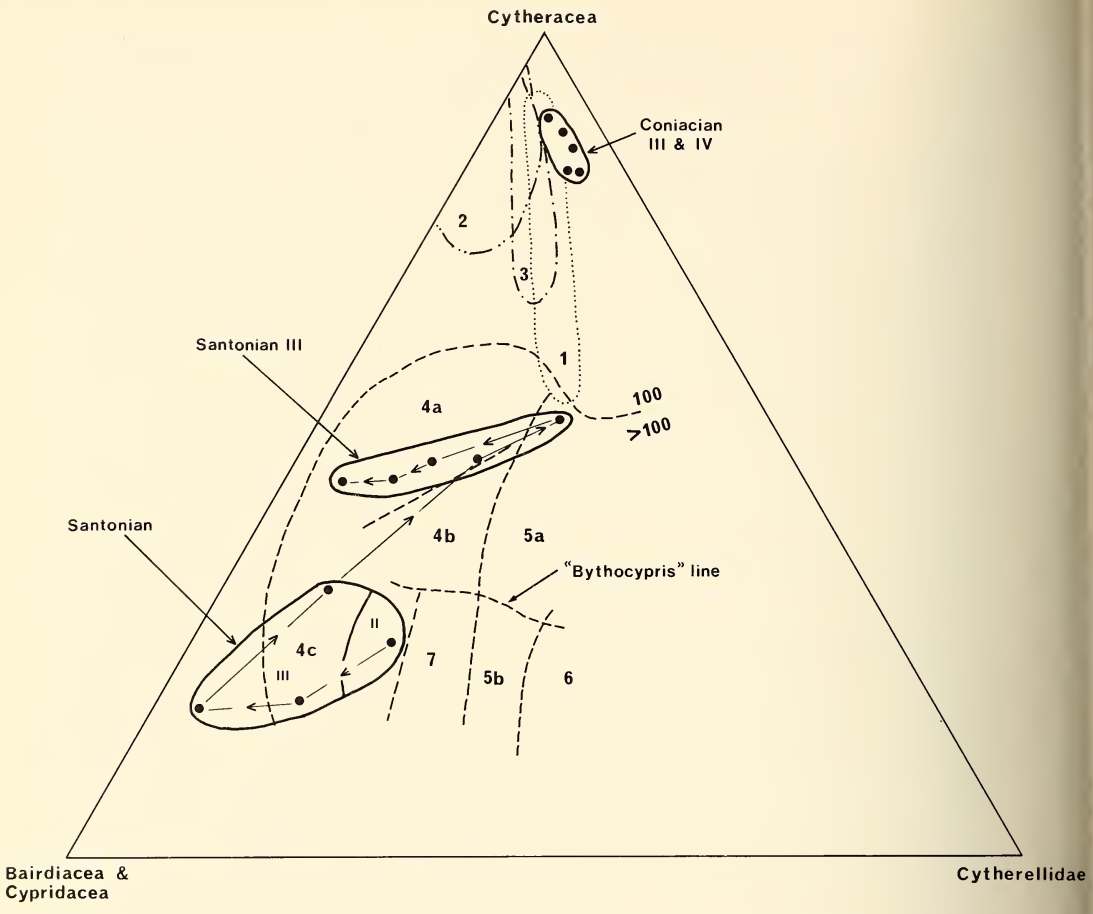

Fig. 39. Cytheracea–Cytherellidae–Bairdiacea+Cypridacea triangular diagram (CCBC plot) of the various populations (solid circles) from the Coniacian to Santonian strata of Zululand. Fields 1, 2, 3, 4a, 4b, 5a, 5b, 6 and 7 have previously been defined by Dingle (1980, 1981). See text for explanation.

The younger Santonian III populations from locality 74 (Table 14) scatter across the CCBC diagram in the vicinity of field 4a (Fig. 39). Comparison with the original ostracod assemblages (Campanian I of BH9) used to establish this field (see Dingle 1981, table 6) shows that the only significant difference is the dominance of *Bythocypris richardsbayensis* in the bairdiacean component of the False Bay samples in contrast to *Bairdoppilata andersoni*, which plays an analagous role in the Richards Bay samples. I have no hesitation in assigning the upper Santonian III populations to this assemblage field and predicting a depositional environment of 100–200 m. Only the position of the sample on the right-hand side of the field is in doubt. It may indicate a temporary water depth shallowing to *c.* 100 m, but because the 'event' is predicted by one sample its

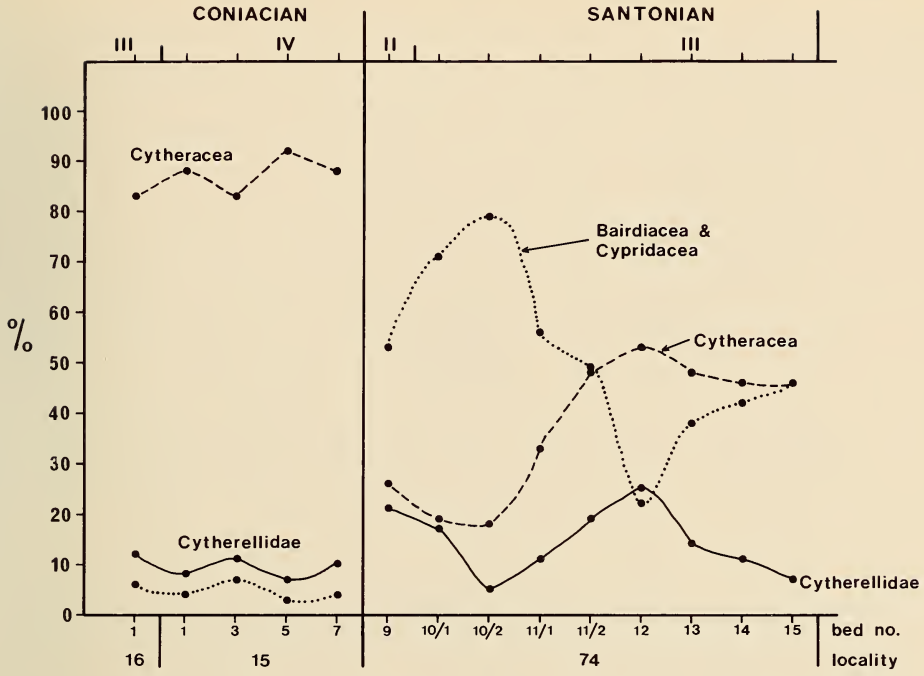

Fig. 40. Temporal trend of major groups (as percentage of total ostracod population) in Zululand outcrops. Data are three-point running means.

significance is difficult to assess, other than to suggest that a somewhat shallower water environment may be located in this field.

Palaeoecological and predicted sedimentary environments for the Santonian section of the Richards Bay BH9 borehole have been fully discussed in Dingle (1980). These data have been incorporated in various figures referred to below.

Dingle *et al.* (1983) have discussed some of the palaeoenvironmental aspects of Upper Cretaceous sedimentation in Zululand, and have stressed the onlapping nature of the Upper Cretaceous transgression that was first recognized by Kennedy & Klinger (1971). The BH9 borehole site lies to the south of the Eteza Fault on the crest of a basement feature referred to as the Richards Bay Arch. Differential vertical movements were recognized between this area and the basin farther north under the Zululand coastal plain. The data acquired during the present study allow modifications to be made to the model presented by Dingle *et al.* (1983).

Figure 42 shows a tentative temporal and spatial correlation of depositional environments along a transect between the False Bay–Nibela Peninsula area, the Mfolozi Valley, and BH9 (100 km in length). The diachronous nature of the post-Turonian transgression is well illustrated, with Coniacian I, Coniacian II,

TABLE 14

Characteristics of Coniacian and Santonian ostracod assemblages from Zululand (Mfolozi Valley and False Bay).

	Coniacian III–IV	Sant. II & Lower Sant. III	Upper Santonian III
Dominant (>20%, >1 sample)	*Brachycythere longicaudata* *Cythereis klingeri*	*Paracypris zululandensis*	*Brachycythere longicaudata* *Bythocypris richardsbayensis*
Secondary (>10%, >1 sample)	*Haughtonileberis haughtoni*	*Brachycythere longicaudata* *Cytherella* sp. *Bythocypris richardsbayensis*	*Haughtonileberis haughtoni* *Cytherella* sp.
Tertiary (>5%, >1 sample)	*Rayneria nealei* *Bythocypris richardsbayensis* *Cytherella* sp.	*Cythereis klingeri* *Paracypris umzambaensis*	*Cytherelloidea newtoni*
Minor (>5%, 1 sample)	*Cythereis mfoloziensis* *Gibberleberis africanus* *Oertliella pennata* *Cytherelloidea mtubaensis* *Cytherelloidea umzambaensis*	*Haughtonileberis haughtoni* *Gibberleberis africanus* *Oertliella pennata* *Cytherelloidea newtoni*	*Bairdoppilata andersoni* *Cythereis klingeri* *Oertliella pennata* *Unicapella stragulata* *Cytherelloidea umzambaensis*
Other features	No *Bairdoppilata* Dominance of *Cytherelloidea* in Cytherellidae	No *Bairdoppilata* Dominance of *Cytherella* in Cytherellidae *Brachycythere longicaudata* is main cytheracean	*Bairdopillata* present
	No. species = 17 Diversity = 15%	No. species = 12 Diversity = 22%	No. species = 15 Diversity = 24%
PALAEOECOLOGY Water depth Equivalent fields on CCBC diagram.	<100 m 1 & 3	?300 m 4c	100–200 m 4a

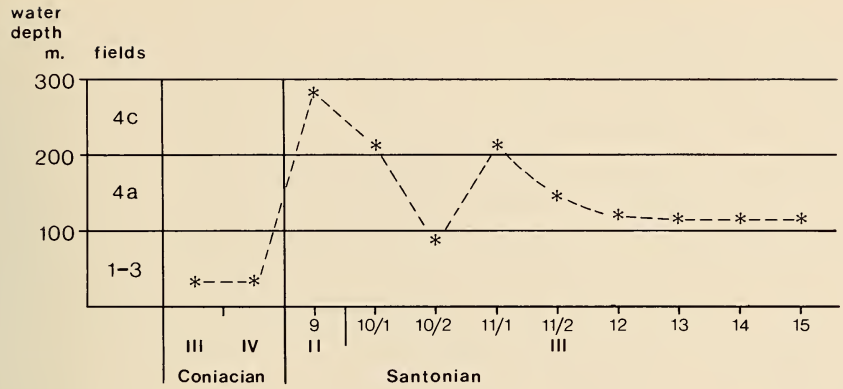

Fig. 41. Summary of predicted temporal water-depth variations at Zululand outcrops based on the CCBC plot in Figure 39. Coniacian localities are in the Mfolozi Valley; Santonian locality (74) is at False Bay. Bed numbers are shown on horizontal axis. Age decreases to the right.

and Santonian II basal sediments at the three localities, respectively, although fossiliferous samples were available only from the first two sites. Despite their age differences, both have very similar ostracod faunas that are characterized by robust cytheraceans *Brachycythere longicaudata, Haughtonileberis haughtoni*, and *Cythereis klingeri*. At BH9, where there is a continuous cored section, the Santonian II to Campanian II sequence appears to show an uninterrupted progression from shallow- (<100 m), through medium- (100–200 m), to deep-(>300 m) water sedimentary environments. Farther north, in the Mfolozi Valley, I have no data to establish the Coniacian V to Santonian I palaeoenvironments, but suspect that it also represents a progression from shallow (Coniacian III–IV), through medium (Campanian II to III), to deep (Campanian IV) water conditions. This correlation suggests that similar sedimentary conditions to those that prevailed during the uppermost Santonian III to mid-Campanian II medium water-depth environments in BH9 were established over the Mfolozi Valley area for the whole of the Coniacian V or Santonian I to lowermost Campanian IV time span.

Information from the False Bay Nibela Peninsula area is less complete. It is reasonable to assume that the earliest sedimentary environment (Coniacian I) was also shallow water, high energy, so that similar ostracod populations to those found at the two southerly sites can be anticipated here. However, I cannot substantiate this assumption. Higher in the sequence, conditions cannot be predicted, and the available data are not easy to assess because only short pre-upper Campanian sections contained ostracod faunas. In particular, the upper Santonian II–III section commences with a relatively deep-water (300 m) ostracod assemblage that is immediately overlain by medium (100–200 m) water-depth assemblages assigned to field 4a on the CCBC diagram. The simplest

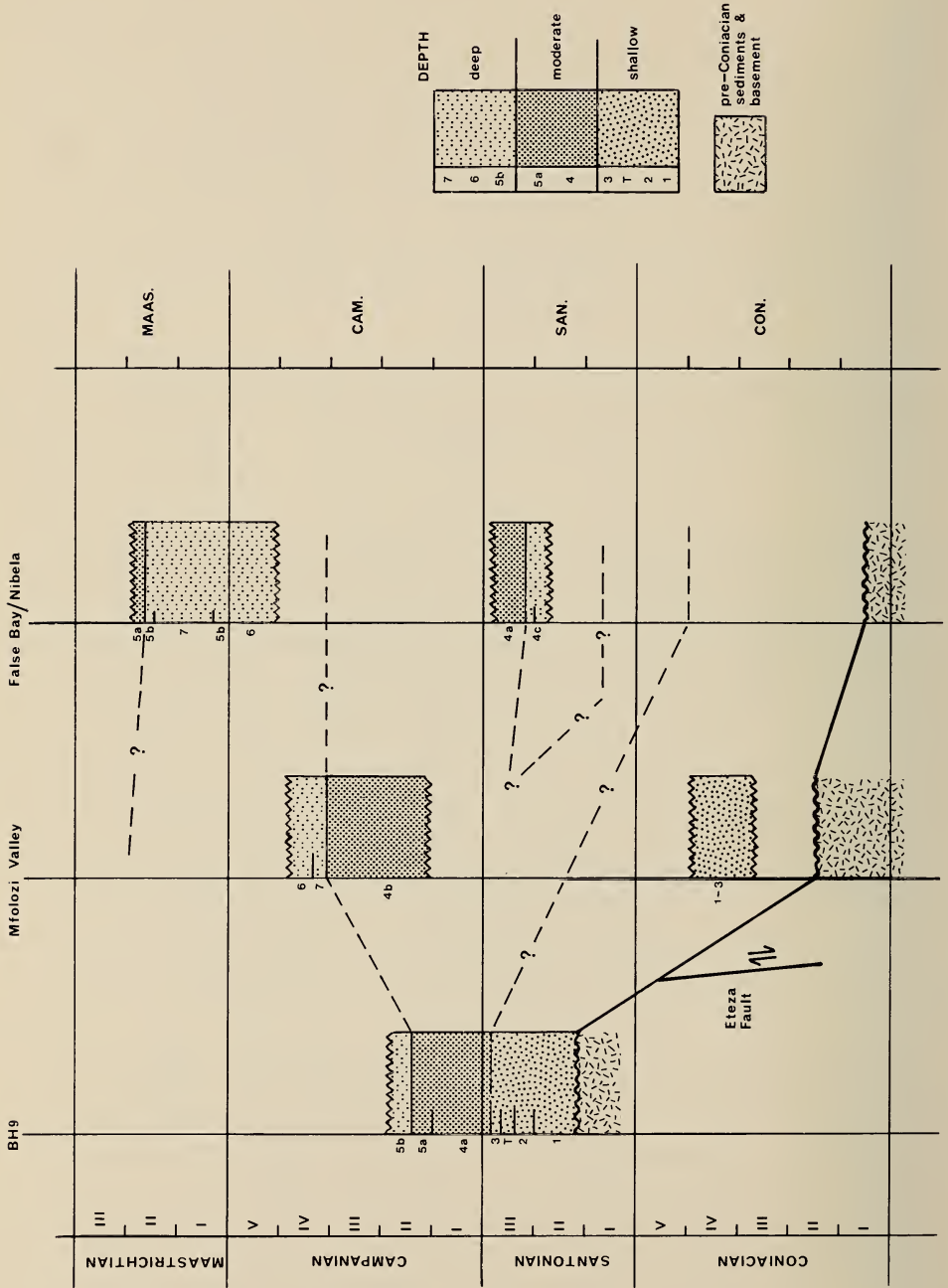

Fig. 42. Temporal and spatial water-depth variations in the Coniacian to Maastrichtian strata of Zululand from the Richards Bay borehole (BH9) (south) to the False Bay–Nibela area (north). Small numbers at left side of columns are fields on CCBC plots (Dingle 1980, 1981, this paper).

correlation (Fig. 42) is that this represents a deep-water episode that may not have penetrated as far south as the Mfolozi area, although critical data around the Coniacian–Santonian boundary are lacking. Deep-water environments were definitely established in the Nibela area by late Campanian times, and, with some fluctuation, persisted until the rapid shallowing that commenced in Maastrichtian II. The diachronous nature of these major sedimentary environmental changes is well illustrated in Figure 42: the shallow–medium boundary ranges from north to south (?late Coniacian to ?early Santonian to latest Santonian) and the medium–deep water boundary ranges south to north (mid-Campanian II to lower Campanian IV to ?Campanian IV).

Considering these data in terms of water-depth curves (Fig. 43) suggests that the sedimentary environments shown on Figure 42 cannot be explained simply in terms of eustacy. Dingle *et al.* (1983) have predicted differential vertical movements between the Richards Bay Arch and the region lying to the north, and in particular, that during Campanian I–II times, the crest of the arch (i.e. BH9 site) subsided more rapidly than the basin to the north (water depths at this time were greatest over the arch). The new data also suggest that once the Mfolozi area had subsided to an approximate water depth of 100–200 m (by Coniacian IV), it remained at this depth until early Campanian time. This presumably resulted from one, or a combination, of the following: eustatic still-stand and no sediment accumulation, sediment accumulation at the same rate as a sea-level rise, crustal subsidence and sediment accumulation compensating for either a eustatic sea-level rise or still-stand. Because there is no evidence for either abnormally thick sediments, or temporally extensive condensed sequences, I favour a slow sediment-accumulation rate coupled with a slow eustatic sea-level rise. This raises a further ambiguity in the False Bay area, where relatively deep-water conditions were followed by shallowing that coincided with the inundation of the Richards Bay Arch. The attainment of deep-water conditions at the northernmost site,

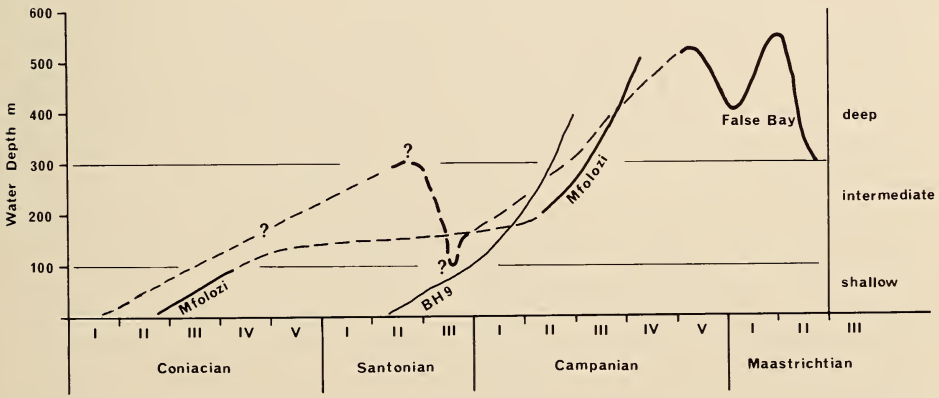

Fig. 43. Water-depth fluctuations during the Upper Cretaceous transgression at three Zululand localities. Based on the CCBC plot (Fig. 39) and Dingle (1980, 1981).

which experienced the transgression earliest, is not difficult to envisage if a faster rate of crustal subsidence compared to the Mfolozi area obtained here, but the Santonian III shallowing suggests either crustal uplift of 100–200 m, rapid sedimentation outstripping the rising sea level effectively elevating the sea floor, or a combination of slight crustal uplift and a moderate increase in the sediment-accumulation rate. Since a period of slow sea-level rise (in the Mfolozi Valley) during Santonian to early Campanian time has already been postulated, the option of an increase in the sedimentation rate perhaps coupled with a decrease in crustal subsidence seems most attractive. As noted earlier, the non-coincidence of the more regularly curved portions of the graphs during early Campanian time strongly suggest that differential crustal movements and sediment accumulation rates must be anticipated over the whole of this region.

In Zululand 34 species have been recognized from Coniacian–Santonian strata, with 17 each from Coniacian and Santonian outcrops, and 24 from the Santonian of BH9. Because of their good state of preservation and completeness of the record, the ranges obtained from BH9 are probably more reliable. Tables 11 and 12 show the ranges of the ostracod species by stages, following the ammonite zonation scheme of Kennedy & Klinger (1975), while Table 15 shows species that are confined to each stage, and Table 16 lists the order of appearance of important Upper Cretaceous species.

It is clear from these data that despite the relative sparseness of many of the assemblages, which in some cases at least was occasioned by poor preservation, the Coniacian ostracod populations contained most of the main elements that characterized later Upper Cretaceous faunas. This indicates that these long-ranging taxa aggressively colonized the continental margins of south-east Africa as soon as local circumstances allowed, following the initiation of the Upper Cretaceous transgression. Table 16, for instance, shows that 14 per cent of the Maastrichtian taxa appeared in the Coniacian, and that this figure grows rapidly to 36 per cent for the Santonian. Prominent in this list are species that form significant components of the overall post-Coniacian populations: *Brachycythere longicaudata, Cythereis klingeri, Haughtonileberis haughtoni*, and *Bythocypris richardsbayensis*. Only four additional long-ranging species joined the list during Santonian time. It can be established, therefore, that the underlying character of the Upper Cretaceous faunas was established rapidly after the Cenomanian–Turonian hiatus, and was not acquired over a long period of time.

Only three species (20%) are confined to the Zululand Coniacian strata (Table 15), two of which are closely related. One (*Cythereis* cf. *luzangaziensis*) is likened to a species from the Turonian of Tanzania, and the other (*Cythereis mfoloziensis*) may be ancestral to the long-ranging *Cythereis klingeri*. None of these three short-range species have been found to occur abundantly, and at this state of knowledge it is not possible to identify taxa that indicate unequivocally a Coniacian, in contradistinction to a Santonian, age. Reliance has to be placed on the fact that certain other taxa, typical of the younger strata, do not occur.

TABLE 15

Age ranges of Coniacian and Santonian ostracods in south-east Africa.

Restricted to Coniacian	
Zululand	Agulhas Bank
Cythereis mfoloziensis	*Apateloschizocythere?* cf. *mclachlani*
Cytherelloidea mtubaensis	*Brachycythere agulhasensis*
Cythereis cf. *luzangaziensis*	

Restricted to Santonian	
Zululand	Umzamba
Cythereis transkeiensis	
Brachycythere pondolandensis	*Brachycythere pondolandensis*
Pondoina sulcata	*Pondoina sulcata*
Cytherelloidea gardeni	*Cytherelloidea gardeni*
Gibberleberis elongata	
	Brachycythere rotunda
	Paracypris umzambaensis
	Veenia obesa
	Gibberleberis africanus
	Paraphysocythere thompsoni
	Brachycythere sicarius
	Cnestocythere? sp. 2091
	Rayneria nealei
	Indet. sp. 2103
	Indet. sp. 2104
	Indet. sp. 2108
	Indet. sp. 2078

TABLE 16

Rates of appearance of Zululand ostracod species.

Long-range species appearing in:			
Coniacian		Santonian	
Brachycythere longicaudata	(–Maas.)	*Cythereis transkeiensis*	(–?Maas.)
Cythereis klingeri	(–Maas.)	*Brachycythere sicarius*	(–Maas.)
Bythocypris richardsbayensis	(–Maas.)	*Haughtonileberis fissilis*	(–Maas.)
Cytherella sp. 1–4	(–Maas.)	*Bairdoppilata andersoni*	(–Maas.)
Paracypris zululandensis	(–?Maas.)		
Rayneria nealei	(–Camp.)		
Haughtonileberis haughtoni	(–Camp.)		
Oertliella pennata	(–Camp.)		
Cytherelloidea umzambaensis	(–Camp.)		

Zululand species extant in:	Percentage appearing in: Coniacian	Santonian
Maastrichtian	5/37 = 14%	9/37 = 24%
Campanian	9/40 = 23%	20/40 = 50%
Santonian	12/33 = 36%	

(upper limits shown in parentheses)

Twenty-six species have been recorded from the Santonian of Zululand, 24 of which occur at BH9, and only 17 farther north. Seventeen of these range into the Campanian, where they constitute 50 per cent of the fauna of that stage. In contrast to the Coniacian, there are two relatively well-represented species that are confined to this stage in Zululand, and which are potentially useful stage indices (Table 15): *Brachycythere pondolandensis* and *Pondoina sulcata*, although both have been recorded so far only from BH9. It is possible that their distribution is climatically controlled because they are more abundant farther south at Umzamba, and this aspect will be discussed later in a regional context. Similarly, there are several other species that are typical of Santonian III strata at BH9 (though not confined to them) that do not occur, or are poorly represented farther north: viz. *Amphicytherura tumida, Cytherelloidea griesbachi, Gibberleberis elongata* and *Haughtonileberis vanhoepeni.*

Considering the Coniacian–Santonian fauna of Zululand as a whole, several species appear to be characteristic of the combined stages (Table 12): *Cytherelloidea newtoni, Gibberleberis africanus*, and *Unicapella stragulata.* The last-named is the earliest-known representative of the subfamily Unicapellinae.

Umzamba

Twenty-three species of ostracods have been recorded from the Santonian strata at Umzamba, eight of which (35%) are restricted to the area (Table 12).

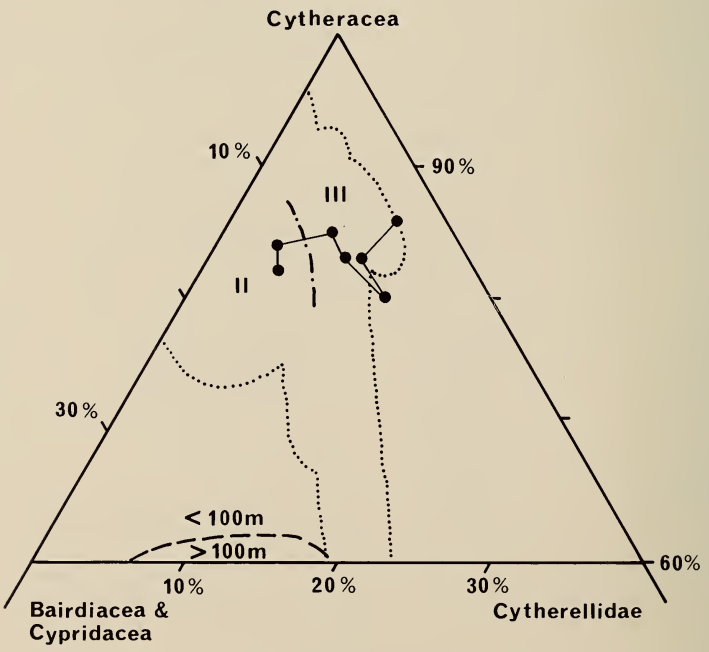

Fig. 44. CCBC plot of Santonian II and III ostracod populations with more than 20 specimens from Umzamba. The data points are joined in ascending order.

This high percentage of endemism gives the Umzamba faunas a distinctive compostion. Because the younger sediments at the Umzamba outcrops are partly decalcified, data on the extension of ostracod ranges into Campanian strata are probably incomplete, but what information there is suggests that several species are confined to the Santonian. This assemblage is considered to be a marker for the 'southern' (Umzamba) Santonian ostracod faunas: *Brachycythere pondolandensis, Pondoina sulcata, Cytherelloidea gardeni, Veenia obesa*, and *Paraphysocythere thompsoni*. The last two species are known only from the Umzamba area and, because they occur relatively abundantly, are particularly useful elements.

Figure 44 shows the ostracod populations (with >20 specimens) from Umzamba plotted on a CCBC diagram. All the samples plot within the shallow-water (<100 m) field and there may be a subdivision between the Santonian II and III populations: the former lie to the left side of the diagram within the field of assemblage 2 from BH9 (Dingle 1980), while the latter lie within the areas overlapped by assemblages 1 and 3 and those from the Zululand outcrops. These data indicate that the Santonian assemblages at Umzamba were deposited in shallow water, with Santonian II possibly having restricted circulation that modified to more open environments higher up the sequence. They also show that the depositional environments at Umzamba during Santonian II and III were similar to those that obtained in Santonian II and III at Richards Bay, and Coniacian III and IV in the Mfolozi Valley.

Borehole J(c)–1

Table 4 shows the distribution of ostracods in the lower part of the J(c)–1 borehole. Two aspects are immediately apparent: the overall sparsity of the fauna (42 valves from 25 available samples, only 12 of which contained ostracods), and the relative lack of cytheracean specimens (12 valves, 29% of total fauna). In addition, many of the carapaces are fragmented, and only 50 per cent of the fossiliferous samples contain more than one carapace. These limitations make any palaeoecological assessment speculative.

The following associations may be significant:

1 981–2 042 m (Santonian)—relatively diverse zone with *Bairdoppilata, Bythocypris, Dutoitella,* and *Cytherella*.

2 054–2 103 m (Santonian–Coniacian)—barren of ostracods, abundant *Inoceramus* prisms and pyrite crystals.

2 115–2 140 m (Coniacian–Turonian)—sparse fauna of *Cytherella* and indeterminate smooth forms.

2 152–2 201 m (Turonian–uppermost Cenomanian)—zone with *Krithe* and *Bairdoppilata*, and indeterminate forms.

2 213–2 237 m (Upper Cenomanian)—zone with cytheraceans, *Bairdoppilata, Bythocypris*, and two indeterminate smooth forms.

2 249–2 297 m (Upper Cenomanian to base of borehole)—zone barren of ostracods except for one pyritic cast of possible *Cytherella*.

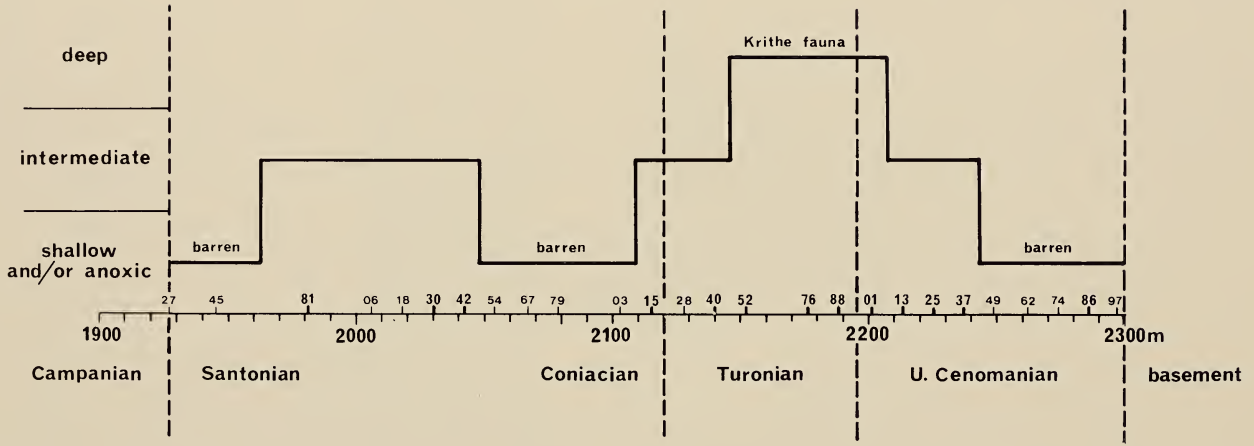

Fig. 45. Speculative environments of deposition and water depth in the lower part of the J(c)–1 borehole. Barren zones are taken to indicate anoxic and/or shallow (i.e. hyposaline) water. *Krithe*-bearing horizons denote relatively deep water, and other faunas are intermediate. Horizontal axis indicates depth downhole in metres, with picked horizons noted above the line (bold numbers indicate ostracod-bearing samples).

The presence of planktonic foraminifera throughout the sequence indicates that the Tugela delta top was connected to the open ocean, but the alternations of barren sequences and the intermittent presence of freshwater charophytes, and a zone with *Krithe* suggests that water depths fluctuated in the manner shown in Figure 45. The two barren sections (2 054–2 103 m and 2 249–2 297 m) are separated by a zone containing *Krithe*, above and below which lie zones containing sparse faunas. The barren sequences may indicate very shallow water (with strong hyposaline characters) and/or periods of anoxic bottom conditions, while the zone with *Krithe* probably indicates moderately deep water (?200 m, see Dingle 1981). This succession may reflect a period of progressively deepening water from Upper Cenomanian to a peak in early–mid-Turonian times, followed by a shallowing and/or decrease in oxygen content of bottom waters, that culminated in the Coniacian barren episode. The Santonian sequences suggest intermediate water depths that possibly shallowed at the end of the period and remained so into the early Campanian (see Dingle 1981, fig. 73). The paradox in this interpretation is that the predicted maximum water depths on the Tugela delta top occur during the Turonian, when evidence from Zululand indicates a withdrawal of the sea and the formation of a major mid-Cretaceous non-sequence. If this interpretation is valid, then the implication is that subsidence on the Tugela delta top was greater than any regional sea-level fall.

Agulhas Bank

Although the Coniacian samples dredged from the Agulhas Bank contained a variety of mollusca, their ostracod faunas were sparse: two species only in sample TBD 510 (*Apateloschizocythere?* cf. *mclachlani* and *Brachycythere agulhasensis*). The former species is close to *A. mclachlani* from the Campanian III of Zululand, but *B. agulhasensis* is distinct from the *Brachycythere* faunas farther north. The paucity of the Agulhas Bank fauna prevents any meaningful biostratigraphic comparisons. From their study of the *Inoceramus* shells, Klinger *et al.* (1980) concluded that the Coniacian depositional environment at site TBD 4510 lay on the inner shelf, with low sedimentation rates and moderately strong bottom currents. This site was only 20 km from site TBD 510, so similar conditions may have obtained during the deposition of the ostracod valves, although we have no additional data to substantiate this possibility.

REGIONAL CONSIDERATIONS

SOUTH-EAST AFRICA

The Coniacian to Santonian ostracod faunas of south-east Africa are of great interest because they document the history of recolonization after the widespread mid-Cretaceous (late Cenomanian–late Turonian) hiatus. The significant dichotomy in the ostracod faunas across this event was recognized by Dingle (1982), but at that time no taxonomic studies had been made on the Coniacian faunas. In this section various aspects of regional biostratigraphy and palaeo-

ecology will be discussed, primarily comparing and contrasting the Umzamba and Zululand regions.

Ostracod zonation

Sufficient data are now available to attempt a preliminary zonation of the Santonian strata of south-east Africa using their ostracod faunas (Fig. 46). Because of regional contrasts in the overall ostracod populations (discussed below), three schemes are needed to effect correlation across the whole Umzamba to False Bay region. The schemes will be defined, then discussed.

Umzamba

***Veenia obesa* Zone**—restricted to early Santonian II. *Definition*: period marked by the presence of *Veenia obesa*, and ending with the first appearance of *Brachycythere pondolandensis* with *Gibberleberis africanus*. *Remarks*: carries a relatively limited fauna that is dominated by *Brachycythere longicaudata*, *Haughtonileberis haughtoni*, and *Pondoina sulcata*, with rare *Brachycythere rotunda*.

***Gibberleberis africanus–Brachycythere pondolandensis* Zone**—range mid-Santonian II to mid-Santonian III. *Definition*: period marked by the presence of *Gibberleberis africanus* together with *Brachycythere pondolandensis*. *Remarks*: can be divided into two subzones. The upper limit is not well controlled between two widely spaced sampling horizons.

***Cytherelloidea gardeni* Subzone**—range mid-Santonian II to early Santonian III. *Definition*: period marked by the presence of *Gibberleberis africanus* with *Brachycythere pondolandensis* and *Cytherelloidea gardeni*. *Remarks*: lowermost part of this subzone coincides with the appearance of several important species: *Cytherelloidea umzambaensis, Cythereis transkeiensis, Paraphysocythere thompsoni*, and *Haughtonileberis fissilis*. Towards the top, *Oertliella pennata* and *Brachycythere sicarius* first appear.

Un-named Subzone—restricted to mid-Santonian III. *Definition*: period marked by the presence of *Gibberleberis africanus* with *Brachycythere pondolandensis* above the last appearance of *Cytherelloidea gardeni*. *Remarks*: during this period, *Veenia obesa* and *Paraphysocythere thompsoni* reach the top of their range, while the local first appearances of *Rayneria nealei* and *Bairdoppilata andersoni* are recorded.

***Amphicytherura tumida* Zone**—range late Santonian III to Campanian (upper limit not known). *Definition*: period marked by the presence of *Amphicytherura tumida* above the last appearance of the *Gibberleberis africanus–Brachycythere pondolandensis* combination. *Remarks*: no species are known to make their appearance in this zone, but the last appearances of *Pondoina sulcata* and *Rayneria nealei* occur near the top.

Richards Bay borehole BH9

***Cytherelloidea newtoni* Zone**—restricted to early Santonian II. *Definition*: period marked by the presence of *Cytherelloidea newtoni*, and ending with the appearance of the *Gibberleberis africanus–Brachycythere pondolandensis* combination. *Remarks*: carries a restricted fauna of *Brachycythere longicaudata, Paracypris* spp., and rare *Cythereis transkeiensis*. At the top of the zone *Cytherella* sp. and *Rayneria nealei* make their local appearance.

***Gibberleberis africanus–Brachycythere pondolandensis* Zone**—range mid-Santonian II to mid-Santonian III. *Definition*: period marked by the presence of *Gibberleberis africanus* together with *Brachycythere pondolandensis*. *Remarks*: carries a diverse fauna, with first appearances of several important species in the lower part. Characterized by the presence of *Brachycythere longicaudata, Rayneria nealei*, and *Cythereis klingeri*. The local range of *Pondoina sulcata* coincides with the lower part of this zone.

***Amphicytherura tumida* Zone**—range mid- to late Santonian III. *Definition*: period marked by the presence of *Amphicytherura tumida* between the last appearance of *Gibberleberis africanus* with *Brachycythere longicaudata* and the first appearance of *Haughtonileberis vanhoepeni*. *Remarks*: no species are known to make their appearance in this zone, but it includes the upper local ranges of *Cytherelloidea newtoni* and *Gibberleberis africanus*.

***Haughtonileberis vanhoepeni* Zone**—range late Santonian III. *Definition*: period that begins with the appearance of *Haughtonileberis vanhoepeni* and ends with the first appearance of *Amphicytherura zululandensis*. *Remarks*: the upper boundary of this zone probably coincides with the Santonian III–Campanian I boundary. This short zone has no short-range species, but is marked by the appearance of *Gibberleberis elongata* and *Oertliella* sp. 476.

Zululand outcrops

Because of the relative sparseness of the faunas and the relatively few outcrops involved in this study, it has not been possible to devise a satisfactory zonal scheme for this area, either internally, or for correlation with regions to the south. As a preliminary measure, almost the whole Coniacian IV–Santonian III sequence has been placed in one zone, which can be subdivided as more data become available.

***Gibberleberis africanus–Unicapella stragulata* Zone**—range mid-Coniacian IV to late Santonian III. *Definition*: period marked by the presence of *Gibberleberis africanus* together with *Unicapella stragulata*. *Remarks*: only the presence of *Unicapella stragulata* distinguishes this zone from rocks of similar ages farther south, while the remainder of the fauna, with *Brachycythere longicaudata, Haughtonileberis haughtoni* and *Cythereis klingeri*, has a similar content to that in the BH9 borehole.

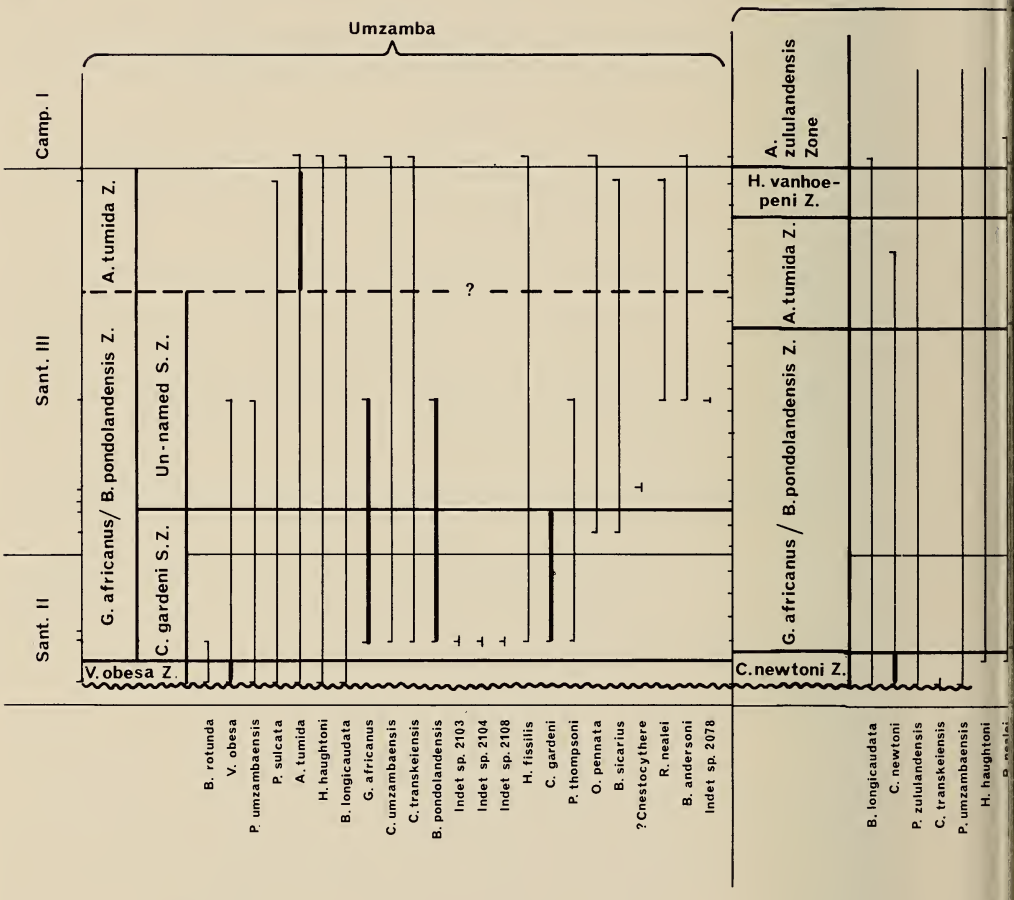
Umzamba
Camp. I
Sant. III
Sant. II
A. tumida Z.
G. africanus/ B. pondolandensis Z.
C. gardeni S. Z.
Un-named S. Z.
V. obesa Z.
?
A. zululandensis Zone
H. vanhoe-peni Z.
A. tumida Z.
G. africanus / B. pondolandensis Z.
C. newtoni Z.
B. rotunda
V. obesa
P. umzambaensis
P. sulcata
A. tumida
H. haughtoni
B. longicaudata
G. africanus
C. umzambaensis
C. transkeiensis
B. pondolandensis
Indet sp. 2103
Indet sp. 2104
Indet sp. 2108
H. fissilis
C. gardeni
P. thompsoni
O. pennata
B. sicarius
?Cnestocythere
R. nealei
B. andersoni
Indet sp. 2078
B. longicaudata
C. newtoni
P. zululandensis
C. transkeiensis
P. umzambaensis
H. haughtoni

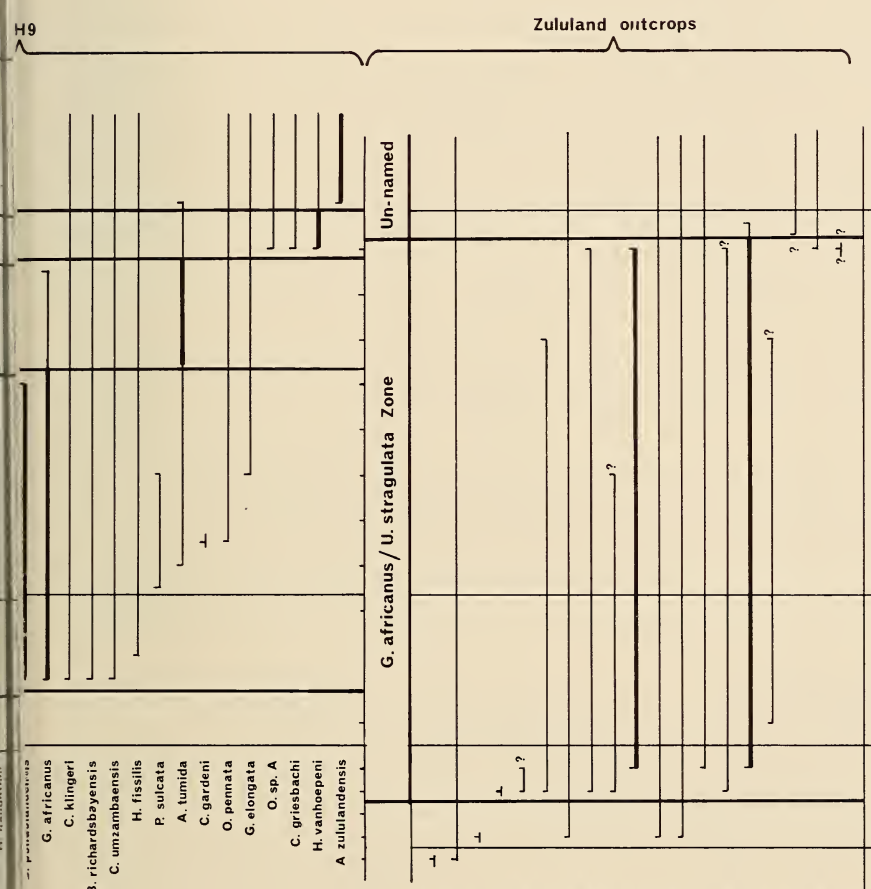

Fig. 46. Basis of proposed ostracod zonation at Umzamba, BH9 (Richards Bay), and the Zululand outcrops in the Mfolozi Valley and False Bay areas. Bold vertical lines indicate zonal boundaries, and bold species ranges are those used in defining zone limits. Ticks on horizontal lines at the top of each locality indicate position of ostracod-bearing samples relative to ammonite zones.
Z = Zone, S.Z. = Subzone.

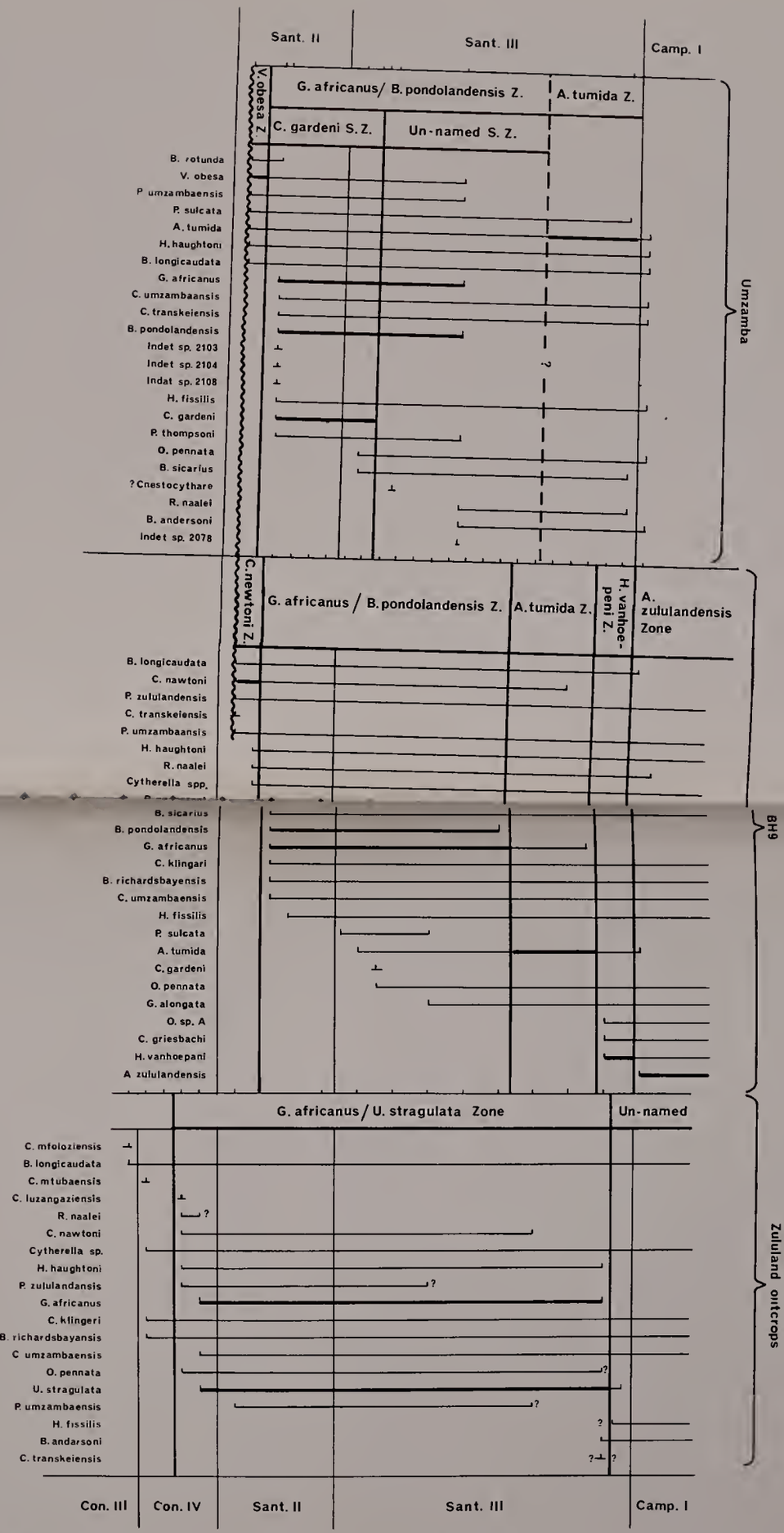

Fig. 46. Basis of proposed ostracod zonation at Umzamba, BH9 (Richards Bay), and the Zululand outcrops in the Mfolozi Valley and False Bay areas. Bold vertical lines indicate zonal boundaries, and bold species ranges are those used in defining zone limits. Ticks on horizontal lines at the top of each locality indicate position of ostracod-bearing samples relative to ammonite zones.
Z = Zone, S.Z. = Subzone.

Figure 47 summarizes the ostracod zonal scheme for south-east Africa defined above and set out in Figure 46. The most complete zonation is that for the Richards Bay area (BH9), where four zones have been recognized in the Santonian II–III sequence. Although the base of this sequence is unconformable on Pre-Cambrian granite, so that it is not possible to define the base of the lowermost zone (*Cytherelloidea newtoni* Zone), its upper limit is probably laterally synchronous with that of the *Veenia obesa* Zone at Umzamba. This is because at both localities the primary control on the range of the overlying *Gibberleberis africanus–Brachycythere pondolandensis* Zone is the vertical distribution of the latter species and I am confident that the range of this species in both areas is very similar, particularly its level of appearance (Fig. 46). North of BH9, in the region of the Zululand outcrops, the *Cytherelloidea newtoni* Zone must be time-equivalent with part of the *Gibberleberis africanus–Unicapella*

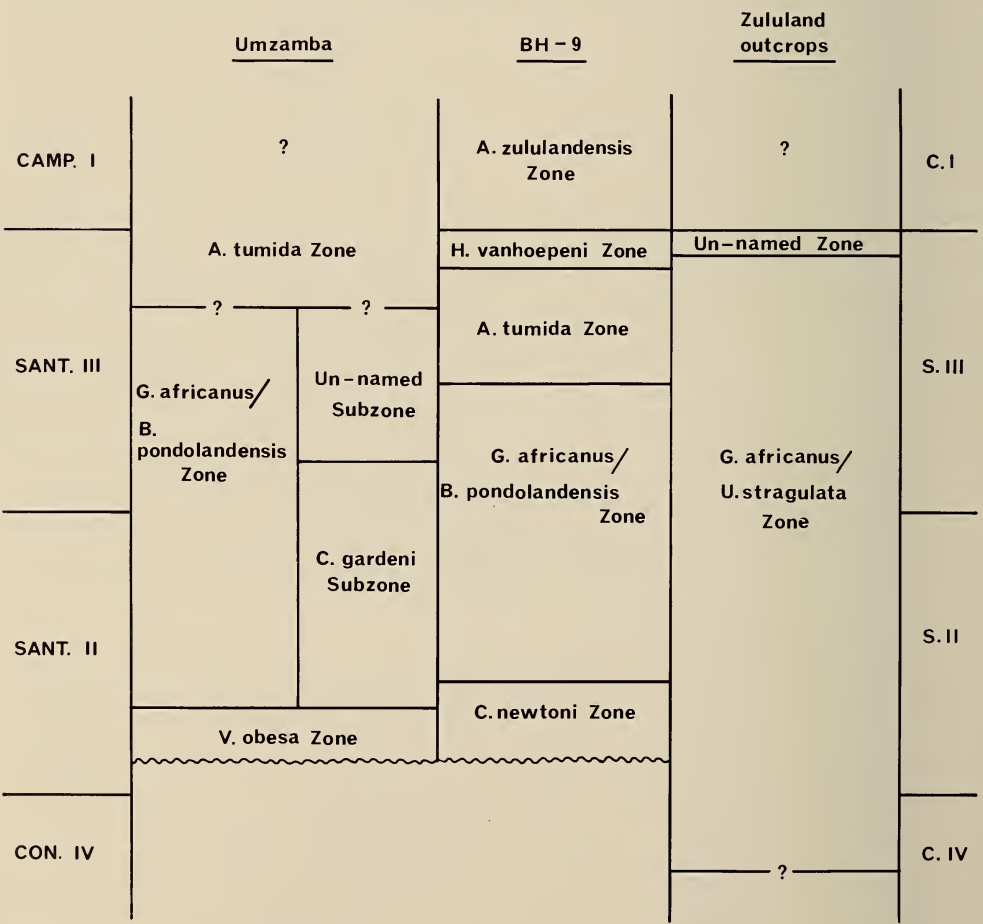

Fig. 47. Summary of ostracod zonation at Umzamba, BH9 (Richards Bay), and Zululand outcrops, and correlation with the ammonite zonation of Kennedy & Klinger (1975).

stragulata Zone, but because *Brachycythere pondolandensis* has not been recognized this far north, the equivalence cannot be assessed.

The upper limit of the *Gibberleberis africanus–Brachycythere pondolandensis* Zone appears to be lower in Santonian III at BH9 than at Umzamba. However, because the samples that control the boundary at Umzamba are widely spaced, this difference may be more apparent than real. In either case, the zone can be correlated between the two faunas because the species used to define it do not appear to be climatically controlled. At Richards Bay, the late Santonian III strata can be placed in a short zone whose upper limit probably coincides with the Santonian–Coniacian boundary (*Haughtonileberis vanhoepeni* Zone). This seems to provide a useful marker between the two stages. Unfortunately, no similar zone can be recognized at either of the other two localities, because sufficiently comprehensive ostracod assemblages from local Campanian I strata are not yet available. At Umzamba I believe that the establishment of two subzones in Santonian II–mid-Santonian III strata will provide additional refinement to age determinations using ostracods. Although a northward extension of the lowermost (*Cytherelloidea gardeni* Subzone) cannot yet be recognized, the one record of the species at Richards Bay does place the relevant horizon at the upper boundary of the subzone in terms of height above the ammonite-defined Santonian II–III boundary.

At present, no satisfactory zonation can be effected for the Coniacian strata in the Zululand outcrops, although the Coniacian IV outcrops have been included in the one zone defined for this area. In particular, the potentially useful species that have been recognized in Coniacian III samples are not yet well enough known to define their ranges.

J(c)–1 and Agulhas Bank

Borehole J(c)–1 lay on the Tugela delta top (Du Toit & Leith 1974; Dingle 1981), approximately 80 km south-west of the Richards Bay area. Despite this geographical proximity, there is a striking dissimilarity between the faunas from the two areas, with no species common. This is particularly so in the cytheraceans, where no genera are common. The presence of *Bythocypris* cf. *richardsbayensis* suggests that there may have been limited contact between the delta top and the Zululand area to the north-east, but the appearance of *Krithe* in the uppermost Cenomanian and Turonian provides further evidence that the sedimentary environments of the areas were markedly different (the earliest record of *Krithe* in the Richards Bay–Zululand area is in Campanian IV of the Mfolozi Valley). Dingle (1981) recognized a similar dichotomy between the two areas in Campanian–Maastrichtian strata, so that the present study indicates that differences in the ostracod faunas were established at the earliest point in the sedimentary history of the delta, and were maintained throughout the remainder of the Cretaceous period.

The two indeterminate cytheraceans (Indet. sp. 2314 and Indet. sp. 2312) in the uppermost Cenomanian apparently have no close relatives either in Zululand

or higher up in the J(c)–1 borehole. Indet. sp. 2314 is superficially similar to *Rocaleberis*, a genus that is first recorded from the Lower Maastrichtian of Argentina, and which is believed to have evolved into the widespread Tertiary taxon *Henryhowella* (Bertels 1976). Until more specimens of Indet. sp. 2314 are available, it is not possible to evaluate any potential relationships, but the palaeogeographic implications for any link of this sort with Argentina would be considerable. The presence of *Dutoitella mimica* in the Santonian extends the lower range of this species, and of the genus in J(c)–1 where it has previously been recorded from the Campanian (Dingle 1981). This confirms a faunal link between the outer Tugela delta top and the Agulhas Bank, which Dingle (1981) detected in Campanian and Maastrichtian strata, and further emphasizes the isolation of the J(c)–1 faunas from Zululand and Umzamba (Fig. 48).

Climatic control

Figure 48 shows the distribution of 24 species of Santonian ostracods between Umzamba, Richards Bay (BH9), and outcrops in Zululand. Previous analyses (Dingle 1980) have suggested that sedimentary environments at the first two sites were similar (Shallow water, <100 m) during Santonian II and III times, so in these cases like is being compared with like. Farther north, where conditions during this period were probably somewhat deeper (200–300 m), comparisons are less meaningful.

Of the 32 species recorded from Umzamba and Richards Bay, 15 are common. Although some of these species are rare and indeterminate, a similarity factor of only 47 per cent between populations of the same age, deposited under similar conditions, and which for the most part are well preserved and well represented, seems significantly low. Table 17 lists the species that are common and restricted to the two areas. Including species which do occur in the other area, but which are rare and restricted in range, 26 per cent of the Umzamba and 38 per cent of the Richards Bay faunas can be considered characteristic of their respective areas. The species that are ubiquitous constitute 43 and 42 per cent of the Umzamba and Richards Bay faunas, respectively. These two faunas are listed here as 'high'- and 'low'-latitude assemblages (the distance is 2,9 degrees). A significant provincialism has also been recorded in the ammonite faunas from the two regions (Klinger & Kennedy 1980).

In assessing the possible causes for this Cretaceous faunal partition, it is necessary to consider the physical setting of the two areas. They lie 320 km apart along a relatively straight coast on which the main intervening feature during early Upper Cretaceous times was the Tugela Delta whose top probably projected seaward, causing an easterly bulge in the coastline (Dingle 1981, fig. 72; Dingle *et al.* 1983, figs 145–146; this paper Fig. 51). Richards Bay lay in the vicinity of a relatively buoyant basement structure (Richards Bay Arch), which was inundated by the Upper Cretaceous transgression in Santonian II times. The modern coastline of Zululand bulges farther eastwards (caused by outbuilding of Upper Cretaceous and Tertiary sediments), but is essentially similar (Fig. 49).

TABLE 17

Spatial distribution of ostracods in south-east African Santonian strata and suggested climatic tolerances. Indeterminate species not shown.

UMZAMBA high latitude 'cool' water 26% of total		ZULULAND low latitude 'warm' water 38% of total	
confined	extends north but rare	extends south but rare	confined
Paraphysocythere thompsoni ***Veenia obesa*** *Brachycythere rotunda*	*Cythereis transkeiensis* *Pondoina sulcata* ***Cytherelloidea gardeni***	*Bairdoppilata andersoni*† *Rayneria nealei*	***Cytherelloidea newtoni*** *Cythereis klingeri* ***Haughtonileberis vanhoepeni*** *Cytherelloidea griesbachi*** *Bythocypris richardsbayensis* *Paracypris zululandensis* ***Unicapella stragulata**** *Gibberleberis elongata***
13% total spp.			29% total spp. in BH9
Ubiquitous, 'intermediate'			
	Gibberleberis africanus *Brachycythere sicarius* *Brachycythere longicaudata* ***Brachycythere pondolandensis***** *Haughtonileberis haughtoni*	*Haughtonileberis fissilis* *Oertliella pennata* ***Amphicytherura tumida***** *Cytherelloidea umzambaensis* *Paracypris umzambaensis*	
	43% spp. at Umzamba, 42% spp. at BH9		

* = Zululand outcrops only
** = BH9 only
† = probably water-depth control
Bold type = zone fossil

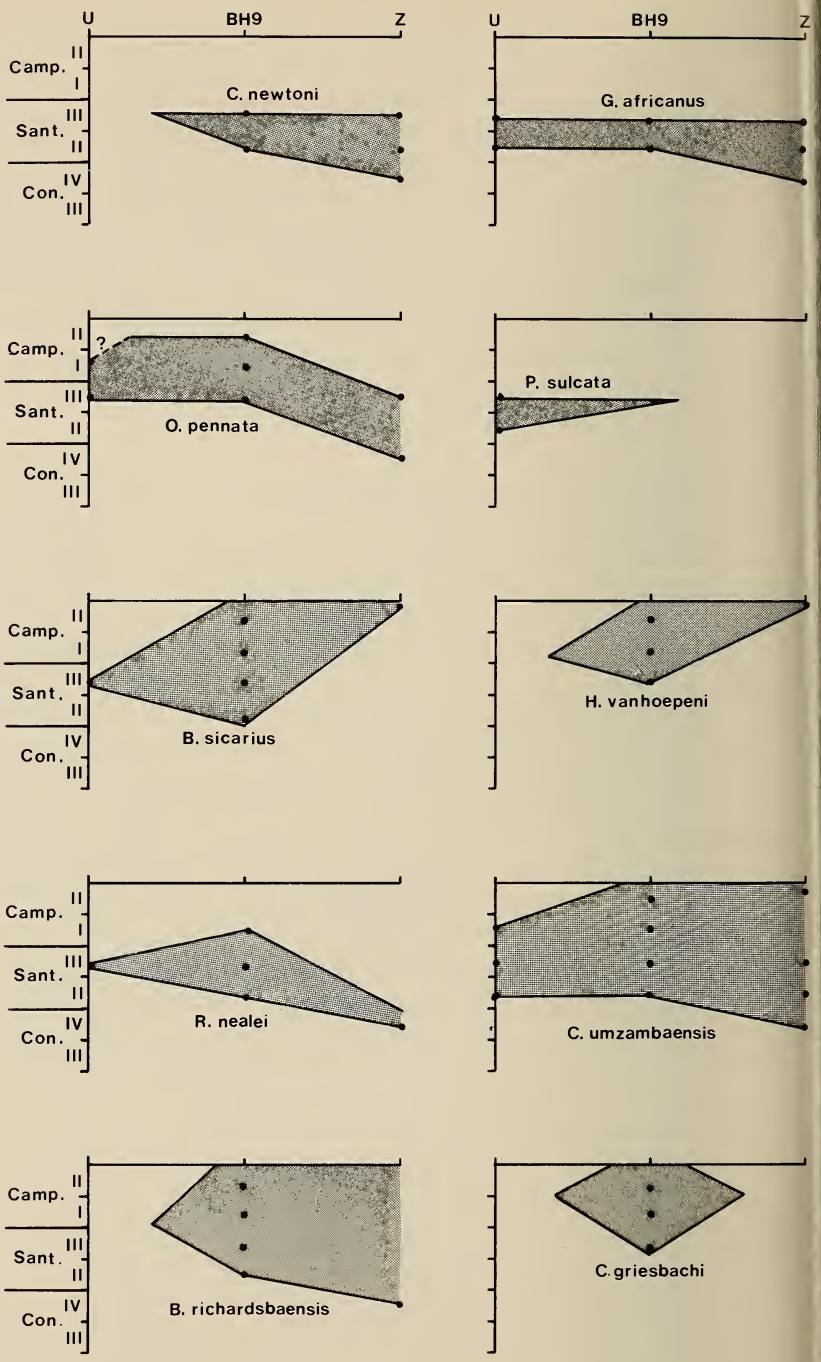

Fig. 48. Temporal distribution of 24 selected species of ostracods between Umzamba (U), Richards Bay (BH9), and the Zululand outcrops in the Mfolozi Valley and False Bay (Z).

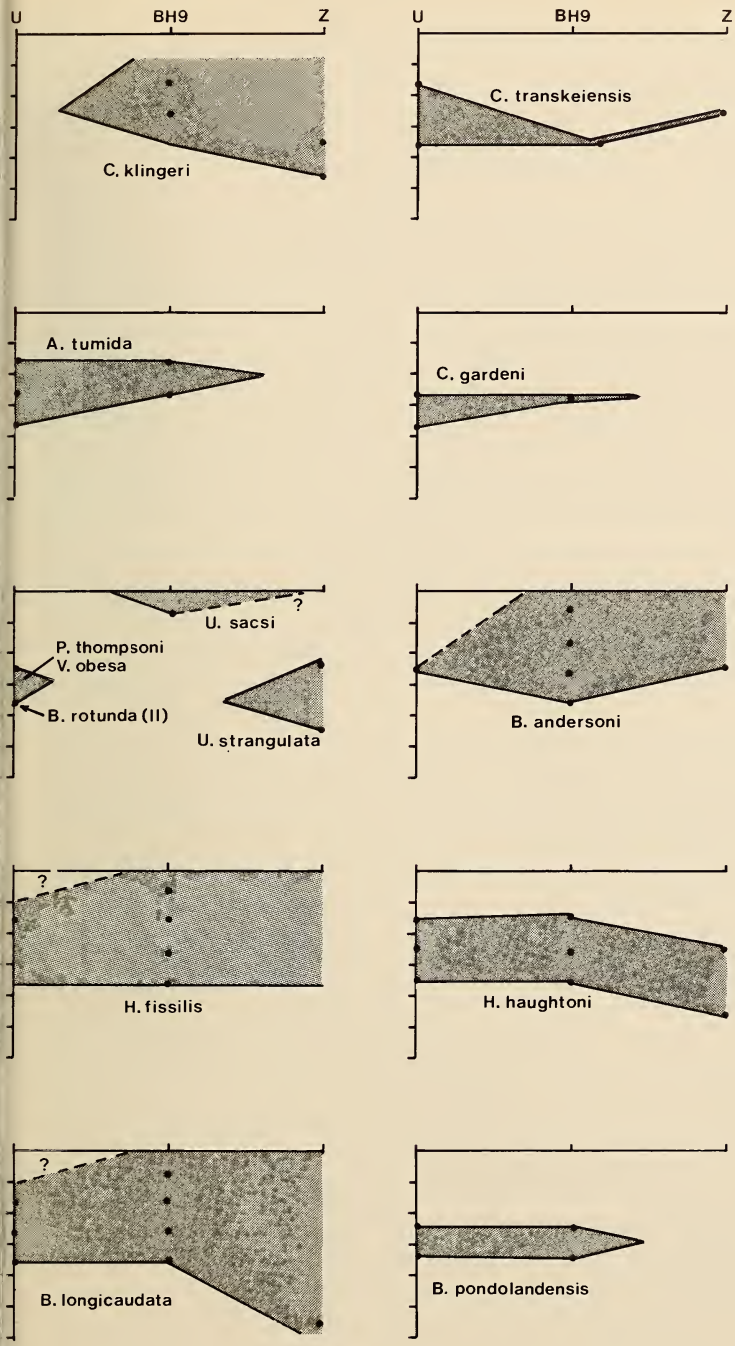
U
BH9
Z
C. klingeri
U
BH9
Z
C. transkeiensis
A. tumida
C. gardeni
U. sacsi
?
P. thompsoni
V. obesa
B. rotunda (II)
U. strangulata
B. andersoni
?
H. fissilis
H. haughtoni
?
B. longicaudata
B. pondolandensis

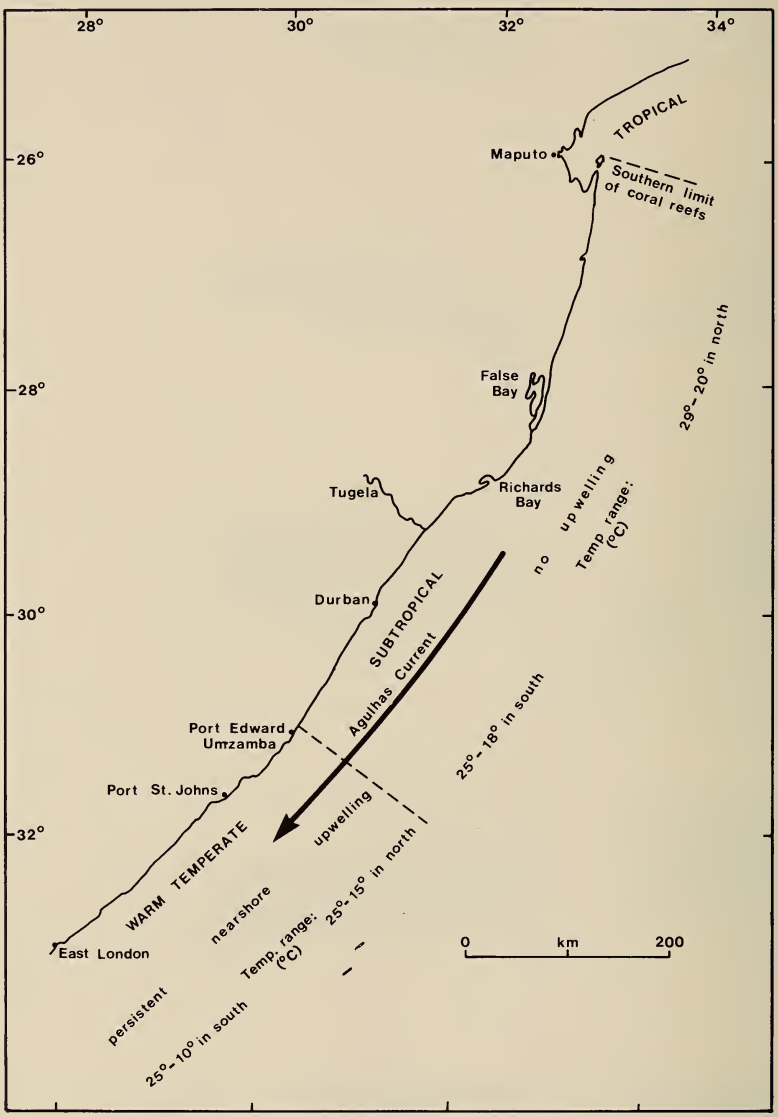

Fig. 49. Modern biogeographical zones of the south-east African coast (Brown & Jarman 1978). Inshore water-temperature data and upwelling characteristics are from Schumann (pers. comm. 1983).

Therefore, there seem to have been no significant physical barriers, beyond those which exist today, to free migration between the two areas, a presumption that is strengthened by the fact that over 40 per cent of each fauna is ubiquitous. Consequently, I surmise that the factors controlling the faunal distribution were related to water-mass properties, e.g. temperature, salinity, and turbidity.

Biogeographical studies of the modern coastal biota have identified three marine provinces along the south-east coast: tropical, subtropical, and warm temperate (Brown & Jarman 1978), with the boundary between the last two lying in the vicinity of 31°S latitude (about 10 km north of Umzamba, Fig. 49). The limiting factor between the subtropical and warm-temperate provinces seems to be the mean minimum water temperatures (see Brown & Jarman 1978), which south of 31°S range 10–15 °C, and north of 31°S range 18–20 °C (see Fig. 49 for further details of inshore water temperatures, which were supplied by E. Schumann (National Research Institute of Oceanology, Stellenbosch, pers. comm. 1983)). This suggests that the faunal discontinuity is related to a difference of 6–7 °C in the mean minimum water temperatures. The key factor here is the occurrence of persistent nearshore upwelling south of Port Edward (just south of 31°S) (E. Schumann, pers. comm. 1983) that modifies the relatively high temperatures of the south-west flowing Agulhas current (up to 25 °C at 31°S). No data are available on the distribution of modern Ostracoda, but these boundaries are clearly defined in the distribution of important taxa such as corals and molluscs.

Comparisons with the present situation cannot be taken far because elements of the oceanographic circulation, in which the western-boundary Agulhas Current is dominant, have not been identified earlier than mid-Tertiary (e.g. Martin 1981), although Haq (1981) has suggested that it was in existence by early Palaeocene times. A speculative Cretaceous palaeocirculation was discussed by Gordon (1973, fig. 4), who predicted a north-east or east-north-eastward flowing current along the south-east coast of Africa in Santonian times, based on the assumption of a more poleward location of the equivalents of the modern southern-oceans low-pressure atmospheric cells. Recently, Barron & Washington (1982) have modelled various atmospheric parameters using a mid-Cretaceous (100 m.y.) global palaeogeography, and concluded that in fact the reverse situation is likely to have occurred: low-pressure cells were located over the oceans adjacent to the southern portions of South America, Africa, and Madagascar–India. In Figure 50 we have used this distribution to speculate on wind and ocean currents. Because south-east Africa lay within the westerly wind belt and a southern-ocean return current can be expected between 55° and 60°S, an eastward-flowing ocean current is predicted along the northern part of the mid-Cretaceous southern ocean, with an east-north-east component off the coast of south-east Africa. This is in fact what Gordon (1973) suggested (for different reasons), although I do not anticipate a major southerly current into the palaeo-Mozambique Channel as he did. It is also similar to that produced from palaeogeographical considerations by Lloyd (1982), and numerically modelled by

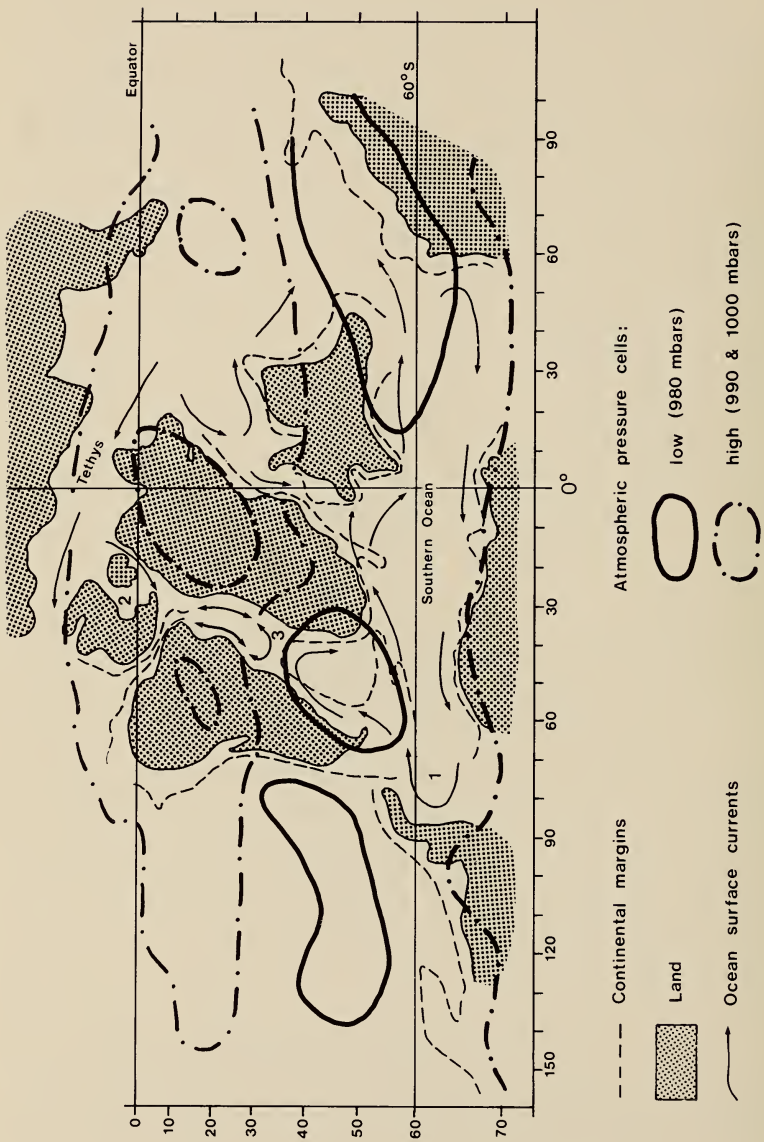

Fig. 50. Southern, South Atlantic, Tethys, and south-west Indian ocean surface water currents in mid-Cretaceous times. Based on the atmospheric pressure modelling and palaeogeography of Barron & Washington (1982). 1 = Southern Ocean retroflexion resulting in a return current. 2 = Temporary trans-Saharan seaway, with currents flowing southward from Tethys. 3 = Narrow northern sector of the South Atlantic, possibly with a monsoonal (reversing) pattern. Zululand lies approximately 50°S 25°W.

Seidova & Yenikeev (1983). Some modification of Barron & Washington's (1982) 100 m.y. model will be necessary for early Santonian time (say 82 m.y.) but the essential geographical features were still in existence at this time, so probably no significant ocean-circulation changes had occurred: a narrow South Atlantic and Southern Ocean; the close proximity of India and Madagascar to Africa; and continuity of a South American–Antarctic–Australasian landmass. In Figure 51 a palaeogeographical sketch of the Umzamba–Richards Bay area in Santonian times is shown, with a north-east flowing offshore current (East Coast Current). Barron & Washington (1982, fig. 2) predict a mean annual range of approximately 12–22 °C in surface temperatures in the vicinity of coastal south-east Africa for mid-Cretaceous times, in comparison with regional averages of 15–24 °C at present (*Times Atlas* 1980). Coastal upwelling in modern times effects a local gradient, lowering the temperature of the higher-latitude sites along the coast by several degrees, with resultant faunal provincialism (Fig. 49). Such a mechanism could not have operated in Santonian times for two reasons. Firstly, the offshore westerly winds would have moved surface water to their left (i.e. inshore), and secondly, the north-east flowing current had its left side to the coast (and dynamic upwelling in the Southern Hemisphere occurs on the right side of currents (G. Brundrit, University of Cape Town, pers. comm. 1984)). In Table 17 the Santonian faunas from these two sites are referred to as 'cool'- and 'warm'-water assemblages (high and low latitude), respectively, but at this stage it is not clear how a significant temperature contrast between the areas was maintained. One possibility is that the boundary between them represents the southernmost limit of penetration by south-west moving inshore cells of warmer water that broke off from the regional anti-clockwise gyre to the north of the Madagascar–India landmass (Fig. 50).

On Figure 51, a temperature gradient across the north-east flowing East Coast Current is indicated, with warmer waters inshore, and cooler temperatures in the deeper and/or more oceanic areas farther offshore. This arrangement is suggested by the faunal differences between the inshore localities of Umzamba and Zululand, and the offshore localities of borehole J(c)–1 on the outer Tugela delta top and the Agulhas Bank. Although there is no substantive evidence for strong links between J(c)–1 and the Agulhas Bank until Campanian times, the presence of *Dutoitella mimica* in the Santonian of J(c)–1 suggests that the environmental conditions responsible for the faunal differences between the inshore and offshore areas around south-east Africa were already established by Santonian times. Water-temperature differences seem the most likely determinant because, although the Tugela delta top was subjected to large salinity fluctuations, there is no evidence that this was the case on the Agulhas Bank.

Recolonization of south-east Africa after the mid-Cretaceous hiatus

Dingle (1982) recognized a major dichotomy in the ostracod faunas of south-east Africa across the mid-Cretaceous hiatus, first described by Kennedy & Klinger (1971). The extent of the non-sequence varies from place to place, and at outcrop in Zululand includes uppermost Cenomanian to lower Coniacian strata

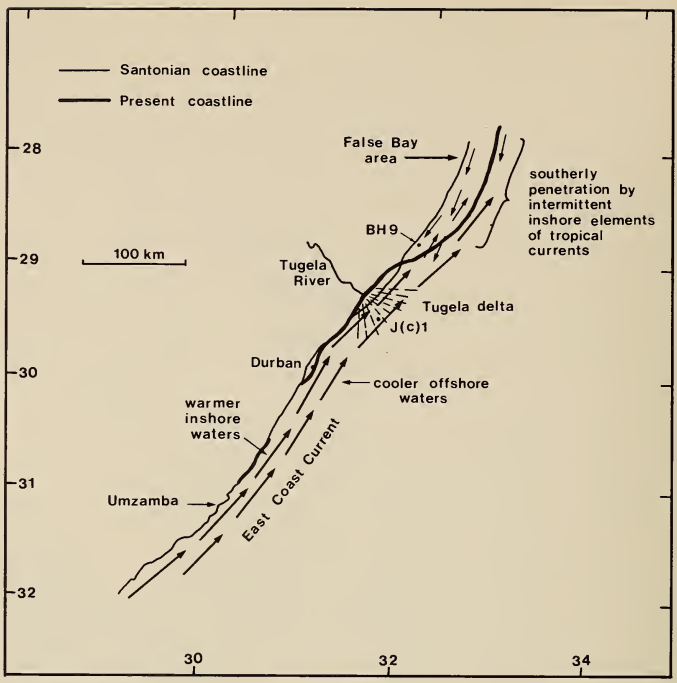

Fig. 51. Santonian palaeogeography of south-east Africa, and predicted nearshore current patterns and temperature characteristics. BH9 locates Richard Bay. Coordinates are for modern location.

(e.g. Kennedy & Klinger 1975). Boreholes closer to the coast in Zululand indicate a shorter break (?late Cenomanian to mid-Turonian—McLachlan & McMillan 1979), and suggest that the earliest sediments of the transgression become older north-eastwards (e.g. Dingle *et al.* 1983). Using Van Hinte's (1976) time-scale, the hiatus across the Mzinene–St. Lucia formations boundary varies from 3 to 6 m.y. in duration.

Figure 52 shows the temporal distribution of key ostracod taxa in south-east Africa in Valanginian to earliest Campanian strata across the hiatus. Pre-Albian assemblages are characterized by various species of genera such as *Progonocythere, Rostrocytheridea, Procytherura*, and *Acrocythere*, while Albian to Cenomanian faunas are characterized by *Arculicythere* and *Isocythereis*. These have been referred to as the South Gondwana ostracod faunas A and B, respectively (Dingle 1984). In addition, they have common elements such as *Majungaella, Sondagella, Pirileberis, Makatinella*, and *Pongolacythere* that give them added distinctiveness. With the exception of *Cythereis*, none of the cytheracean genera present prior to the mid-Cretaceous hiatus have representatives above the Cenomanian in south-east Africa, and even in this case no species are common (*C. agulhasensis*, Albian, Agulhas Bank; and *C. klingeri, C.* cf. *luzangaziensis*, and *C. mfoloziensis* in the Coniacian of Zululand). The South

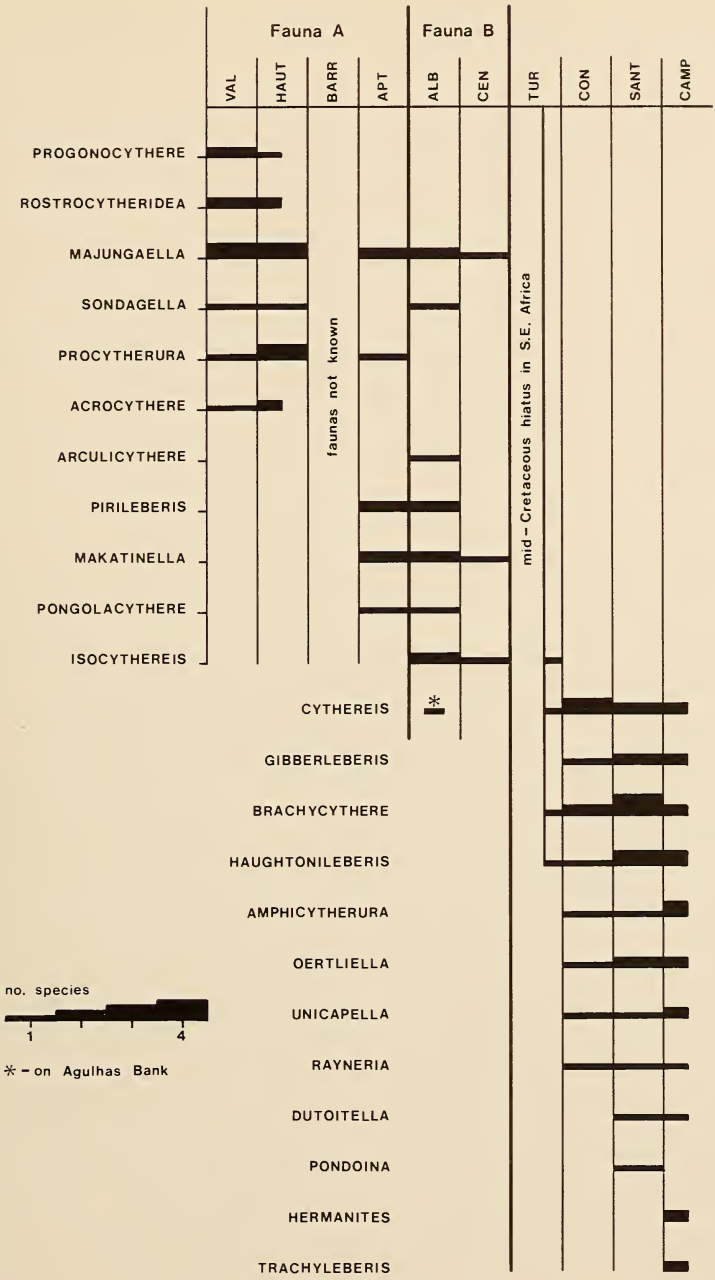

Fig. 52. Distribution of the main cytheracean genera in south-east Africa for Valanginian to Campanian time. Turonian occurrences are for Tanzania as re-interpreted from Bate & Bayliss (1969). Numbers of extant species are indicated by thickness of bars. Note the major Cenomanian–Turonian/Coniacian dichotomy. Faunas A and B are the South Gondwana faunas of Dingle (1984).

Gondwana faunas are Cytheruridae–Schizocytheridae–Progonocytheridae-dominated (Table 18).

TABLE 18

Cytheracea in south-east Africa shown as number of species (in parentheses) in families, as percentage of cytheracean element. (After Dingle 1982, 1984, this paper.)

	Haut.–Val.	Alb.–Cen.	Coniac.	Santonian
Collisarborisidae		10 (1)		
Schulerideidae		20 (2)		
Brachycytheridae			11 (1)	17 (4)
Cytheruridae	30 (6)			
Schizocytheridae	15 (3)	10 (1)	*	8 (2)
Trachyleberididae	5 (1)	30 (3)	89 (8)	46 (11)
Cytherideidae	10 (2)			4 (1)
Bythocytheridae	5 (1)	10 (1)		
Progonocytheridae	25 (5)	20 (2)		8 (2)
Loxoconchidae	5 (1)			
Indet.	5 (1)			17 (4)
Total no. spp.	(20)	(10)	(9)	(24)

* = present on Agulhas Bank

Dingle (1982) characterized post-Coniacian faunas as Trachyleberididae–Brachycytheridae–Schizocytheridae-dominated, and Table 18 and Figure 52 show that these higher taxa were all represented during Coniacian times. In other words, elements that dominated during much of Upper Cretaceous time were also aggressive recolonizers of the region after the non-sequence, in particular the long-ranging cytheracean species *Brachycythere longicaudata, Haughtonileberis haughtoni*, and *Cythereis klingeri*, medium-ranging cytheracean species such as *Gibberleberis africanus* and *Oertliella pennata*, and long-ranging non-cytheracean types such as *Bythocypris richardsbayensis* and *Cytherelloidea umzambaensis*. It is interesting to note that the earliest known member of the subfamily Unicapellinae (which forms a minor, but distinctive element of Campanian–Maastrichtian faunas) occurs in the Coniacian IV of Zululand. The total failure of the original cytheracean taxa (South Gondwana fauna B) to regain niches is a phenomenon of considerable significance, because although the sedimentary environments of Albian–Cenomanian and Coniacian–Santonian strata at Zululand outcrop sites were probably not strictly comparable, with the latter probably somewhat deeper (compare Fig. 39, this paper, and fig. 41 in Dingle 1984), the two were sufficiently similar to indicate that a combination of phylogenetic and regional palaeogeographic factors was responsible. This question will be examined in the next section.

GREATER AFRICA AND GONDWANALAND

Aspects of ostracod distribution in the South Atlantic during Cretaceous times have been considered by Krömmelbein (1976), Bertels (1977), Dingle

(1982), and Tambareau (1982*a*, 1982*b*) amongst others, and the latter references contain a comprehensive compilation of specific citations. These works have shown that the major south-east African mid-Cretaceous faunal dichotomy, which has been referred to in a previous section, is not present in west Africa and Brazil, and recent studies in north Africa (e.g. Bismuth *et al.* 1981) indicate that it is also not present along the south-west shores of Tethys. It is present in Iran (Grosdidier 1973) and Tanzania (Bate & Bayliss 1969). The problem is therefore twofold: when did the faunal change take place in south-east Africa, and why?

The difficulty in assessing the precise timing is caused by the non-sequence in uppermost Cenomanian to Turonian strata in south-east Africa, but can be tackled by considering the regional distribution of two key taxa: *Brachycythere longicaudata* and *Haughtonileberis haughtoni*. These are particularly well suited because there are numerous records of the two genera from greater Africa (Tables 6, 9); in south-east Africa the two genera, and in particular the species selected, are diagnostic elements in the post-Turonian populations (Figs 46, 48). Figure 48 shows that in Zululand *B. longicaudata* is known from Coniacian III, and *H. haughtoni* from Coniacian IV. Given the limitations of the sample distribution, both species can be considered amongst the earliest (and most abundant) colonizers of the area during the Upper Cretaceous transgression. Neither genus is present in underlying Albian–Cenomanian Mzinene Formation strata. SEM photographs of material originally described by Bate & Bayliss (1969) show that both species occur in the Upper Turonian of Tanzania (recorded as *B.* aff. *sapucariensis* and *Curfsina turonica* (paratype, BMNH Io783)). The Cenomanian–Turonian succession appears to be complete in Tanzania, but a faunal dichotomy with some of the significant characters of that noted in south-east Africa is also present here: neither *Brachycythere* nor *Haughtonileberis* occurs in the Cenomanian; and *Majungaella*, which occurs in the Albian and Lower Cenomanian, does not extend into the Turonian. In eastern Africa, therefore, the dichotomy occurs between the local top of the Lower Cenomanian (with *Rotalipora appenninica* and *Planomalina buxtorfi*), and local base of the Upper Turonian (with *Globotruncana helvetica* and *G. linneiana*, amongst others, see Table 5). In fact it could lie within the Cenomanian because Bate & Bayliss (1969: 120) record a possible intra-Cenomanian hiatus above which *Majungaella* does not occur (in beds with *Rotalipora greenhornensis* and *R. cushmani*). The latter possibility can also not be ruled out in Zululand, because the highest record so far for *Majungaella* is Cenomanian III (Dingle 1984). (No ostracod fauna was recovered from Cenomanian IV, which is probably upper *R. cushmani* Zone.) In view of the fact that Bate & Bayliss (1969) did not describe large faunas and had no ostracods of Lower–Middle Turonian age, it seems more appropriate to assume the less precise age for the faunal change at this stage of our knowledge. On the basis of ammonite faunas, Reyment & Tait (1972: 93) postulate a late Lower Turonian date at which 'nekroplanktonic ammonite shells were able to drift with oceanic currents over the entire Atlantic'. Reyment *et al.* (1976) show a series of palaeogeographies in which the various west African–Brazilian–north

African connections developed in Albian–Turonian times, and concluded that free surface-water connections between north-west Africa and the south-west Indian Ocean were established by Middle Turonian times. This accords with our data, with the exception that no trans-Saharan connection was postulated before the early Turonian (Reyment *et al.* 1976; Reyment 1980*b*). The occurrence of *Brachycythere* gr. *sapucariensis* in the Cenomanian of Tunisia, Gabon, and north-west Brazil (see Table 6) shows that at least temporary communication must have been established by early Cenomanian times, presumably across the Sahara, but conceivably around north-west Africa across the Brazil–west Africa land bridge (Fig. 53A).

Neither *B. longicaudata* nor *H. haughtoni* has been recorded from west Africa, Brazil and north Africa, but both of the genera involved have a longer history in these areas than in the western Indian Ocean region (Tables 6, 9): *Brachycythere* gr. or cf. *sapucariensis* appears in the Lower Cenomanian of Tunisia and Upper (possibly Lower) Cenomanian of Gabon, and ranges into the Lower Coniacian (Brazil), while several species of '*Haughtonileberis*' have been recorded from Gabon (Grosdidier 1979), the earliest of which is Upper Albian. In addition, four other species of *Brachycythere* occur in Lower Turonian, or older

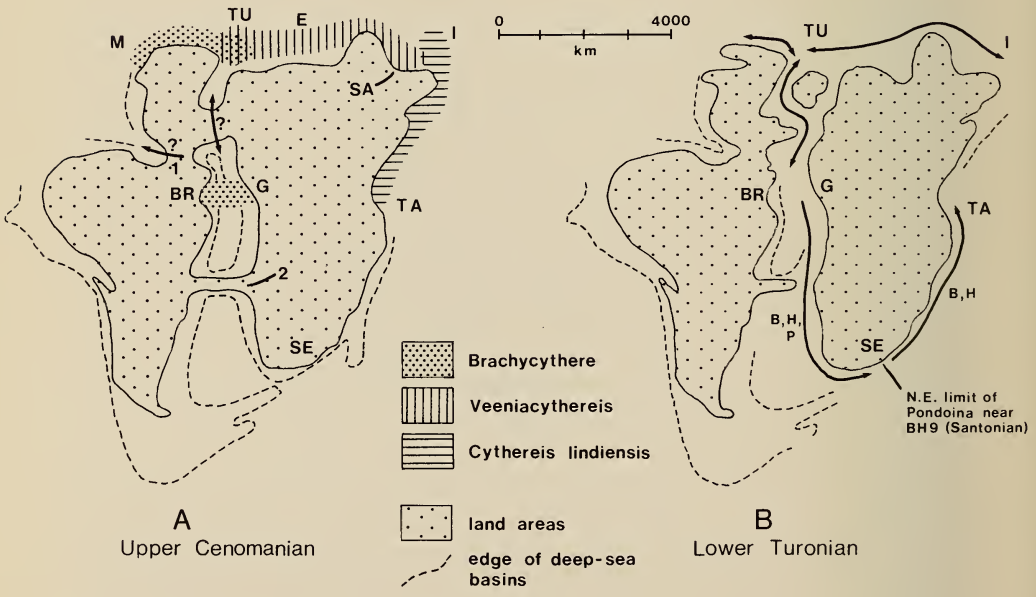

Fig. 53. Cenomanian and Turonian ostracod distributions, migrations, and intercontinental relationships. A. Upper Cenomanian. B. Lower Turonian.
Abbreviations—large type: M = Morocco, TU = Tunisia, E = Egypt, SA = Saudi Arabia, I = Iran, TA = Tanzania, SE = south-east Africa, G = Gabon, BR = Brazil; small type: B = *Brachycythere*, H = *Haughtonileberis*, P = *Pondoina*. 1 = Brazil–west Africa land bridge, 2 = Walvis–Rio Grande land bridge. Arrows denote migration routes.

strata of north Africa. *Brachycythere sapucariensis* is very close to *B. longicaudata*, and its wide geographical distribution suggests that it was probably ancestral to the latter.

From the above, it is clear that *Brachycythere* was widespread in the Equatorial Atlantic–south-west Tethys, and *Haughtonileberis* was widespread in the northern part of the South Atlantic before either genus appeared in the western Indian Ocean sometime between the Middle Cenomanian and Middle Turonian. In east Africa, they displaced the extant fauna, and in south-east Africa they colonized inshore areas during the Turonian–Coniacian transgression. Significantly, the first appearance in Iran of *Brachycythere* (five species) was in ?Coniacian–early Santonian strata (Grosdidier 1973). The questions to consider now are why did these taxa infiltrate new areas, why were they so successful, and why was there a phylogenetic 'explosion' in the newly colonized areas (many of the post-Turonian genera in south and east Africa are endemic)?

Table 6 shows that *Brachycythere* spread rapidly along the southern shores of Tethys between Morocco and Iran during Lower Cenomanian to Coniacian times. Grosdidier (1973) records a major faunal break in the latter region across a late Cenomanian to ?Coniacian–early Santonian hiatus, where the older fauna, characterized by *Cythereis* (three species), *Veeniacythereis jezzineensis*, and *Dordoniella?* is replaced by one characterized by *Brachycythere* (five species), *Veenia, Pterygocythere?, Ovocytheridea, Buntonia*, and *Cythereis*. Because *Cythereis lindiensis* is recorded in the Cenomanian of both Iran and Tanzania, indicating that there was faunal contact between the two areas in pre-Turonian times, it is superficially tempting to suggest that *Brachycythere* arrived in east Africa, and even south-east Africa, via Arabia. Other evidence does not support this suggestion, however, and in particular we can cite the restriction of *Pondoina* to Gabon (Turonian), Brazil (Coniacian), and south-east Africa (Santonian) (Krömmelbein 1972), and the non-occurrence of *Haughtonileberis* in Arabia and *Veeniacythereis* in the South Atlantic and western Indian oceans. These distributions suggest two dispersion routes out of the Equatorial Atlantic (Fig. 53B). They were favoured by different genera, so that the partitioning of the original (Cenomanian–Turonian) Gabon–Brazil fauna resulted in two generically distinct younger faunas along the southern shores of Tethys and in the western Indian Ocean.

Figure 50 shows that the region in which early evolution of *Brachycythere* and *Haughtonileberis* (Albian–early Cenomanian) took place lay in low latitudes, presumably in warm waters as part of a 'tropical' population. This suggests that water temperatures would have been a limiting factor in any migrations, at least during the early part of their development, although these genera must have been inherently more tolerant than the bulk of the Equatorial Atlantic–Tethyan tropical fauna, which never managed to achieve significant expansion into the Indian Ocean: for example *Ovocytheridea, Veenia, Veeniacythereis, Buntonia, Glenocythere*, and *Schuleridea* (see Tambareau 1982*b* for a summary). A second factor limiting migration would have been the palaeogeography of the